Laboratory Testing for Adfreeze Bond of Sand on Model Steel Piles

Joey Villeneuve, B. Sc.A.

Thesis submitted in partial fulfillment of the requirements for the
Master of Applied Science degree in Civil Engineering

Under the supervision of
Dr. Julio Angel Infante Sedano, P. Eng

Department of Civil Engineering
University of Ottawa
Ottawa, Ontario

Abstract

This study explored the available adfreeze data published in literature and the techniques used to obtain it. Two methods were selected and modified to complete series of adfreeze bond test. A model pile pull-out method consisting of pulling a pile out a large specimen of soil was the first method used. The second method was modified from an interface shearing apparatus developed by Dr. Fakharian and Dr. Evgin at the University of Ottawa in 1996 and allowed preparing, freezing and testing the specimen in place.

The material and soil tested for this study were provided by EXP Services Inc. The model pile, a galvanized HSS 114.3 x 8.6 section, is commonly used to install solar panels. Soil was taken from a future solar farm site in proximity to Cornwall, Ontario.

The study had for objective to develop a low cost adfreeze laboratory testing method. Limitations of the technics and apparatus used were observed. While the results of a model pile pull-out test compared to previous data publish by Parameswaran (1978), the interface shear series of test presented more limitations. The interface shearing method has been previously study by Ladanyi and Thériault (1990).

Issues with the interface shear method due to the water content of the soil as well as the range of normal stress applied to the specimen both during testing and freezing. The data obtained was inconclusive and the method will be studied in future research program.

This studied approach the adfreeze testing with new improvement. The main contribution of this study is the data obtained by measuring and observing adfreeze of ice poor sand with varying water content. The measurements allowed to study the effect that increasing water content has on the interface bond strength.

The modifications made to interface shear apparatus are also major new contribution provided by this research. The apparatus was converted in a small freezer chamber using insulation panel and vortex tubes. Which was used to freeze the specimen in the testing chamber and testing adfreeze in place without handling the shear box arrangement.

Acknowledgements

The author would like to express his most sincere appreciation to his research supervisor, Dr. Julio Angel Infante Sedano, for his great support, knowledge, help and guidance throughout the preparation, design, setup and test series. Dr. Infante Sedano was an invaluable member of the group that help put this research together.

The author also wishes to thank Dr. Sai Vanapalli, Dr. Mamadou Fall and Dr. Mohammad Rayhani for serving as members of the examination committee.

The author would also like to thank his laboratory assistant Mathieu Villeneuve, Camille Montour and Frederik Hupe for their long hours spent in the laboratories and the help they brought in the preparation of the specimen.

Thank you to the staff of the department of Civil Engineering of the University of Ottawa for their help and particularly to Mr. Jean Claude Celestin and Mr. Muslim Majeed for their exception technical knowledge and support.

Nothing would have been possible without the financial support of the University of Ottawa and EXP Services Inc. with Mr. Mansour Navidpour who provided the material.

Thank you to all.

Table of Content

Table of Figures

Table of Tables

Chapter 1. INTRODUCTION

Given that the greater part of Canada's territory is situated north of the 49th parallel, it experiences some of the hardest winters in the world. The frost seasons are therefore very long and even continuous in some part of the country. Because of this, the formation of frozen soil is then unavoidable. In the northernmost latitudes, part of the frozen soil remains frozen year-round leading to the formation of permafrost. Since 50% of the country is covered by some type of Permafrost (Harris S.A, 2015), studies of frozen soils are therefore relevant to the Canadian reality.

Permafrost is a soil condition for which, by definition, the soil needs to remain permanently frozen for at least 2 consecutive freezing seasons (or 2 years). This type of soil condition can be found north of the 50th parallel or in high mountain ranges. On the other hand, the frost front can be observed at latitudes as low as the 40th parallel in North America and down to the 30th parallel in Asia (Phukan, 1978). The seasonal ground freezing limit is defined by engineers by a frost penetration depth of 300mm (Andersland, 2004). Canada, Russia and Greenland have the biggest permafrost cover of the entire world: 50%, 60%, and 100% of their total area respectively. In other countries, such as the Scandinavian nations, Western Europe, the United States and China, engineers have to contend with seasonally frozen ground. The study of frozen soil needs a different approach than the classical soil mechanics. A fourth solid phase is found in frozen soil: ice. This fourth phase combined with the three classical phases (solid soil, water and air) at different ratios will modify the original soil properties.

Frozen ground has a very broad definition. Most simply, it is defined as a soil or a rock at a temperature below 0°C, independent of the water content (Andersland, 2004). Even if this definition includes dry soils, frozen soils are generally considered to consist of four phases: soil grains, ice, unfrozen water and gas. The ice, in any concentration, is an important bonding agent that fuses the soil or rock particles together similarly to cement in concrete. It increases shear strength and makes the soil impervious to water seepage.

Frozen soil mechanics is a relatively young field of geotechnical engineering. The earliest research in the domain dates back to the 1960s. Major advances were made during the mid-1970s and 1980s, when demand for petroleum lead the industry into northern latitudes (Arenson et al., 2007). These studies brought the first design criteria for foundations, pavements and investigation methods for frozen soils. However, the late 1980s depression delayed new research for nearly a decade (1990s). It was not until the mid-2000s that interest for the domain arose anew.

Frozen soils are still not well understood today. Researchers such as Andersland, Arenson, Ladanyi and Morgensten have pioneered the domain and explored practical fields and theoretical aspects of it. It was quickly found that classical soil mechanics was not representative of frozen soil conditions. The presence of ice as a bonding agent not only influences strength and permeability, but particle interaction and internal stress distribution.

1.1.Problem Statement

Many types of piles have been used in permafrost. The range of material used includes timber, steel and concrete (Heydinger, 1987). Steel H-piles, corrugated metal piles and circular HSS piles are the types most commonly used. Timber piles are usually tapered with the tip downward to facilitate installation or upwards when greater uplift resistance is needed. (Crory, 1966) Pre-tensioned precast concrete piles are manufactured to withstand handling and driving stress. Cast in place concrete piles are not recommended due to the heat emitted during curing. The most advanced type of piling systems now used includes freeze pile and thermosyphon. Freeze piles are formed with interior tubing allowing cooling fluid to circulate and evacuate heat from the ground therefore maintaining it frozen. Thermosyphon piles are sealed with an anti-freeze fluid which boils at the target ambient temperature. The vapour thus formed transports the excess heat to the surface where the fluid condenses and flows back in the pile. The heat is then dissipated at the surface, and the soil surrounding the pile remains frozen.

Canada has a standard for thermosyphon pile design, CAN/CSA-S500-14; Thermosyphon foundations for buildings in permafrost regions and a standard for permafrost protection CAN/CSA S501-14; Moderating the Effects of Permafrost Degradation on Existing Building

Foundations but no frozen soil foundation design standard exists. The Canadian Foundation Engineering Manual doesn't cover any design aspect of deep foundations in frozen soil conditions with the exception of frost heave and frost susceptible soils. It provides a general value for adfreeze of 65 to 100 kPa for fine grain soils and 150 kPa for saturated frozen gravel. Experience is the only guideline in frozen ground foundations.

It is well known that pile foundations in frozen soil conditions rely mainly on the adfreeze bond to carry loads and the end bearing capacity is generally neglected (Ladanyi and Theriault, 1990). The implication is that in the active zone (the area subjected to freezing and thawing cycles), the combined effect of the adfreeze bond, and the expanding nature of freezing water can lead to an upward force acting through the structure's foundation piles. The adfreeze force can be so large that the entire structure can be lifted without it touching the ground.

A considerable amount of information and observations are available on the adfreeze bond of specific soils, but little applicable design methods and standard testing methods. Therefore, this research looked into comparing results of two different testing techniques similar to the ones found in literature. The testing also observed the effect of the adfreeze bond on ice poor soils, considering specimens with different water contents before freezing, as well as different net normal stresses.

1.2.Objectives

The objectives of this study were to;

1) Put in place a pull-out testing procedure, easy to implement in laboratory. Achieving cheap and easy laboratory testing method to demonstrate the potential of adfreeze testing.
2) Measure and observe adfreeze bond strength. While there is various research presenting measured adfreeze values, there is still gaps in the data and observation.
3) Use an interface testing apparatus to test adfreeze bond under direct shear. Modified direct shear box have previously been used to test interface friction.
4) Create an apparatus able to freeze and test specimens in place limiting handling of fragile samples.

5) Test and compare pull-out and direct shear procedures in interface apparatus.

1.3.Scope of Research

The objectives of this research described in the previous section were achieved at the Geotechnical Laboratory and the Structural Laboratory of the University of Ottawa. Adfreeze bond was measured and observed by a Universal Testing Machine (UTM) and a Cyclic 3-D Simple Shear Apparatus for interface testing.

The testing procedures for pull-out testing was developed using easy to procure material such as off the shelf thermistors, shop fabricated steel elements and a commercial freezer. The observation and data of this new adfreeze testing method where compared to the data and observation from literature push-through testing.

The interface test series relied on a freeze/test in place sequence developed specifically for the current adfreeze testing program. The results and observations of the data were compared to available literature data obtained using a comparable interface testing method.

The present study covered adfreeze bond testing for a pile shape and material commonly used for solar panel installation in a soil provided by a consultant studying the feasibility of a solar park near the municipality of Cornwall, Ontario. The novelty of the testing program relied on the adfreeze tests that were conducted.

1.4.Outline of Thesis

This thesis is arranged in chapters dividing the different testing method and finale discussion of the results. “Chapter 2: Literature Review” presents a summary review on previous knowledge of frozen ground. The key topics of review covered research and testing of adfreeze bond, soil freezing process and effect of water/ice content.

“Chapter 3: Model pile pull-out test” presents the soil, material and equipment used for a model pile pull-out testing program. This section presents the detailed procedure for large specimen

preparation and freezing as well as the apparatus setting. The results and observations of the test program as summarized at the end.

“Chapter 4: Soil Interface Testing” presents the material relation used for interface and model pile testing as well as the equipment used to determine the comparison. The important modification made to the apparatus to allow freeze/test in place are detailed. The chapter concludes with the observation and results obtained from the series of tests.

“Chapter 5: Testing method discussion” discusses the observation made during each testing procedures and the issues encountered. This section presents the feasibility of low cost adfreeze testing by comparing results with known values and discussion available in literature.

“Chapter 6: Conclusion” presents a summary and conclusion of the research program. Some recommendations for further research on the subject are also summarized.

Appendices show all the detailed data collected from the testing procedures as well as shop drawings for the fabricated equipment used during the pull-out tests.

- Appendix A: presents the individual test results of the pull-out test series
- Appendix B: presents the individual test results of the shear interface test series
- Appendix C: presents the set-up and material drawing for the pull-out test series

Chapter 2. Literature Review

The studies introduced in Chapter 1 lead to the first design criteria for foundations, pavements and investigation methods for frozen soils. Due to the late '80s depression it was not until the mid-2000s that new interest for the domain manifested itself.

Adfreeze or pile-soil interface bond is the main contributor to frozen ground bearing capacity. It is also a component resisting the heave forces in permafrost regions (Parameswaran, 1978). However, while designing piles and other types of foundations in seasonally frozen ground, the active layer is mostly ignored. Designers assume no influence from the active layer and simply design from under the assumed. Some exceptions are found depending on the project specifications.

2.1. Frozen ground

Frozen ground or frozen soil is defined as:

"Soil or rock with a temperature below 0°C" (Andersland, 2004)

or

"Ground with a mean soil temperature below the freezing point" (Zang et al., 2003)

These definitions encompass all soils and rock with a temperature below the freezing point of water independently of their water content. Although the definition includes dry soils, frozen soils are generally considered to be composed of four phases: soil grain, ice, unfrozen water and gas. The ice, in any concentration, is an important bonding agent that fuses the soil or rock particles together as cement does for concrete. Thus, it increases shear strength and makes the soil impervious to water seepage.

The large increase of soil strength is commonly used by construction engineers designing for frozen soils. Excavations and slopes are more stable, the bearing capacity of foundations is

increased, and contaminants are locally constrained by ice. These are some of the advantages of working with frozen soils. Its major disadvantage, however, is that a frozen soil quickly loses its improved properties when thawing.

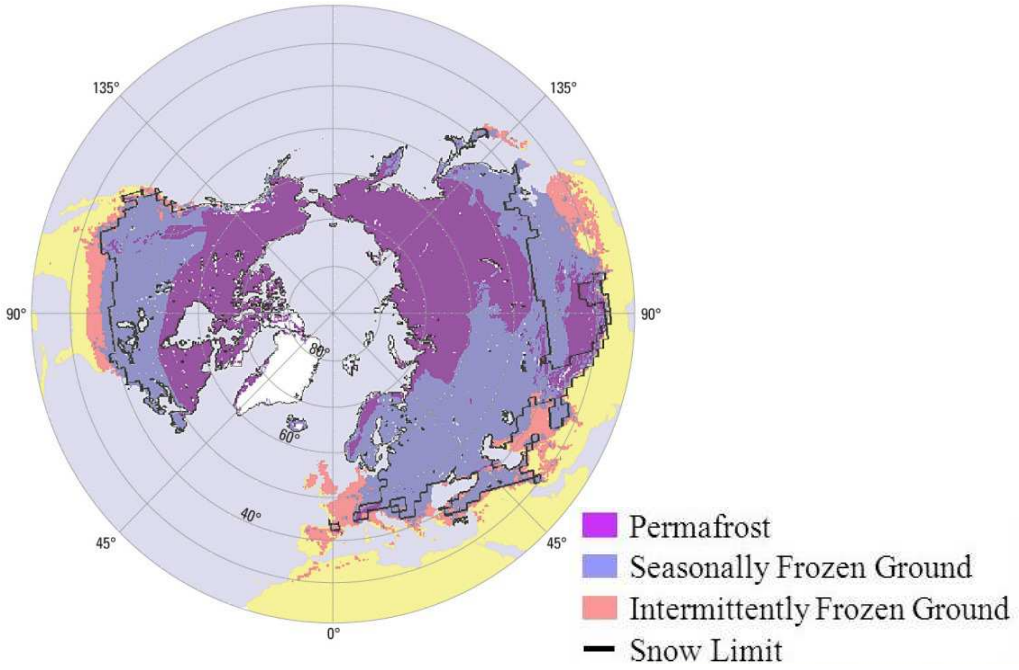

Figure 1: Distribution of frozen ground in the Northern Hemisphere (from Zhang et al., 2003)

The strongest frozen soil condition is known as permafrost. It is often described as a unique material. Permafrost is defined as a soil condition where the soil needs to be permanently frozen for at least 2 consecutive freezing seasons (or 2 years). On the other hand, seasonal ground freezing limit is defined by engineers by a frost penetration depth of 300 mm (Andersland, 2004).

According to Zhang (2003) permafrost covers 25.6% of the land in the Northern Hemisphere, which is approximately 24.91 million square kilometers while seasonally frozen ground coverage is about 50.5%, which represents 48.12 million square kilometers. Another 6.6% (6.27 millions square kilometer) is defined as "intermittently frozen ground". Intermittently frozen ground is a near surface freezing during 1 to 15 days of the year. Figure 1 demonstrates the regions affected by these types of ground freezing.

2.2. Soil Temperature Observation

When considering frozen ground and permafrost, temperature is critical (Hammer et al, 1985). In permafrost the temperature is always close to 0°C at the lower extremity and at least one time a year it warms to temperatures above 0°C at the surface. This thawing layer is commonly called the active layer and is only seasonally frozen. Figure 2 shows the typical temperature profile of a permafrost ground during freezing and thawing season.

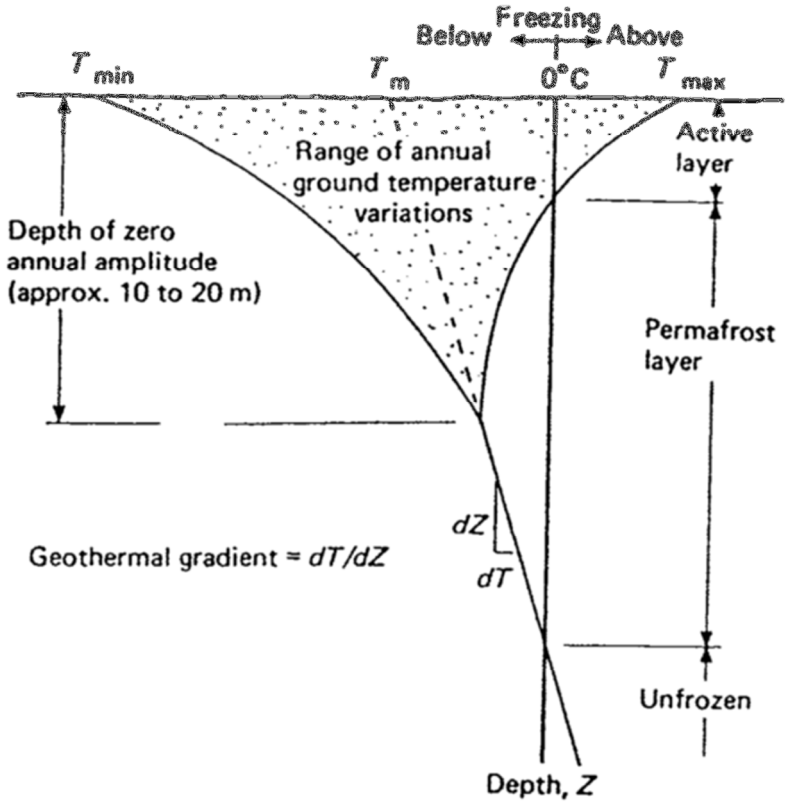

Figure 2: Typical permafrost ground temperature (from Andersland, 2004)

The first soil temperature readings were made by Williams in 1789 using a mercury-in-glass thermometer embedded 255 mm below ground (Miller, 1985). He took readings from May to November in a wooded and a pastured area and accompanied his readings with visual observations. Not only was the effect of vegetation observed, but the effect of snow cover during winter time was also studied. Today thermometry is still used to measure and understand the effect of land coverage on ground temperature.

Today, various alternatives to the mercury thermometer exist to measure temperature. Temperature can now be read using many sensor properties like dimensional change (mercury/glass and bimetal thermometers), chemical change (frost tube, Figure 3) or electrical change (thermistors, resistance thermometers and thermos-couple). It can also be measured by indirect methods such as infrared or optical pyrometer.

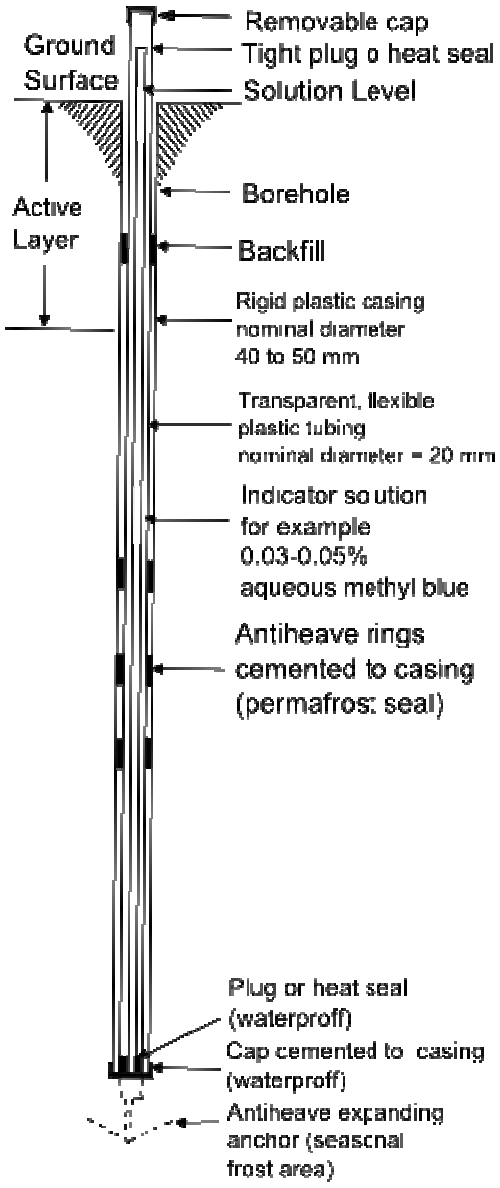

Figure 3: Frost tube for measurement of rate and depth of thaw or seasonal frost penetration (Ladanyi and Johnston, 1978)

The appropriate methods of measuring ground temperature will depend on the accuracy, location and frequency of reading needed. Field conditions and laboratory conditions sometimes require the use of different methods, some being available only in laboratory. Today's sensors can measure temperature to an accuracy of 0.1°C off-the-shelf (Miller, 1985). The work done by Williams (1789) illustrates one of today's problems. Most Temperature data for Canada's frost zones comes from dispersed weather station and published data from passed research. The data has global representation and doesn't represent local fluctuation of micro climates.

2.3. Frozen Ground Sampling

Sampling is an important step in preparing any field design. The data acquired from field samples range from particle size distribution to creep behaviour, thaw consolidation and strength. The type of sampling and testing procedures selected depend on many factors. Among those, the size of the engineering structure is the main factor influencing both the method and the number of samples. The type of frost or permafrost will guide the method, depth and size of samples to be taken, and the data required will dictate the method of sampling. Location also affects the sampling technique. As is often the case in arctic areas, smaller equipment is the only option for sampling since the locations are commonly only accessible by helicopter (Andersland, 2004).

Sampling techniques used in frozen ground are similar to the ones used in unfrozen soils, but care must be taken to avoid thermal disturbances. Samples and observations can be taken from natural exposition, like exposed river banks, gullies and landslide scarps. Test pits are also a common option; sampling can also be done from the wall or bottom, as well as excavated by hand or excavator to depths of 8 to 10 m. Most often, however, data is obtained from boreholes which can be drilled with heavy equipment or hand equipment (Figure 4). Drilling equipment varies in size and therefore can be transported in by helicopter (Veillette, 1975).

Figure 4: Removing a sample from a core barrel (SnowNet, 2009)

If not tested immediately the frozen sample will need to be insulated and kept at the appropriate temperature equivalent to the temperature on site. Various methods are used for this purpose; some circulate diesel fuel, brine, alcohol and other types of antifreeze fluid in sleeves or compartment around the sample. However, the fluid may contaminate the sample or thaw the surface. If the specimen is large enough; undisturbed samples can be obtained by removing the affected layer. Other methods will use a modified insulated sampling tube or heavy walled tubes.

During transport the samples need to be protected from moisture loss, sublimation, thawing and even temperature change (Baker, 1976). Samples are wrapped in cellophane and placed in sealed polyethylene bags from which the air has been vacuumed out. The sample is then transported in a cooler or small portable freezer. Appropriately prepared samples can be kept in acceptable conditions for periods of 8 months or more. These sampling procedures can be extensive, precise and intricate, and consequently present many opportunities for error, or be disturbed by many components.

2.4. Freezing process

Soil freezing occurs when the soil temperature drops below 0°C. However, water in soil does not freeze uniformly below 0°C. It freezes gradually over a range of temperature that depends on the heat capacity of the soil (H), the latent heat of freezing (L), the soil bulk density (ρ_{soil}) and the

volumetric ice content (θ_{ice}). Figure 5 provides the unfrozen water content change in function of temperature. The change in total heat is then balanced by the change in latent heat. Giving a ground thickness (z), the change in temperature (T), overtime (t), given a heat loss/input, (q_h) can be expressed by (Stähli, 2005):

$$\frac{\partial(HT)}{\partial t} = L\rho_{soil}\frac{\partial\theta_{ice}}{\partial t} + \frac{\partial}{\partial z}(-q_h) \quad (1)$$

From the heat transfer equation presented above, the soil freezes from the surface down until heat is reinserted or the system reaches equilibrium from underground sources of heat.

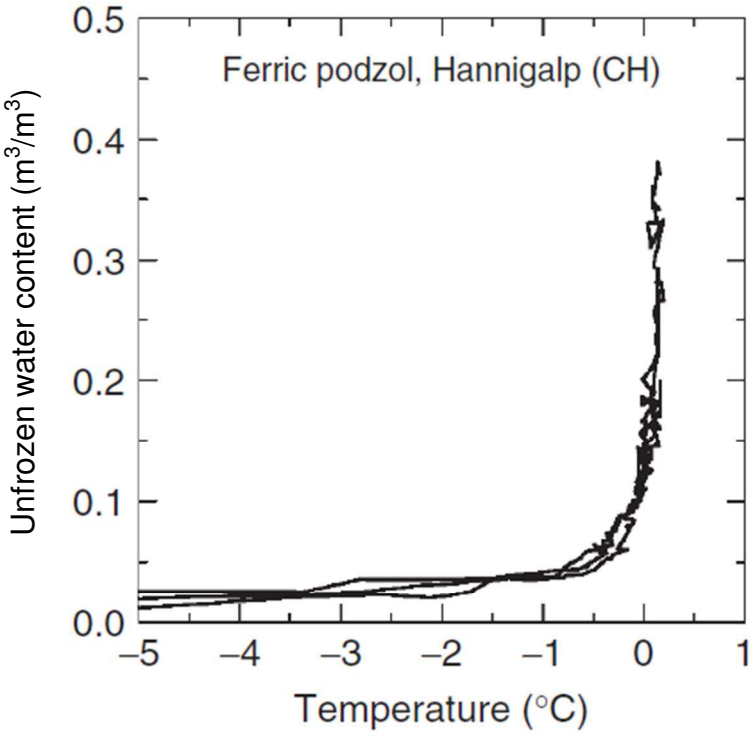

Figure 5: Soil freezing characteristic curve of sandy loam (from Stähli, 2005)

From available data, clays freezes at lower temperatures than sandy soils (Stähli, 2005). Even at a temperature below -5°C, a fraction of the water remains unfrozen due to thermodynamic principles described in the following section. Miller (1965) put forward the idea that the same state of moisture can be achieved by a freezing/thawing process as it is in a drying/wetting

process. The drying/wetting process is demonstrated for ice free soil on the soil water characteristic curve (SWC) and the freezing/thawing process on the soil freezing curve (SFC).

The SWC is in function of matric suction describe in equation (2) by ψ_{aw} as the difference in pore air pressure (u_a), and pore water pressure (u_w).

$$\psi_{aw} = u_a - u_w \quad (2)$$

The SFC is presented in function of the state of water ϕ_{iw} by equation (3) as the difference in pore ice pressure (u_i), and pore water pressure.

$$\psi_{iw} = u_i - u_w \quad (3)$$

Miller (1963) presented the idea that the data from a same soil at same densities and having experienced a similar history would directly relate ($\psi_{aw} = \psi_{iw}$) (Black & Tice, 1989, Stähli, 2005). The experiment of Koopmans and Miller (1966) supported this hypothesis when the same soil is used. The state of the water was calculated from the unfrozen water content using Equation (6), explained in the next section, from temperature values of the SFC. For colloidal soil, fine grained soils where water is affected by absorption space, the curve showed superimposed while for granular soil where capillary effect is important on water, a correction factor needed to be used to account for the difference in surface tension (y_{aw}, y_{iw}), Equation (4).

$$\psi_{aw} = (y_{aw}/y_{iw})\psi_{iw} \quad (4)$$

Many researchers have provided evidence supporting Miller's hypothesis (Koopmans and Miller (1966), Black & Tice(1989), Spaans and Baker (1996) by comparing the obtained SWC and SFC for various type of soil. Figure 6 shows the similarity of both curves by superimposing on the other.

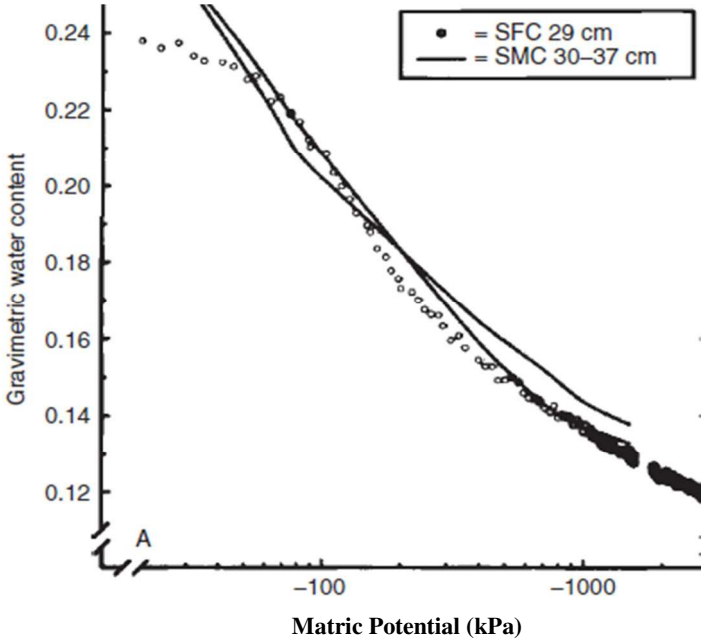

Figure 6: Similarity of the SWC and SFC for a laboratory tested silty loam (from Stähli, 2005)

2.5. Effect of pore water pressure

Frozen ground behavior under the increase of hydrostatic pressure is the result of a combination of mechanical and thermodynamic effects. The mechanical component governs the stress sharing and the thermodynamics governs the pressure melting phenomena.

If only mechanical effects are considered in a fully saturated soil is frozen (no unfrozen water phase) and exposed to hydrostatic pressure under undrained conditions, the pressure increase on the pore matrix can be represented by a modified Skempton's B value (B_f).

$$B_f = \frac{\Delta u_m}{\Delta \sigma}\left[1 + n\frac{\left(\frac{C_m}{C_s}\right) - 1}{\left(\frac{C}{C_s}\right) - 1}\right]^{-1} \quad (5)$$

Bishop presented this equation in 1973, where $\Delta\sigma$ is the increase in hydrostatic pressure, Δu_m is the resulting increase in the pore matrix stress, n is the porosity, C_m the compressibility of the

pore matrix, C_S the compressibility of the soil grains, and C the compressibility of the soil skeleton. For saturated dense sand, nearly all pressure is transferred to the pore matrix (Ladanyi 1985).

However, when considering a three-phase material such as frozen ground with unfrozen water, the pore water pressure increase may be much smaller. Wissa (1969) assumed that the ice would cement the soil grains which greatly reduce the compressibility of the soil skeleton. It was found that cement-stabilized sand would have a typical B value of 0.575 under hydrostatic pressure. The conclusion is that a sudden increase in pressure will stress the ice more than the unfrozen water. This increase in stress leads to thermodynamic consequences involving pressure melting phenomena.

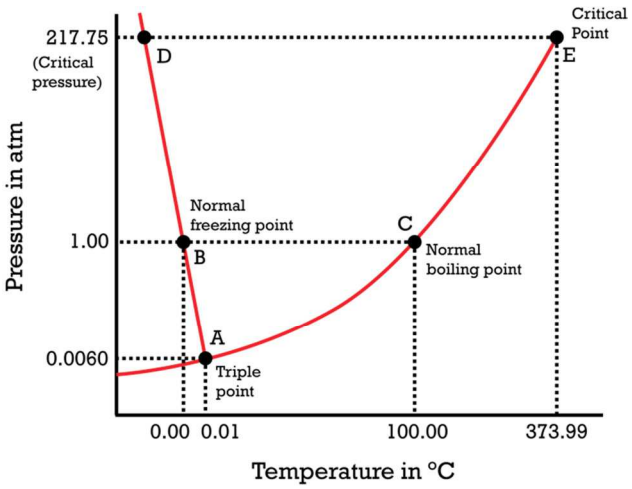

Figure 7: Water phase diagram (by: Christopher Auyeung)

The stress in a soil is highly concentrated at small contact points between the grains. In frozen soils this contact area will include a layer of ice between the particles. From the water phase diagram shown in Figure 7, water will not freeze at normal freezing temperature under high stress. The effect is even larger when minerals are dissolved in the water.

The pressure melting phenomenon happens when the stress is high enough and/or when the temperature changes during the test. If the stress path crosses between phases the ice will melt

and influence the pore water pressure. When the process is non-isothermal the relationship for ice and water coexisting is defined by Clausius-Clapeyron equation (Hillel, 1980)

$$\frac{du_W}{\gamma_W} - \frac{du_i}{\gamma_i} = \frac{LdT}{T} \quad (6)$$

where γ_w=1000 kg/m3 is the density of water, γ_i=916.8 kg/m^3 is the density of the ice, L=3.336x10^5 J/kg is the latent heat of water, dT=T_0-T is the difference between normal freezing temperature of pure water, T_0=273.15 K and the actual temperature, T, of the system. The equation becomes:

$$du_W = 1.091du_i + 1.221dT \quad (7)$$

It is important to note that *u* is in MPa and T in Kelvin. For the interface condition dp_w=dp_i=dp, which gives the freezing-point depression for ice (Andersland, 2004).

$$\frac{dT}{du} = -0.0743\ K/MPa \quad (8)$$

Meaning that a pressure of 13.5 MPa is needed to reduce the freezing point of water by 1°C. Under normal condition, if it was not for grain-to-grain contact area, there would be very little melting.

For an isothermal process, dT=0.

$$du_w = 1.091du_i \quad (9)$$

From which it can be concluded that pore-water pressure follows closely the pore ice pressure as long as there is no phase change.

This melting phenomenon is also a governing factor of frozen soil consolidation. Since the small ice-particle contact area can increase the local stress by a factor of 10 to 500 compared to the global normal pressure of the element, (Arteau, 1984) the local melting water must also migrate to dissipate pore water pressure adding time to the process. For example, frozen sand has a typical hydraulic gradient of approximately 10^{-13} m/s and a coefficient of consolidation of 10^{-8} m^2/s, which would require 7 months to consolidate a 100 mm long by 50 mm in diameter test specimen. The majority of the published triaxial test results should be classified as unconsolidated-undrained tests. An exception has to be made for specimens consolidated before freezing (Goodman, 1975).

2.6. Rheology of soil and ice mixture

Rheology is defined as "the study of the deformation and flow of matter" in terms of stress, strain, temperature and time (Arenson, 2015). The thermo-mechanical properties of frozen soil are highly influenced by all four criteria. Stress and strain relates to melting pressure; temperature modifies the amount of unfrozen water; and time is a major factor for creep, consolidation and strength.

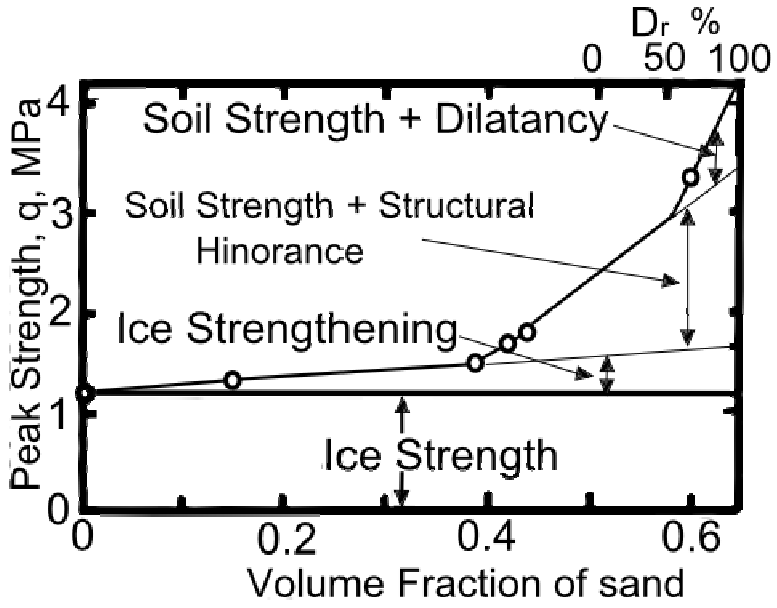

Figure 8: Failure mechanism map of unconfined compressive strength of frozen Ottawa sand at -7ºC and a constant strain rate of 4.4 x 10^{-4} s^{-1} (From Andersland, 2004)

Ladanyi (2003) concluded that the behavior of mixture depends on the characteristics of the constituting solid and liquid as well as their relative proportion in the mixture. Ting et al. (1983) summarized the work and concluded that the peak strength is governed by one of three criteria depending on the volume fraction of sand. Figure 8 shows the failure mechanism of frozen Ottawa sand at different sand volume fraction. Ting et al.'s concluded that up to a grain volume (Volume solids/Volume Total) fraction of 0.4, the behaviour is governed by the pore ice. For fraction greater than 0.4 the friction resistance between the particles intervenes; and for a ratio greater than 0.6, the dilatancy caused by interlocking of dense sand adds to shear strength.

Ladanyi (2003) approximated the results by this equation

$$q_{u,mix} = q_{u,ice}(1 + 14.1C^4) \qquad \text{For } 0<C<0.65 \qquad (10)$$

where C is the volume fraction of sand, and $q_{u,ice}$ is the shear strength of pure ice.

$$q_{u,mix} = q_{u,ice}(1 + 14.1C^4) \qquad \text{For } 0<C<0.65 \qquad (11)$$

However, when the amount of ice decreases the cohesion decreases and eventually the strength reverts to the one of dry soil. Figure 9 shows the effect of water content on compressive strength.

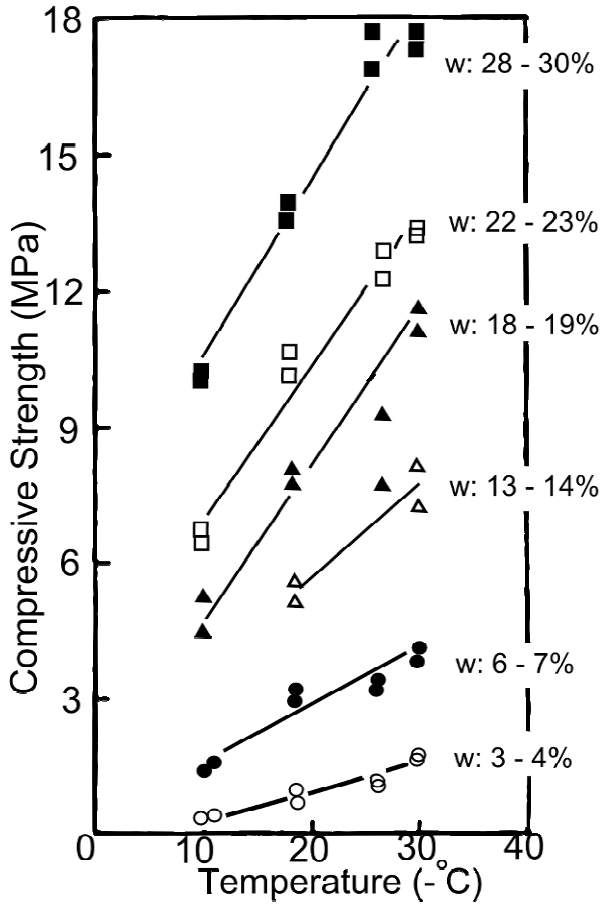

Figure 9: Relationship between uniaxial compressive strength of frozen sand with temperature at different water content. (Ladanyi, 2003)

Andersland & Ladanyi (1994) presented an empirical formula to account for this effect.

$$q_u(\text{kPa}) = 15.5w(\theta + 15°\text{C}) - 1373 \qquad (12)$$

Where q_u is the uniaxial compressive strength, w is the total water and ice content and θ=-T°C is the frozen temperature of the soil.

It was found that stress-strain behaviour of frozen soil is similar to the behaviour of ice. Gold (1970) presented the 4 responses shown in Figure 10 where ice is tested at small strain rates ($<10^{-5}$/s), response A, to higher rates ($>10^{-2}$/s), response D.

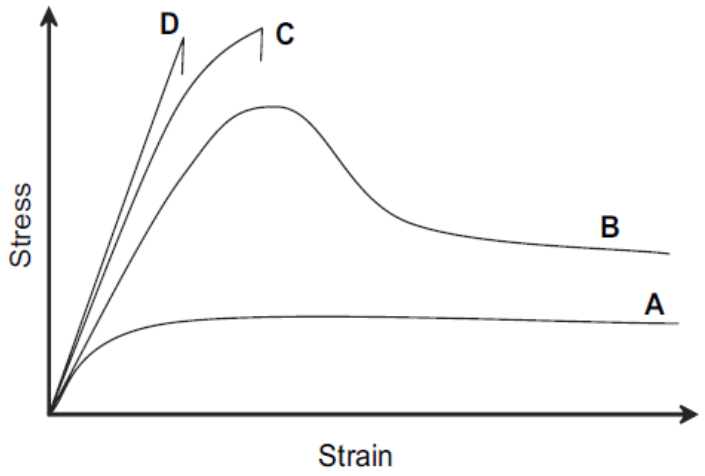

Figure 10: Stress-strain behavior of ice under different strain rate A) ductile behavior with strain hardening, B) dilatant behavior with strain softening, C) brittle behavior with failure after yield point, D) brittle failure (Arenson et al., 2007)

However, the stress-strain response of a frozen soil is not only dependant on strain rate but also depends on volumetric ice content as shown previously. Figure 11 demonstrates the response of frozen soil to both the volumetric ice content and strain rate (Arenson & Springman, 2005).

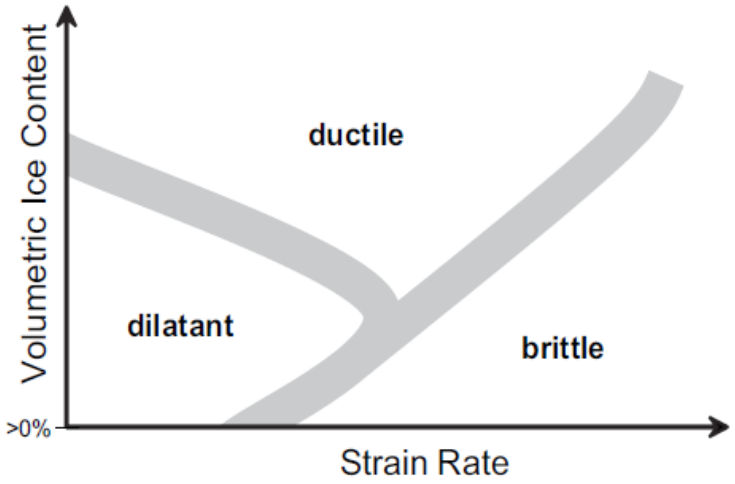

Figure 11: Stress response of frozen ground as a function of strain rate and volumetric ice content (Arenson et al., 2007)

An increase in the testing strain rate will influence the strength measured as well as the response of the frozen sample. A low ice content soil shows a dilatant response and a high ice content soil as a ductile response. As described by Gold (1970) and Arenson et al. (2007) a soil with high volumetric water content will respond like pure ice.

2.7. Frost Heaving

Expansion is associated with soil freezing. It is well known that freezing water will expand by 9%+. However, this 9%+ expansion doesn't lead to a 9%+ increase in the volume of voids of the soil. This happens as the water is being expelled from the soil during the freezing process. is due to the water being expelled in the process.

For silty soils, the freezing process depends on the rate at which the temperature decreases (or drops). When the freezing rate of a saturated specimen is large, the water freezes in place. If the temperature is gradually lowered, the ice tends to accumulate in layers of clear ice parallel to the surface exposed to the freezing temperature. As a result, frozen silty soils consist of layered ice and soil (Andersland, 2004). For this to occur, water must migrate through the ground. The thickness of the layers of ice depends on the freezing rate and the availability of water to the freezing front. Figure 12(a) shows a closed system where there is no excess water available, Figure 12(b) shows a system where there is excess water migrating towards the freezing front and Figure 12(c) shows a system where a layer of permeable soil is blocking the water to travel up to the freezing front.

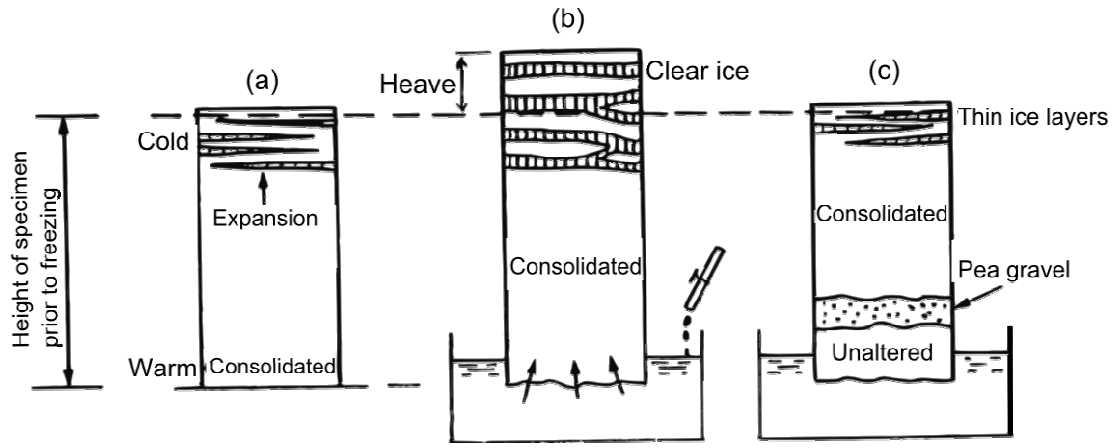

Figure 12: Ice formation in soils: (a) closed system (b) open system (c) drainage layer (from Andersland, 2004)

For in-situ freezing conditions in fine grain soils, the water would migrate from the water table (free water layer) by capillary effect. The distance between the freezing front and the water table has to be smaller than the height of the capillary rise of the soil. The maximum rise (h_c) can be approximated by the relationship:

$$h_c(m) = \frac{0.03}{d(mm)} \qquad (13)$$

Where *d* is taken as 20% of D_{10}.

Since the water table is continuously replenished, ice lenses can, in theory, continuously grow. While growing, the ground above the ice layers rises. This is called frost heave, and a heave of 150 mm is not uncommon in regions that experience moderate winters (Andersland, 2004). Since frost heave is dependent on the underlying soil profile, a coarse soil situated between the water table and the freezing front, will negate the capillary effect and the upper zone is considered a closed system (Figure 12 (c)).

The stress exerted from frost heave can commonly reach over 2000 kPa (Domaschuk, 1982), giving important force to the effect of this uplift on both shallow and deep foundations. For region susceptible to frost heave, on clay and silt consolidated deposits, foundations are installed

under the maximum frost front. However, for deep pile foundations the frost heave forces are exerted directly to the structural member through the increase skin friction of adfreeze bond.

The frost heave is usually non-uniform since the permeability and shear strength of each frozen ground is highly dependent on temperature change, permeability and water content/availability. And so, highway structures constructed on frost sensitive soils will experience increase in roughness and bumps. When the warmer temperature of spring thaws inter-particle ice and ice layers, the soil becomes over saturated by water. Since the frost thaws from the top down, the additional water will not drain until the underlying frozen soil thaws. During this time the soil is mushy and loses most of its bearing capacity which can severely impair the pavement (Andersland, 2004). This also gives reason to the half load condition implemented in the spring.

2.8. Adfreeze

The interface between the pile and the soil under frozen condition is commonly call adfreeze. It has also been designated as adfreeze strength (Weaver and Morgenstern, 1981), adfreeze bond and frozen pile-soil interface (Parameswaran, 1978) in the literature. It represents the bond created along the surface of the pile when freezing. It has two components, adhesion due to ice and friction due to soil grains.

Literature shows the major factors influencing adfreeze as being: ice content (Weaver and Morgenstern, 1981), temperature (McRoberts and Nixon, 1976) and pile material (Phukan, 1978).

Data on adfreeze is important when it comes to calculating bearing capacity. This data has been measured since the 1930's, which most of it has been derived from tests carried in the field on undisturbed soils. (Parameswaran, 1978; Tsytovich, 1975; Vyalov, 1965). Several empirical techniques were developed from this information.

In general, the condition presented in Equation (14) must be met for a pile installed in frozen ground condition to support the loads.

$$P + \tau_f A_f + \tau_d A_d > D_L - \tau_h A_h \quad (14)$$

The condition requires the design load (D_L) and the effect of frost heave stress (τ_h) through the pile contact area (A_h) are counteracted by the pile end bearing capacity (P), the adfreeze strength of the pile-soil interface(τ_f), pile-frozen soil interface (A_f), friction stress between the pile and unfrozen layer of saoil (τ_d) and the pile-soil interface of that layer (A_d).

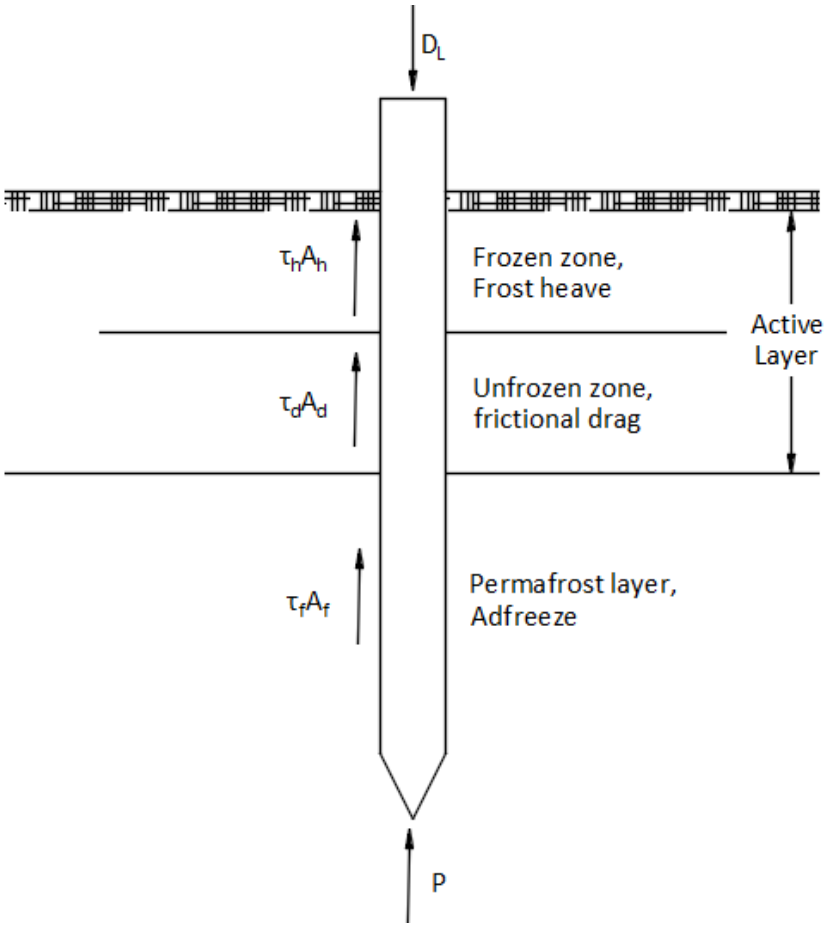

Figure 13: Pile foundations bearing capacity schematic in permafrost (from Parameswaran, 1978)

Adfreeze bearing capacity ($\tau_f A_f$) is determined at the ultimate point of rupture of the bond. Literature shows a brittle rupture (high peak) and a small residual resistance curve after failure. Some typical curves for different pile material are presented in Figure 14.

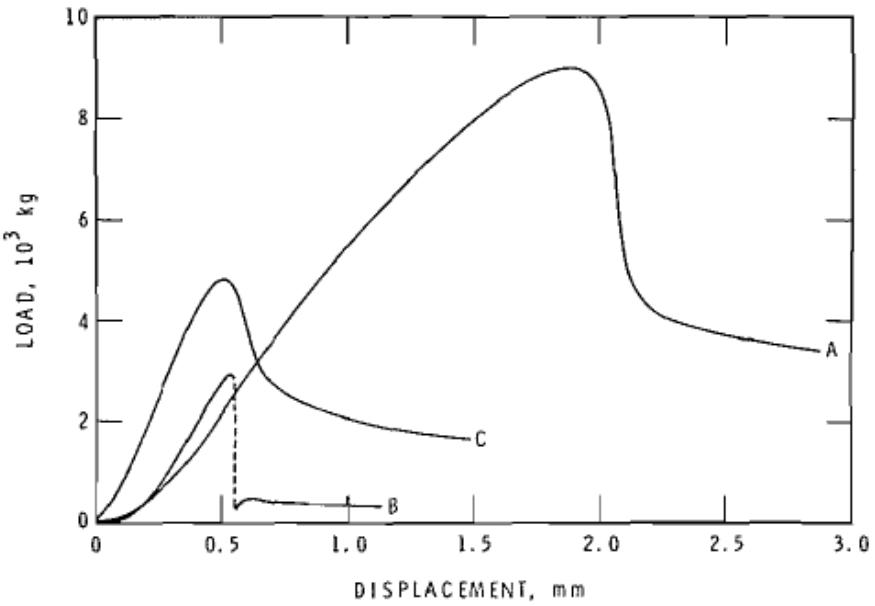

Figure 14: Adfreeze load-displacement curves for piles in frozen sand: (A) untreated B.C. fir, (B) painted steel and (C) concrete (from Parameswaran,1978)

2.9.Ground freezing applications

Typical application of frozen ground includes access shafts, deep excavations, tunnels, ground water control, containment of hazardous waste and a variety of special projects. Some applications require freezing the ground. It is possible to create artificial frozen soils by installing refrigeration pipes which cool the soil by circulating a cooling fluid in an inner tube within the soil mass to be frozen and returning it in an outside space between two tubes (Figure 15). This technology is frequently used to support excavations and block water flow (Figure 16).

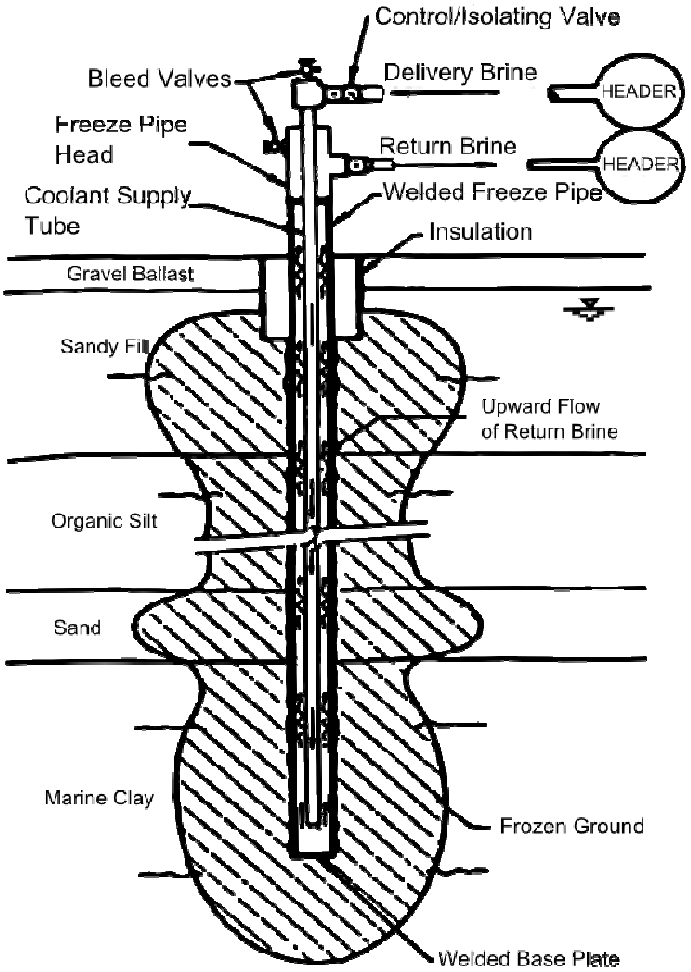

Figure 15: Ground freezing tube (freeze pile) (Andersland, 2004)

The high strength, the stability and very low permeability of frozen grounds are the advantages that engineers can exploit in their designs. The use of freezing tubes allows freezing of the ground in any geometry. Figure 17 shows the use of these systems for tunnel and shaft excavation. They can also be used to create impermeable walls to control water seepage and contaminant transport.

Figure 16: Ground freezing tubes used to excavate (a) tunnel (Frank Coluccio Construction, 1996) and (b) shaft (BDF, 2009)

Ground freezing is also used to obtain undisturbed cohesionless soil specimens. It is complicated to obtain undisturbed samples of sand and gravel due to their lack of cohesion, which prevents the soil from keeping its shape in a sampling tube. If properly frozen the sample should not be altered by heaving. Studies have shown that if the confining pressure is maintained and drainage is not prevented during freezing, the volume change is negligible and soil strength is not altered upon thawing (Marcuson, 1979). To accomplish such conditions, the soil needs to be frozen at a slow rate and be provided with a free draining boundary on the unfrozen side. Samples can then be taken by core drilling and thawed after confining pressure has been reapplied.

This technology can also be applied to pile foundations to ensure proper freeze bonds and bearing capacity. However, structures commonly built on permafrost will be done so on shallow foundations and on a non-frost susceptible soil pad with the ends of the pipe ducts exposed to air. The ducts are open in the fall to let cold air freeze and closed during summer to limit heat transfer. This method has proved efficient, inexpensive and easy to use.

Figure 17: Duct-Ventilated fill foundation (ZHDC,2011)

2.10. Adfreeze testing by push through

This method used by Parameswaran (1978) to facilitate constant rate testing for various pile material also allows testing for different pile type, shape and size. The procedure uses a large plexiglass box (304.8 x 304.8 x 304.8 mm) (B) on an aluminum base (D). The base has a centre orifice allowing the test pile to be push through. A temporary plug (C) allows the installation of the pile and soil sample without leak. A schematic of the setup can be seen in Figure 18.

Once the pile is installed and the soil is compacted and saturated, the box is placed in a cold room to freeze. The soil temperature is monitored by a thermistor (T) placed during the compaction procedure. After freezing, the sample is lifted and installed on four legs (F) placed on the testing machine, situated in the cold room. The plug (C) is removed and direct-current differential transducers (DCDT) are positioned on the pile, to measure its displacement while a ram (E) pushes down at a constant rate.

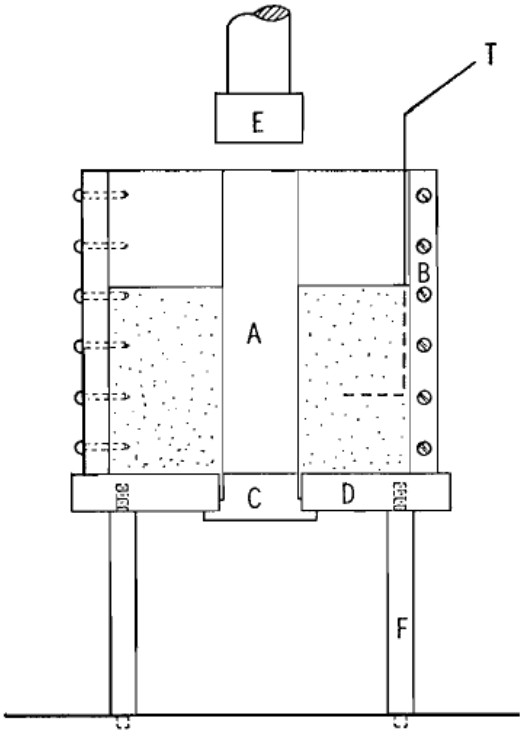

Figure 18: Schematic diagram of push through testing apparatus (Parameswaran, 1978)

The results of this study showed that two determinant factors, the type of material and roughness of the pile, influenced its response. The different type of material and response obtained are shown in Figure 14. Rougher and untreated surfaces show a more ductile response while smoother surfaces and treated surfaces show a more fragile and brittle behaviour.

The study also showed the effect shear rate has on the measured adfreeze strength. Table 1 shows the peak adfreeze strength measured under different shear rate. It was also found that the adfreeze strength (τ_f) follows the same power-law form as frozen soil deformation under compression and shear which is represented by:

$$\tau_f \sim \acute{I}^m \qquad (15)$$

where $\acute{I}$ is the shear rate and m is a material constant.

Fragile failure indicating clean quick shearing of the interface bond was noted for all material types at higher shear rates and not only for smoother/finer particle with lower coefficient of friction. No testing was conducted to observe the effect of ice-poor frozen soil in the study.

Table 1: Values for peak adfreeze strength for various pile type under constant shear rate (Parameswaran, 1978)

Cross-Head speed (Í) ($mm \cdot min^{-1}$)	Adfreeze strength (τ_f), MPa						
	B.C. fir	Concrete	Painted Steel	Creosoted B.C fir	Spruce	Unpainted steel	Steel H-Section
0.0005	1.14	0.525	0.497	0.403	0.96	0.527	0.64
0.001	1.175	0.553	0.496	0.487	0.863	0.76	0.513
	1.29					0.609	
0.002	1.113	0.671	0.648	0.69	1.122	0.68	0.648
	1.247			0.505			
0.005	1.61	0.733	0.677	0.72	1.196	0.806	0.691
0.01	1.56	0.866	0.679	0.813	1.167	0.734	0.695
		0.94				0.745	
0.02	1.936	1.16	0.973	0.92	1.461	0.868	0.854
0.05	2.231	1.293	1.026	0.875	1.29	1.181	0.852
					1.506		
0.01	2.42	1.611	1.146	1.22	1.542	1.364	0.983
						0.704	

The same set up was later used to test adfreeze strength of pure ice and saline ice water on piles for pier and bridge application (Parameswaran, 1980).

2.11. Adfreeze testing by interface shearing

Interface shearing was used by Ladanyi and Thériault (1990) to measure adfreeze strength and observe the relationship to shear strength of the soil and the healing process of adfreeze under creep loads.

A double shear apparatus was developed by Thériault (1988) which consist of 3 shear boxes mounted on a standard shear-rate-controlled testing frame, Figure 20. The apparatus was positioned in a cold room set at -2 ± 1°C. To maintain a better control on the temperature of the sample, antifreeze fluid was circulated around the sample. This system was controlled by a thermistor placed in the shear box. This allowed monitoring the temperature and controlling the bath circulation system. The variation of temperature could then be kept below 0.1°C.

The test series included direct shear tests with sand and silt, interface shear with both soil and steel and aluminum, and bond healing test between both soil and frozen sand or steel. All tests were conducted at a shear rate of approximately 16.9 mm/day (0.012 mm/min).

Adfreeze bond healing is the process under which adfreeze strength is recuperated over time under in-situ stress or normally applied load in laboratory.

The results of the study made on air free samples showed that the adfreeze bond is essentially brittle (as shown by Parameswaran, 1978). Ladanyi and Thériault (1990) presented another observation, the residual strength representing a small fraction of the peak strength after the brittle failure but increases with confining load as presented in Figure 19.

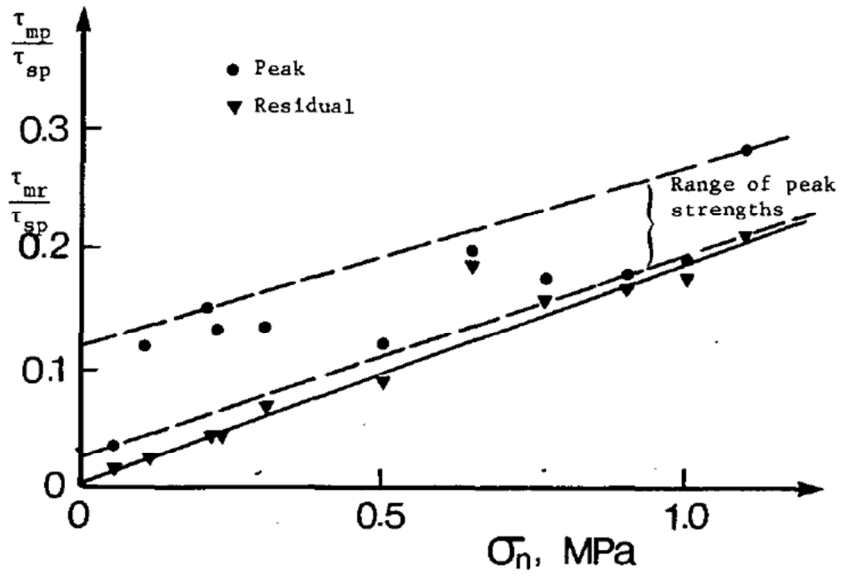

Figure 19: Adfreeze bond of frozen sand against steel express in function of shear strength of the frozen sand (T=-2 °C) (Ladanyi & Thériault, 1990)

As for the healing process, the adfreeze strength may only be fully recovered under relatively high normal pressure in the order of 500 kPa. For lower normal stress the bond may only partially heal. For fine soils like silt where the relative content of unfrozen water is higher, the healing process was more pronounced. However, for sands, it was found that a very minimum healing process occurred, showing that the process is favorized by the unfrozen water content and the ability for that water to travel in the soil (Ladanyi & Thériault, 1990). For the tested silt, the unfrozen water content was found to be 14% higher than in the tested sand.

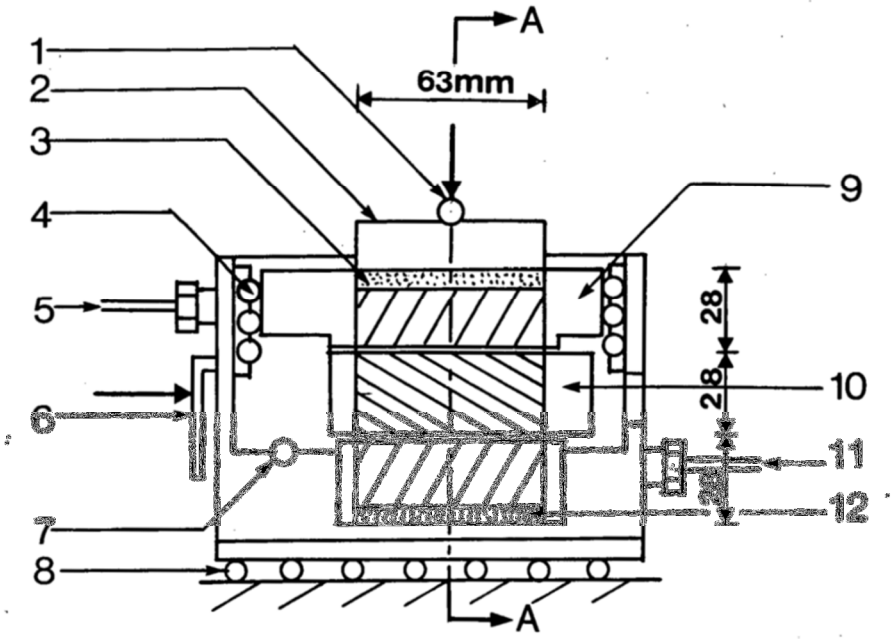

Figure 20: Longitudinal cross-section of the double shear apparatus: 1. Vertical load application; 2. Loading platen; 3. Porous stone; 4. Cylindrical bearings; 5. Antifreeze out; 6. Horizontal load application; 7. Thermistor; 8. Ball bearing; 9. Upper shear ring; 10. Central shear ring; 11. Antifreeze in; 12. Lower shear ring (from Ladanyi and Thériault,1990)

The study was not able to fully answer its purpose and it was suggested that larger scale testing and observation would be needed to fully answer the concerns of adfreeze bond.

2.12. Adfreeze relation to shear strength

A considerable bank of data on adfreeze strength has been published over time. Weaver and Morgenstern (1981) analysed the available data and related the long-term shear strength to the adfreeze bond strength.

It was concluded that the relationship between the long term unconfined compressive strength and the measured adfreeze bond strength can be represented by a coefficient relationship.

$$\tau_{lf} = ms_{lt} \quad (16)$$

where τ_{fl} is the long term adfreeze, s_{lt} is the long-term shear strength of the soil and *m* is the material coefficient. Table 2 shows the proposed coefficient put forward by Weaver and Morgentstern (1981).

Table 2: Shear to adfreeze bond coefficient presented by Weaver and Morgenstern (1981)

Pile type	m
Steel	0.6
Concrete	0.6
Timber (uncreosoted)	0.7
Corrugated steel pipe	1

Ladanyi and Thériault (1990) later showed that the value of *m* is also dependent on the normal stress applied to the soil even if that assumption was considered negligible by Weaver and Morgenstern (1981). Showing that the long-term pile capacity was not only dependent on long-term adfreeze, but also depended on the residual friction angle at the interface and by correlation, total ground lateral pressure (Aldaeef & Rayhani, 2018). Ladanyi and Thériault (1990) ameliorated the equation by adding the contribution of the residual friction angle and presented the following equation:

$$\tau_{lf} = ms_{lt} + \rho_{h,tot} tan\phi_{res} \quad (17)$$

where $\rho_{h,tot}$ is the total lateral earth pressure and Φ_{res} is the residual angle of friction.

2.13. Conclusion and direction

The available literature showed limited knowledge of frozen ground. Most practical applications involving frozen ground relies on past experiences and field data only. The science behind the process and effect of freezing has been studied and developed, however no major link to practical field applications have been made.

When it comes to adfreeze strength and testing, useful practical data has been obtained from full scale field test. Those tests are mostly only conducted for a specific project and can be difficult, or impossible to generalize due to outside uncontrollable parameters such as temperature variation, climate and soil history (Andersland, 2004).

Laboratory test data is limited since it requires special facilities (freezer chambers) and engineering practitioners often don't see the need to test soils which in most cases are known to perform well. Since Weaver and Morgenstern (1981) presented a relationship between shear strength and adfreeze, it provided a quick and conservative way to account for the effect of adfreeze.

The available adfreeze data from literature generally considers the phenomenon under air free conditions and little is known about the effect of variable water content. This study will consider only ice poor soil and observe the effect of modifying the water content of the specimens before freezing.

Another discrepancy from the available research is the incompatible results obtained by different testing methods. Even when testing similar soils, the push through method used by Parameswaran (1978, 1980) and the interface shear method developed by Thériault (1980, 1990) show a significant difference. This study will analyse two different methods of testing and discuss the test results from the test series and from literature.

Chapter 3. Model pile pull-out test

3.1. Introduction

This chapter presents and provides the details of the first series of test conducted in this study to measure adfreeze shaft resistance. Adfreeze strength was measured by pulling out the model pile installed in frozen sand. The nature of the pull-out test allowed measuring only skin friction developed at the soil-pile interface by measuring the force applied and the responding displacement.

The objective of this phase of the study was to measure the effect of embedment depth and ice content on adfreeze bond strength. The soil and part of the equipment used was provided by a consultant interested in studying the adfreeze bond of typical eastern Ontario sand on piles used to install solar panel arrays.

Freezing was achieved using outdoor temperature during the winter and in a modified freezer during the warm seasons. Temperature was monitored using commercial USB thermistor compatible with a Raspberry Pi computer. The key details of the equipment used during the test program are described in this chapter. The chapter also summarize the results of the program.

3.2. Pull-out apparatus

The University of Ottawa structure laboratory is equipped with a Galdabini Sun 60 material testing machine. This testing apparatus is equipped with a 750 000 N load cell able to test in tension and compression. It has a 625 mm wide testing space between the load arms and a head clearance of approximately 900 mm to permit safe testing. Figure 21shows the machine with the installed testing setup.

Figure 21: Galdabini Sun 60 set up with frozen soil test box

The samples were installed in a heavy steel box 600 mm by 600 mm by 600 mm. The interior volume of the boxes were able to accommodate 534 mm x 534 mm x 572 mm (l,w,h) specimens. The boxes were completely sealed, impermeable, and insulated using removable foam panels on all faces. Shop drawings are available in Appendix C.

The Galdabini Sun 60 is equipped with linear potentiometer transducer (LPT) connected through built-in serial ports. LPT measure the movement of a slider short circuiting over a potentiometer, the movement of the sliders modifies the resistance of the circuit. The change in resistance is calibrated to the movement of the arm, see Figure 22.

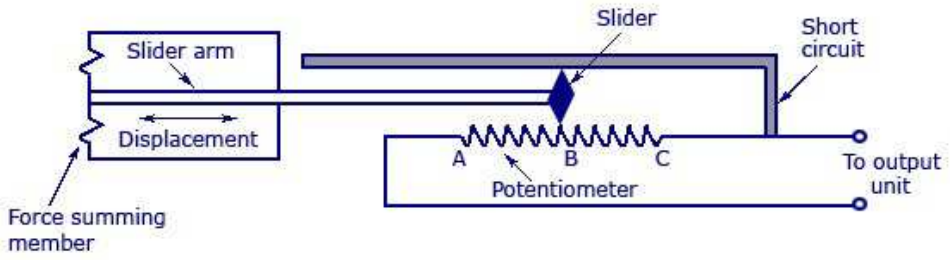

Figure 22: Linear potentiometer schematic (http://www.instrumentationtoday.com)

The machine is also able to register self-movement of the loading arm. To avoid any slack in the system to be registered in the displacement, the LPT was used and internal displacement measurements were ignored. The LPT was fixed directly to the pile and measured displacement from the box edges, Figure 27.

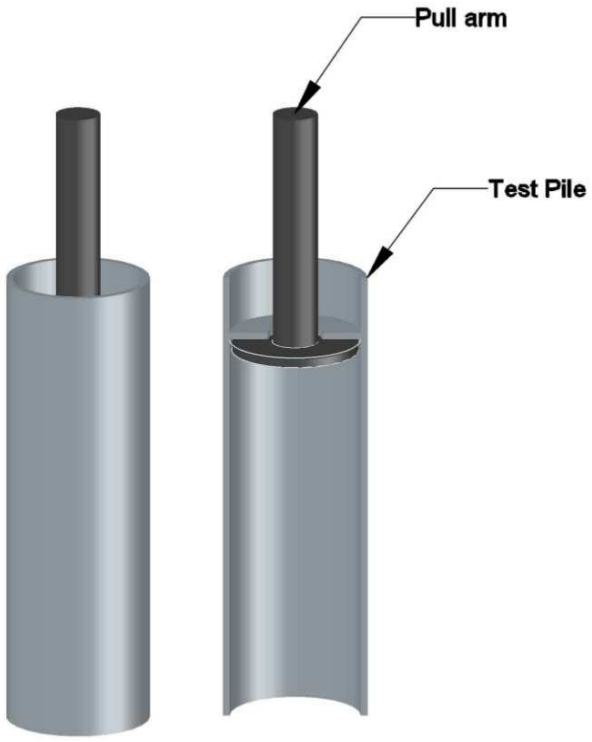

Figure 23: Pile pull arm attachment set up full view (left), cut view (right)

The boxes were fixed to the machine by first installing a heavy 25 mm thick plate to the testing table using four large machine bolts. The box was installed on the plate using a fork lift and attached to the plate using eight grade 10 bolts around the perimeter HSS frame of the box. The testing arm was then able to clamp on the pulling bar installed on top of the pile, Figure 23.

The piles provided for the program where galvanized HSS 114.3 x 8.6 lightly corrugated. Roughness measurements are available in Chapter 4, Table 5: Roughness measurement of tested pile and various galvanized steel plates and sheeting.

Each testing pile was outfitted with a steel plate welded directly into the hollow core. A hole was drilled in the plate to insert a puling bar. The bars were approximately 19 mm in diameter. Another plate was welded at one end of the rod. When inserted in the pile the two plates would transfer the load to the pile. Figure 23 shows the pile attachment. More drawings are available in appendix C describing the box and attachment to the testing machine.

3.3. Tested soil properties

The soil provided for testing was taken from a potential solar panel field located in proximity to Cornwall, Ontario (Canada). The soil composed the surface layer of the site. The received soil had an average gravimetric moisture content of 12%. A series of standard test was conducted to classify the soil.

The results of a sieve analysis are presented in Figure 24 and the results for the coefficient of uniformity (C_u) and the coefficient of curvature (C_c) are presented in Table 3. According the unified soil classification system (USCS) the soil can be classified as well graded sand (SW).

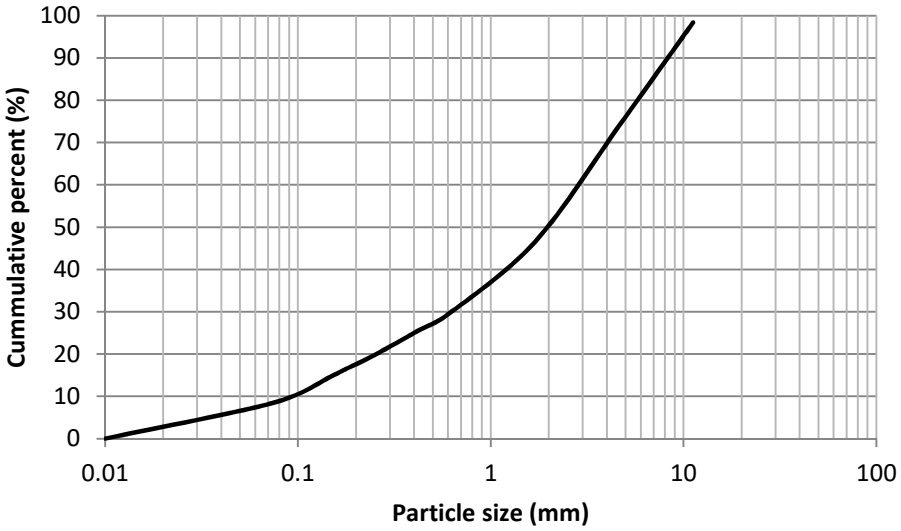

Figure 24: Cornwall sand Grain size distribution

Table 3: Soil grading coefficients

Parameters	
D_{10} (mm)	0.086
D_{30} (mm)	0.570
D_{60} (mm)	2.010
C_U	23.37
C_C	1.88

Due to the natures of both testing method studied a standard Proctor compaction test (ASTM D698) as well as static compaction test were conducted. As described below in this chapter, a drop hammer was used to compact and prepare the sample for the model pile pull-out program and static compaction was used to compact the smaller samples for interface sample, Chapter 4.

The static compaction tests were conducted to establish the best static load that will approach the Proctor results. The loads of 750 kPa and 1125 kPa were tested and plotted on the same graph as the Proctor results, Figure 25. The curves show that a static compaction of 1000 kPa will provide the best approximation to the Proctor compaction curve (Catana, 2006). The maximum dry

density and optimum water content from the Proctor test was 2026 kg/m^3 and 11.6 % respectively.

A standard specific gravity test (ASTM D7263) provided a value of 2.65.

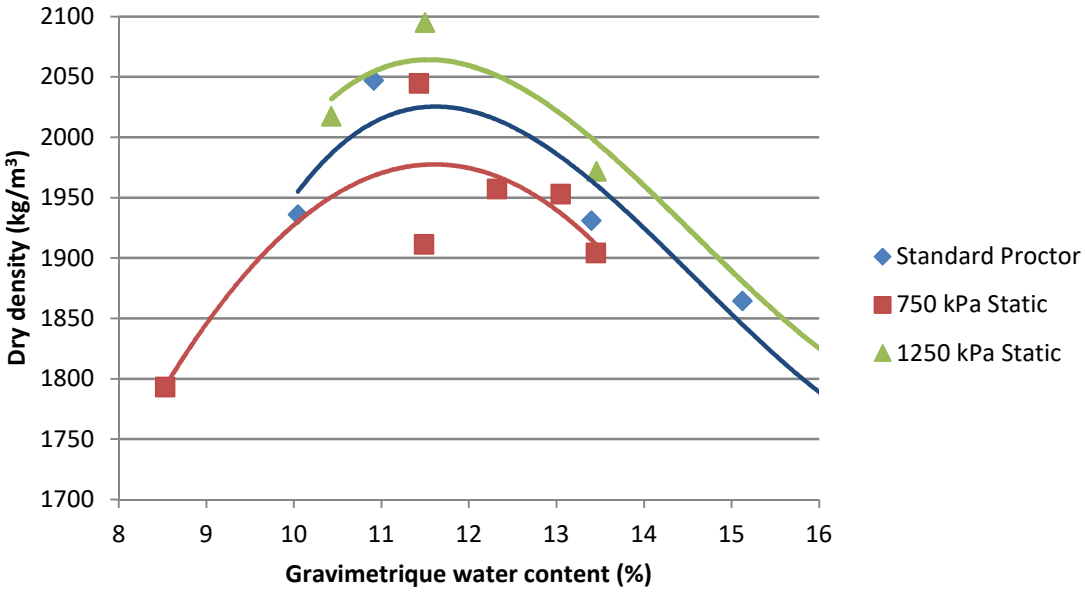

Figure 25: Proctor and static compaction curve

3.4.Sample preparation

The empty steel box was first filled with a 50 mm thick compacted layer of the same soil to be tested. The purpose of this bottom layer is to avoid any steel on steel bond to be created or ice accumulation bonding the bottom of the pile. This step was added following the first test conducted at full depth of the box. The pile was then inserted, centred and levelled using four temporary wooden struts.

The maximum embedment depth that the setup allowed to test was 572 mm, however at that depth the pile was resting on the metal bottom of the box and the forces damaged part of the equipment. The tests were then conducted avoiding metal on metal contact and at depth starting at 521 mm with the exception of a test at 533 mm which rested directly on the bottom of the test box.

The sand was then mixed with water to achieve predetermined water content and compacted in lifts of 50 mm with a custom drop hammer to approach the proctor curve as much as possible. The process was repeated until the desired sand thickness was achieved. The struts were removed when the sand could support the pile. Density was measured after the test was completed to avoid disturbance. The standard test method for density and unit weight of soil in place by the rubber balloon method (ASTM D2167) was used to obtain the average density of the sample.

Temperature could be monitored in real time using waterproof USB DS18B20 thermistor by Adafruit. The sensors have an accuracy of ±0.5 °C from -10 °C to 85 °C.

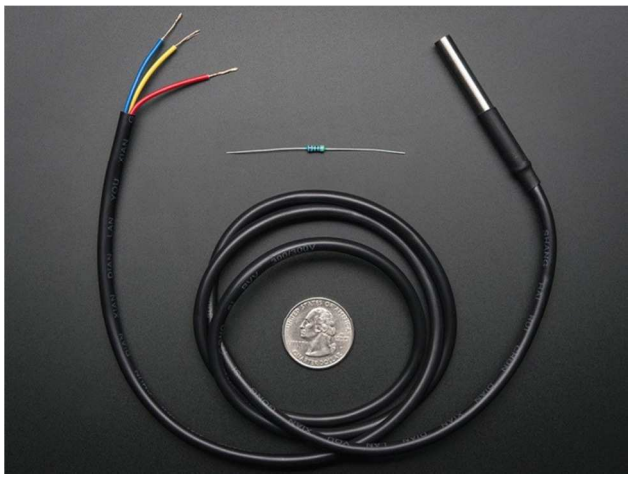

Figure 26: Waterproof DS18B20 Digital temperature sensor (Adafruit)

Three USB thermistors were inserted between the centre lifts 25 mm from the pile, in the center of the pile and the box's wall and 25 mm from the wall. A fourth sensor was inserted in the center of the pile and the box's wall before the last lift. Those thermistors allowed real-time monitoring of the sample temperature during testing.

The samples were frozen in an extended upright household freezer during summer and outside during winter time. The temperature inside the freezer reached -8 °C. Exterior temperature during January and February 2015 was on average -22 °C. The sample was tested while internal temperature was lower than -5 °C.

3.5. Test Settings

The test setup required a minimum of five days to freeze uniformly. The test box was moved and lifted using a fork lift. It was slowly installed and fix to the testing table to avoid disturbing the sample. Foam insulation panels are attached around the box to minimize heat exchange with the surroundings. The LPT is installed with a holding arm and bolted through a threaded hole on top of the pile, Figure 27. The USB thermistors are connected to a Raspberry PI computer used to take readings during testing. A wireless interface (SSH) to the Raspberry PI allowed the data to be transferred for analysis.

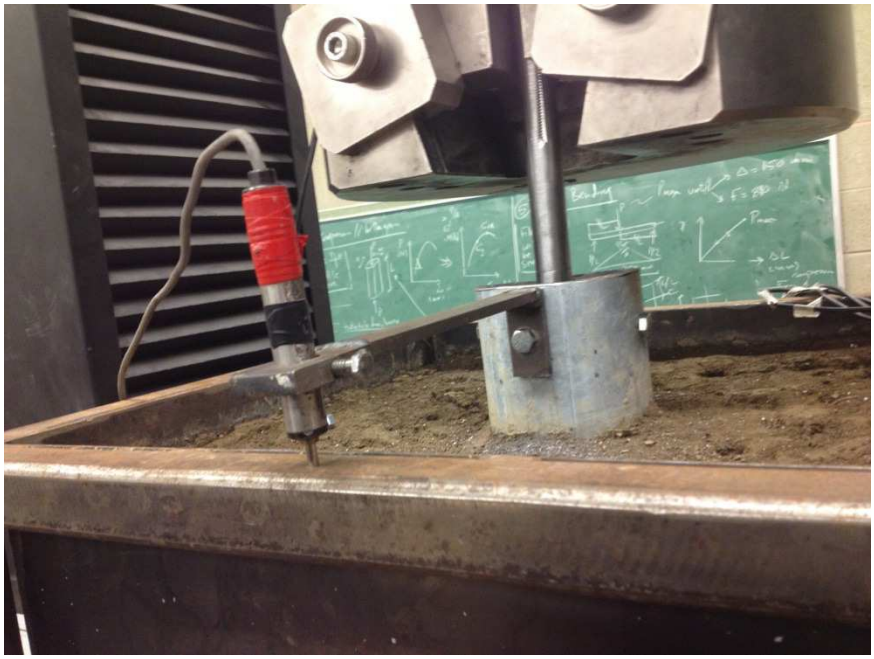

Figure 27: Attachment and LPT set up to the model pile

The Galdabini Sun 60 was set to pull at a rate of 0.1 mm/min, the slowest the equipment can be set to keep the data file small enough to be analyzed. The tests were estimated to take 30 to 40 min which would create 36000 to 48000 data points. The testing machine recorded time, displacement and force.

3.6. Test results

Individual force vs displacement (p-δ) results can be found in appendix A. During testing it was found that the bond was very fragile and could easily be broken. Some of the tests were disturbed during installation and the maximum bond was then lost, only residual strength could then be tested. The following, Table 4, provides a summary of all the samples tested and if the results were used in the study. The reason samples were ignored can be found on individual test results in the appendix.

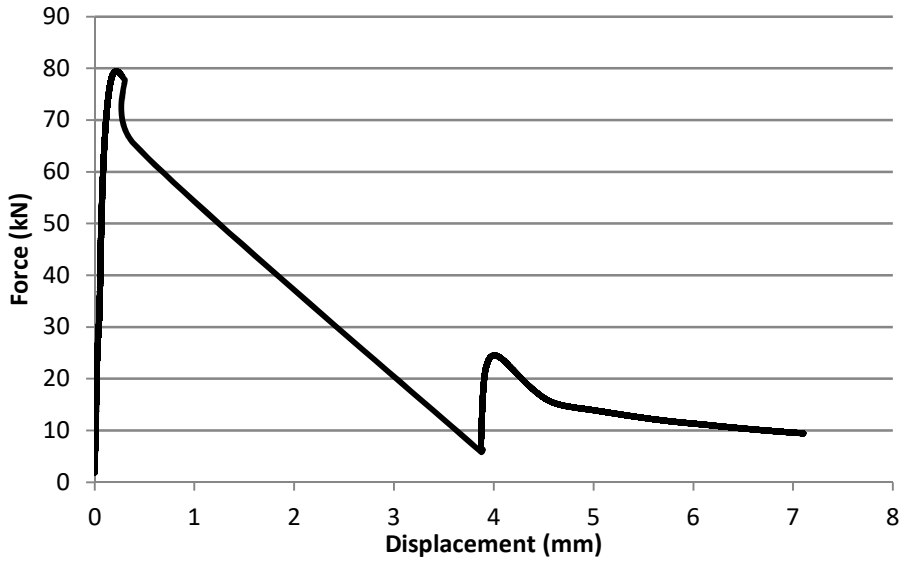

Figure 28: Typical force-displacement curve results

The samples had a high maximum strength which was very brittle. Residual strength was taken as the second peak.

Table 4: Pull-out test summary

Test Name	Embedded depth (mm)	Maximum strength (kPa)	Residual strength (kPa)	Water Content (%)	Dry Density (Kg/m3)	Relative Density (%)	Used/ignored
Pull out 1	533.4	553.4	N/A	17.1	N/A	N/A	Ignored
Pull out 3	533.4	N/A	218.5	13.1	N/A	N/A	Residual Only
Pull out 4	520.7	635.4	N/A	14.1	N/A	N/A	Used
Pull out 5	428.62	N/A	N/A	13.7	2087.8	102.3	Ignored
Pull out 6	419.1	623.6	222.0	12.9	1943.6	95.3	Used
Pull out 7	427.8	517.2	159.6	11.6	1662.3	81.5	Used
Pull out 8	406.4	N/A	186.0	8.8	1912.6	93.8	Residual Only
Pull out 9	406.4	497.2	129.0	10.3	1621.3	79.5	Used
Pull out 10	406.4	255.5	69.3	7.7	2102.8	103.1	Ignored
Pull out 11	406	519.0	146.4	9.5	1797.2	88.1	Used
Pull out 12	304.8	281.7	95.4	8.3	1904.6	93.4	Ignored
Pull out 13	304.8	318.1	99.5	9.9	1904.9	93.4	Used
Pull out 14	301.6	386.1	117.2	8.9	1695.0	83.1	Used

To verify soil compaction a compaction curve was compared to the standard proctor test. The dry density on the sample was found using a field balloon test at four different positions (ASTM D2167 – 15). The first test was taken 25 mm under the surface and the others at intervals of 50 to 100 mm depending on total embedment length. The curve obtained from the average densities within the testing box is comparable to the standard proctor tests as presented in Figure 29.

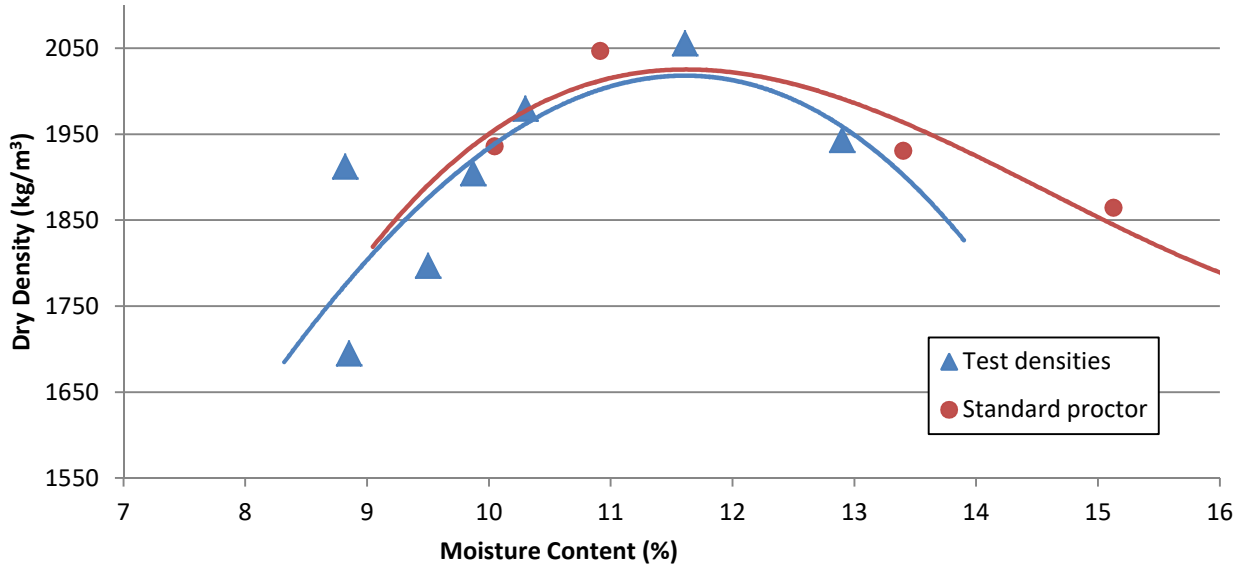

Figure 29: Proctor vs tested dry densities

To observe the effect that moisture content (w(%)), depth (mm) and density (kg/m3) have on the adfreeze strength, each were plotted on different graphs separating peak and residual strength.

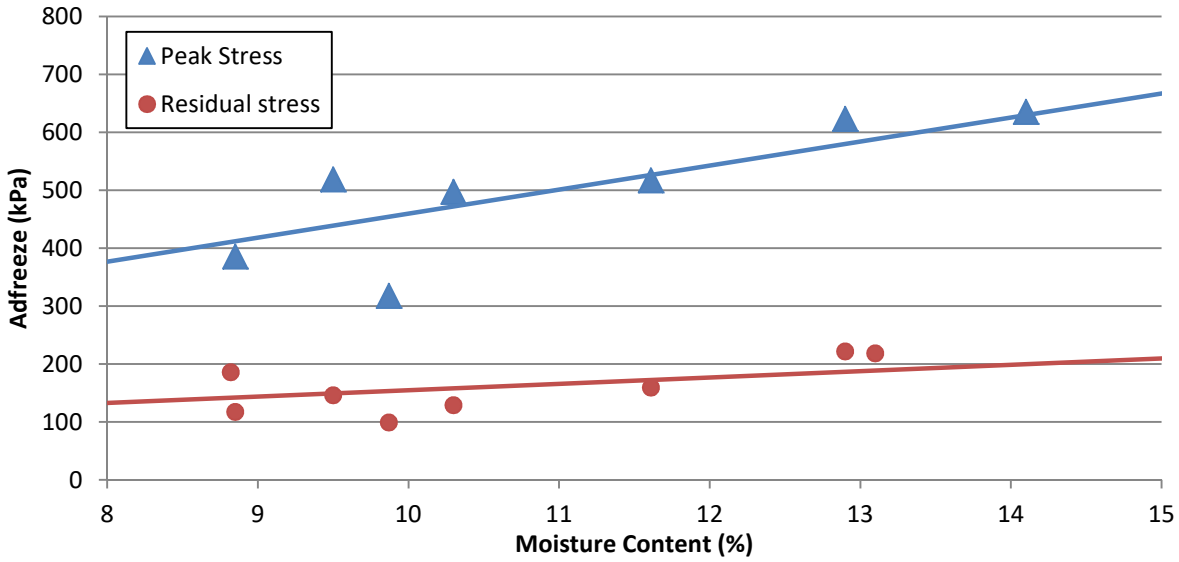

Figure 30: Adfreeze Strength in Function of Moisture Content

The moisture content, even more importantly the fraction of unfrozen water in soil, is known to influence the strength of frozen soil (Yong, 1962). The shear strength of frozen soil can both be

reduced and increased by raising the water content of the soil. The strength increases until the soil is saturated once the saturation content is passed the sample will then lose strength by increasing its water content. When the volumetric water content is increased passed a threshold value of 10% (Arenson, 2007) the water act more like “Dirty Ice”.

Dirty ice acts very closely to pure ice; it represents water with a volume fraction of soil below 0.5. The relationship and effect of volume ratio is presented on Figure 8.

Figure 30: Adfreeze Strength in Function of Moisture Content, shows the curve approaching full saturation. The degree of saturation for the compaction used for testing was found to be between 16 and 17%. As described by Weaver and Morgenstern (1981) the relationship between shear strength of the frozen soil and its adfreeze coefficient is proportional. It is then expected that over saturated soil samples will demonstrate the same behaviour under adfreeze testing.

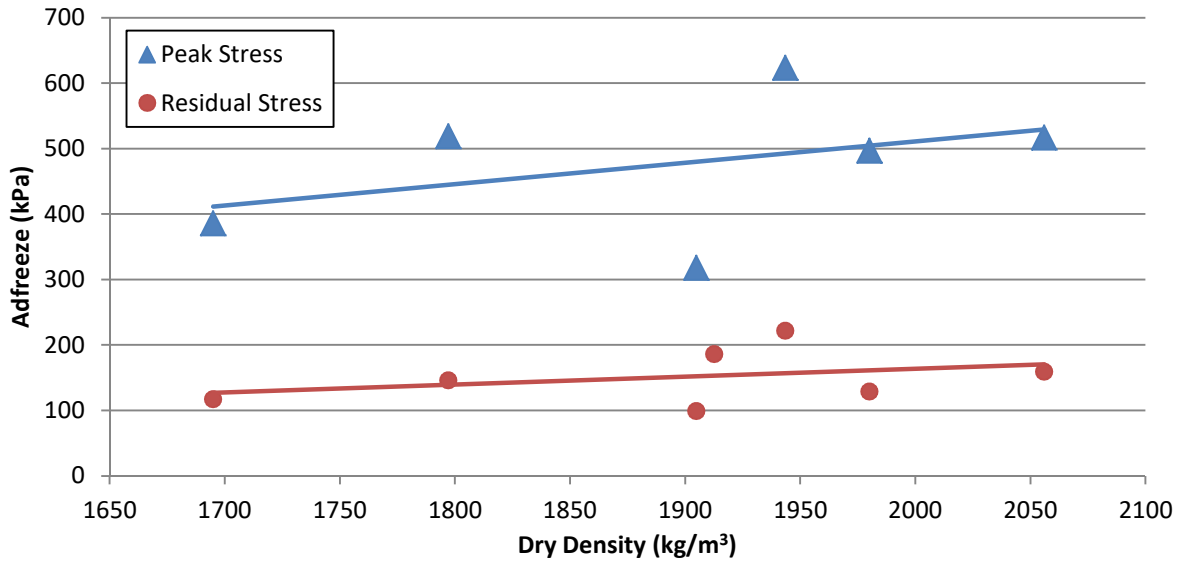

Figure 31: Adfreeze strength in function of density

Figure 31 shows that density has little effect on bond strength. The majority of the bond strength gained by freezing comes from the ice (Aldaeef & Rayhani, 2018). Unfrozen water form penetrates between the steel and the soil as well as all the imperfection in the materials. When freezing, water expands and cements the interface (Wissa, 1965) between soil particles and the pile material. This cementing effect increases the interface bond in some conditions up to 10

times the thawed bond. Even if the particles are closer the interlocking effect is not significantly increased since most of the load is transferred through the ice (Ladanyi 1985).

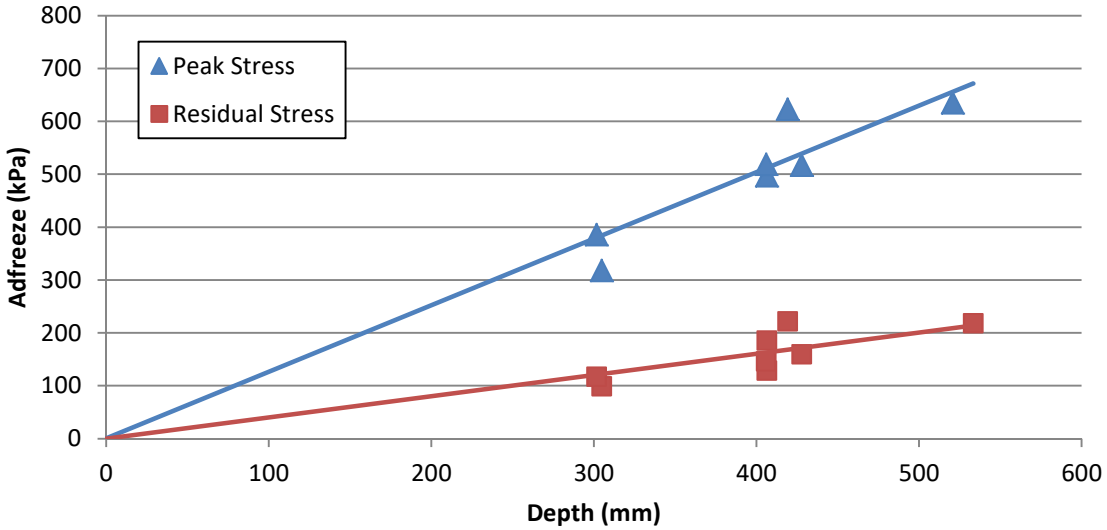

Figure 32: Adfreeze strength in function of embedded depth

3.7. Observations

3.7.1. Fragile bond

During the testing procedures it was found that the bond is fragile. The sample loses its peak maximum adfreeze bond if it had been exposed to vibration or a shock. On two occasions the forklift used to install the sample on the testing machine was holding the box too high and the pile came in contact the machine's arm. The unquantifiable shock seemed to be insignificant at the time the lateral load was applied. From the adfreeze peak strength, however, it was found that displacements on the order of 0.5 mm were sufficient to break the bond. The piles reached their maximum capacity between 0.3 and 0.6 mm of displacement.

Pull-out tests 3 and 8 shown in appendix present the results of the disturbed samples. This level of sensitivity is due to the shallow embedment depth. The lateral resistance of these small piles is small especially for the small displacement needed to break the adfreeze maximum bond.

3.7.2. Effective bond depth

The lateral pressure was assumed to be negligible around the tested piles due to the shallow absolute depth of their embedment. Figure 6 show the soil separating from the surface of the pile. The extent of the effect could not be measured and was not visible for all piles. The lower the water content of the soil the more visible the crack was. The same trend was observed for shallow embedment depth: the shallower the pile embedment, the larger the crack that would be formed.

The effect for small diameter-shallow piles might be important in affecting the capacity of the pile. Different experiments should be done to establish if there is an effective depth to be used in calculating capacity of piles in frozen ground. The installation method and type soil may also influence this behaviour.

Figure 33: Soil interface separation at the surface of the sample

Chapter 4. Soil Interface Testing

4.1. Introduction

This chapter presents the equipment and method used to test adfreeze bond using a direct shear interface apparatus. The apparatus was modified and outfitted with refrigeration equipment to enable in place tests at freezing temperatures. First, surface testing was conducted to ensure the interface tested was of similar roughness as the model pile tested in Chapter 3. Secondly a range of normal stress was chosen for testing from the literature review. Finally, compaction and preparation of the sample was done to approach the same conditions tested in Chapter 3.

The results and observation are presented following the testing procedure. The objective of this part of the experimental program is to measure adfreeze bond using a small size sample in a soil-interface testing apparatus like apparatuses found in practical testing laboratories.

4.2. Soil-Interface apparatus

In frozen ground it is a common practice to consider the soil-pile interface as the only load transfer mechanism (Ladanyi and Theriault, 1990). By doing so, the end-bearing capacity is ignored, and the system is simplified to the material and soil interface. For axially loaded elements such as piles the system can be represented by a flat surface of the pile material in contact with soil under a normal force.

An automated three-dimensional interface testing apparatus was developed and presented by Fakharian and Evgin in 1996 at the University of Ottawa. This apparatus can be programed and modified easily for a range of interface testing. A schematic of the machine is presented in Figure 34. Its small size and testing enclosure made it easy to convert into a cold room using insulation panels and refrigeration equipment. It makes this apparatus one of the first to freeze and test samples without require handling the specimen after freezing.

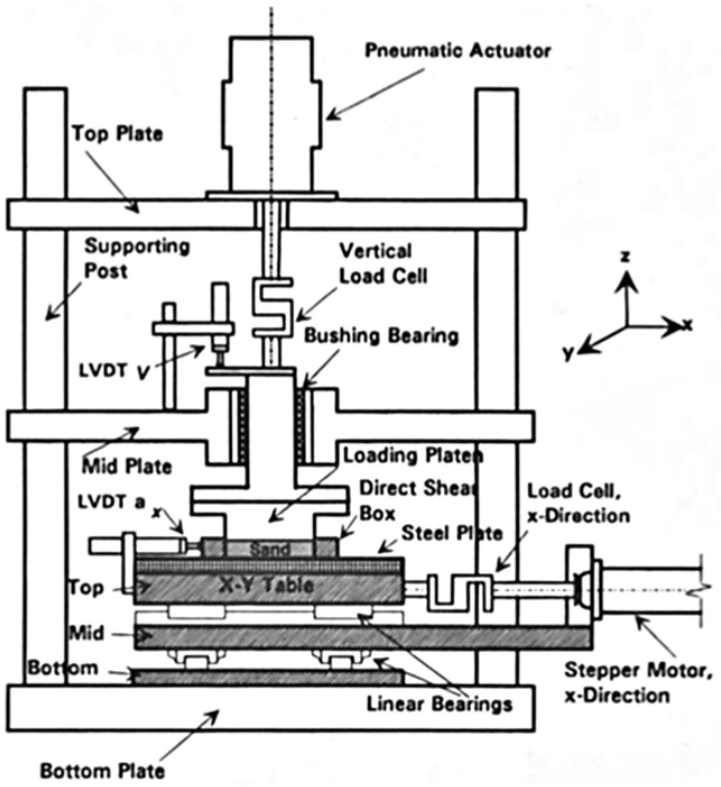

Figure 34: Schematic of Fakharian's 3D interface apparatus (C3DI) (from Fakarian & Evgin, 1996)

While the tests for this research were completed in a 2D plane, the apparatus was developed for 3D monotonic and cyclic testing. It is composed of a reaction frame designed to withstand horizontal and vertical loads of 25 KN. Those loads are resisted by 600 mm by 600 mm aluminum plates. The bottom and middle plates are to provide horizontal reaction while the top and bottom provide vertical reaction.

The test is conducted in between the bottom and middle plates on a set of 600 mm by 600 mm tables connected through linear bearings. The top testing table is then free to move in the X-direction and the middle table is free to move in the Y-direction about the bottom plate, and that without rotation about the vertical axis. Programmable ball screw stepper motors are used to advance each table in the desired direction while transferring the reaction to the table below while a load cell between the ram and the table reads the applied load.

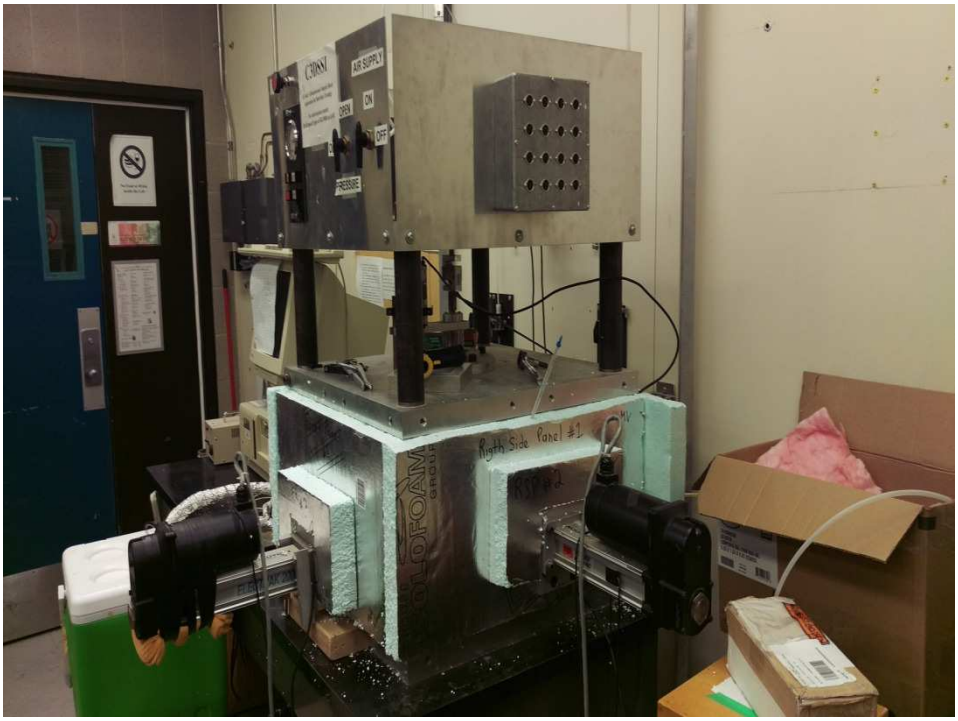

Figure 35: Foam insulation panel covering the testing chamber of the C3DI

The normal load is applied by a pneumatic actuator from the acting from the top of the frame. It applies a load in the Z axis through vertically mounted bushing bearing fixed against X-Y plane movement. The load is then applied through a loading plate that fits in the 100 mm by 100 mm direct shear box in which the soil sample is prepared. An LPT is fixed to the middle plate to measure normal displacement of the specimen. (for more details, Fakharian & Evgin (1996))

To adjust the apparatus for freezing interface tests, the testing chamber between the bottom and middle plates was fully enclosed within insulation foam panels, as shown in Figure 35. The inside view of the testing table and normal load plate is shown in Figure 36. The figure also shows tubes, which can be use to circulate a fluid through the testing table for gradient temperature testing, however, those were not used for this series of tests, as the tubes were disconnected, and the interface plate was thus subjected only to the temperature of the insulated chamber. The bolted plates were used to hold the sample and shear box in place for preparation and installation. The LPT seen in the foreground was used to measure displacement in the X axis. The load cell on the right leads to the Y axis stepper motor not used for these tests. The X axis set up is the same on the far side of the table.

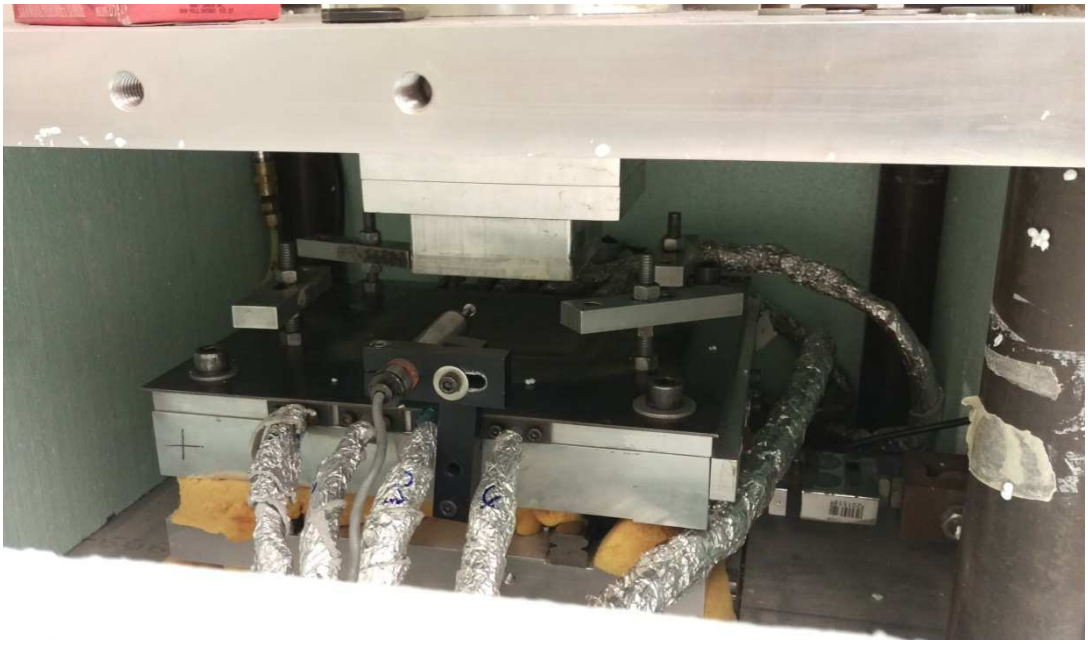

Figure 36: Interface testing table inside the insulated chamber

4.3. Freezing equipment

The testing chamber was refrigerated by 2 electrical refrigeration box panel able to cool air down by 20°C from the ambient temperature and 2 vortex tubes which injected air between -7 and -6°C in the chamber. This system was able to freeze and keep the testing table at a temperature of -4 ± 0.5°C. Being able to freeze the specimen within the testing enclosure protects the fragile adfreeze bond from potential disturbance during transportation.

4.3.1. Refrigeration panels

The refrigeration panels used were taken off an Igloo Iceless Thermoelectric Cooler, Figure 37. The panel is specified to refrigerate and keep the temperature of the cooler box 20°C below ambient temperature. Two panels were glue and seal to the foam insulation around the testing chamber allowing proper ventilation for the refrigeration system. Using this system allowed to stabilize and avoid temperature fluctuation in the chamber. They were not the main source of cooling.

Figure 37: Colling equipment: Igloo Iceless Thermoelectric Cooler (left) (Terapeak.com), Exair vortex tube (rigth) (exair.com)

4.3.2. Vortex tubes

Vortex tubes are a reliable, low cost and maintenance free solution for cooling small areas. They require only a steady flow of compress air to operate. As shown in Figure 38, the input compressed air is separated in two different streams of different temperature. The apparatus uses a vortex to split the denser colder air particles from the warmer lighter air. The Exair Model 3210 vortex tube can output a temperature range from -46°C to 127°C depending on the temperature, pressure and flow rate of the feed compressor. The preferred temperature can be set using the adjustable valve on the warm outflow side of the tube.

Two Exair Model 3210 vortex tubes were installed to push freezing air in the testing chamber. The laboratory is equipped with compressed air lines able to provide the required flow of 4.8 l/s at 6.9 Bar of pressure for the proper function of the vortex. The tubes were set to provide a continuous flow of air at a temperature of -7°C.

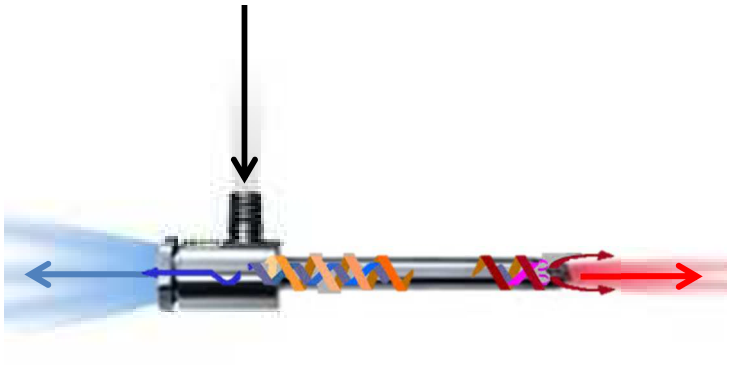

Figure 38: Vortex tube output (modified from Streamtek.com)

4.4. Test surface

To properly select the material tested for both test method and for equivalent test results, the galvanized pile was compared to the plate material by roughness. The Hommel Tester T500 shown in Figure 39, used with a standard pick-up T5E was used to measure the roughness of the circular pile and several galvanized steel plates. The apparatus reads average roughness (R_a), maximum range of roughness (R_T) and average peak roughness (R_Z) at a precision of 0.1 µm.

The tester drags the pick-up over a pre-set travel length and measures the vertical displacement of the stylus, situated at the end of the pick-up, as it travels. A default travel length of 10mm was used. Sample roughness profiles from Hommel are shown in Figure 40, Figure 41 and Figure 42.

Figure 39: Hommel tester T500 Roughness meter (http://granat-e.ru/t500)

Ra is defined by the arithmetic mean of the profile deviation from the center line over the measuring length (l_m). Graphically, it is the area between the roughness profile and its center line, Figure 40. It is calculated by integrating the displacement of the stylus over the travel length, Equation (18).

$$R_a = \int_0^{l_m} |y| dx \qquad (18)$$

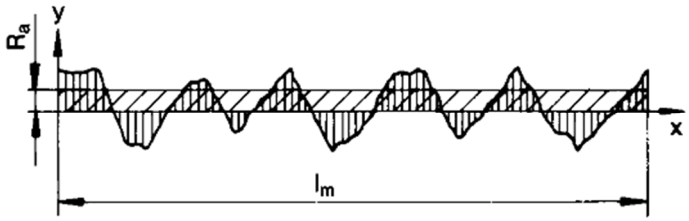

Figure 40: Roughness profile with average roughness (Hommel)

R_T representes the maximum vertical displacement of the stylus over the travel length. It is defined by measuring the maximum peak value (R_P) and the lowest valley value (R_V) peak of the graphical representation and adding them together, Figure 41.

$$R_T = R_V + R_P \quad (19)$$

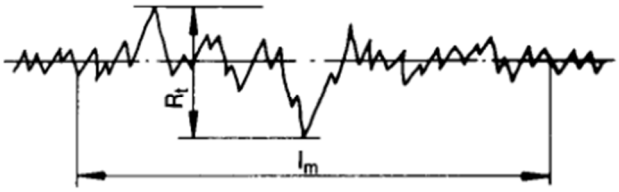

Figure 41: Roughness profile with maximum roughness (Hommel)

R_Z is taken as the mean of the absolute value of the five (5) highest peak (Y_P) and five (5) lowest valleys (Y_V). It represents the average maximum displacement of the stylus over the travel length.

$$R_T = \frac{1}{5}\left(\sum_{i=1}^{5}|Y_{Pi}| + \sum_{i=1}^{5}|Y_{Vi}|\right) \quad (20)$$

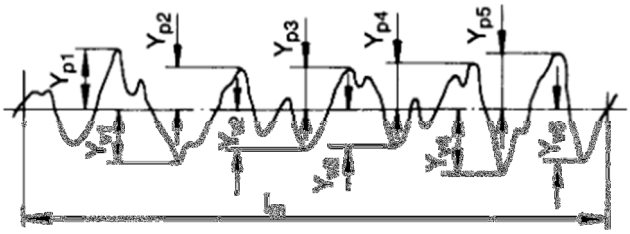

Figure 42: Roughness profile with average peak roughness (Hommel)

A variety of galvanized steel plate and sheeting were tested to find the best match to the surface of the piles tested in the pull-out series of tests. The results of the measurements are presented in Table 5. The measurements were done at multiple locations and directions on the surface of the pile and plating. The best comparable sheeting material available was the corrugated galvanized sheeting 1. Two sheets of the material were cut and fitted to the testing table of the apparatus for testing.

Table 5: Roughness measurement of tested pile and various galvanized steel plates and sheeting

Pull-Out test pile							
R_z (μm)	4.76	7.66	8.76	7.9	19	14.48	8.64
R_a (μm)	0.6	0.96	1.7	1.5	4	2.52	1.26
R_T (μm)	6.06	10.26	11.14	9.24	23	17.22	12.6
Galvanized plate corrugated 1							
R_z (μm)	23.76	17.78	16.76	18.6			
R_a (μm)	3.74	2.5	2.66	2.5			
R_T (μm)	31.22	23.3	18.9	28			
Galvanized plate corrugated 2							
R_z (μm)	36.8	31.7	34.1	34.2			
R_a (μm)	8.6	5.7	5.4	5			
R_T (μm)	43.5	32.7	44.7	43.8			
Galvanized sheeting 1							
R_z (μm)	1.94	1.62	3.22	2.44			
R_a (μm)	0.34	0.24	0.58	0.44			
R_T (μm)	2.42	2.28	4.26	3.04			
Galvanized sheeting corrugated 1							
R_z (μm)	9.3	8.92	10.04				
R_a (μm)	1.34	1.28	1.44				
R_T (μm)	12.04	11.68	12.6				

4.5. Sample Preparation

The interface apparatus was developed to test 100 mm by 100 mm samples with a maximum thickness of 23 mm. The sample is prepared in an aluminum direct shear box 25 mm thick with a 100 mm square opening. The underside of the box is lined with a Teflon layer to minimize friction and prevent sand from leaking under. The shear box is shown in Figure 43 during the preparation of a sample.

To prepare the sample, the shear box is first installed on the testing table and centered down with the vertical load ram. Once in place the box is fixed to the table using the available clamps

attached to the table. The top part of the table is then removed from the machine for proper handling and access.

Figure 43: Shear box with Teflon layer (left); Sample being compacted in load frame with proving ring(centre); Sample after compaction (right)

A dry sample of soil is then manually mixed with the calculated amount of water to achieve the target gravimetric water content for the specific test. The box is then filled with the well mixed soil and levelled out. To reach the maximum dry density achieved from the standard Proctor test, the box is put in a loading frame where it is compacted under static load using a ram, a jack and a calibrated proving ring to monitor the load. See Figure 25 for compaction test, the sample are compacted at 1000 kPa before being removed from the loading frame. To be properly prepared the sample needs to be approximately 5 mm from the top of the shear box after compaction. If the sample is found to be too thin or not leveled after compaction, more soil is added and the re-compacted.

A plastic wrap film is put over the sample to avoid the soil freeze-bonding to the load ram during the freezing. The table is reinserted in the testing chamber and fixed in place. The chamber is already at the target temperature.

The load ram is lowered on the sample and the target normal load is applied using the manual configuration of the pneumatic actuator. The clamps holding the shear box are removed since the

ram is now holding the setup in place. The X-Axis LPT is then replace and adjusted to be ready for testing.

The foam panel is put back in place and the sample was left to freeze for 30hrs. A thermometer is inserted through one of the insulating panels to monitor the temperature in the chamber with an accuracy of 0.5 °C.

4.6. Test Settings

Once the sample is ready and frozen for testing, a computer running a Benchmate™ based software will automatically control the test. The system comprises the testing apparatus and transducers, interface unit (hardware), and the software itself. The software can control; the normal load through automatic commands to the actuator; the push/pull rate of the stepper motor, as well as monitoring the displacement and loads on the sample in all directions. The output provided is a comma separated data file (.csv) providing the readings of all transducers (LPTs and load cells) every 5 seconds for the duration of the entire testing procedure.

The step motor controlled the shearing for this set up to push or pull the table while testing. For one test the table is pushed by the stepper motor while for the other, the table is pulled. This is done so that the motor stays within its working range while allowing enough movement for the test. The testing range of the motor is approximately 14 ± 1 mm. This range is the maximum movement that the table can accommodate without reaching the limit of the linear bearings. The program was set to allow a maximum movement of 7 mm in either direction during the tests.

For this research the parameters that varied were the normal load and the water content of the sample. The chamber temperature and the strain rate were kept constant through the entire testing series. The sample water contents were 9, 11 and 13% and each were tested under normal loads of 350, 400 and 450 kPa. The temperature of the chamber was kept at -4 ± 0.5°C. The stepper motor was set to strain the sample at a rate of 0.1 mm/min.

The software requires a maximum displacement for each test. By default, the value is set at 5 mm for either direction. For the current tests, the value was set to 7 mm which is the maximum the software allows for each testing sequence.

After the test was completed the specimen was removed and a sample was taken to measure the water content.

4.7. Test results

For this research three normal stress values were used. Since the apparatus maximum capacity is set to be 500 kPa the testing stresses selected were 350, 400 and 450 kPa. Five tests were completed for each normal stress. The moisture content used to test was 9, 11 and 13%. Some tests were doubled when the results or curve obtained deviated from previous tests. More importance was given to the 11% moisture content due to it being the optimum water content of the soil.

Some issues arose for the 13% moisture content specimens. The sample at this water content could not retain all its water which would then seep out from under the shear box. This, in turn, resulted in the shear box becoming cemented to the testing table, falsifying the test results. Consolidation of the sample is required in future test series.

Individual test results and curves are available in appendix. A summary table is presented under Table 6. Maximum peak adfreeze bond stress, residual strength and moisture content of each test is indicated and classified by normal pressure. The name of each test follows this format: “normal stress (kPa)”, “F (frozen)”, “moisture content (%)”, “Alphabetical counter”. For example, a test conducted under 350 kPa of normal stress with 11% moisture content which is the third repetition is indicated by “350F11C”. In preparation for testing multiple specimens, dummy tests were conducted to calibrate and test the apparatus. Some tests were completed in the frozen state while others were conducted under room temperature using the tested soil or a dummy block. The dummy block was a steel block placed in the shear box which allowed the calibrating the machine by simulating a test sequence.

Table 6: Interface shear test results

Name	350F09A	350F09B	350F09I	350F11I	350F13I
Normal Stress (kPa)	350	350	350	350	350
Peak Strength (kPa)	175.6	190.5	296.3	450.8	143
Residual Strength (kPa)	N/A	N/A	111.2	120	N/A
Moisture content (%)	9	9	9	11	13

Name	400F09A	400F11A	400F11I	400F11J	400F11K
Normal Stress (kPa)	400	400	400	400	400
Peak Strength (kPa)	246.8	177.6	52.9	195.2	185.1
Residual Strength (kPa)	N/A	N/A	29.8	105.1	N/A
Moisture content (%)	9	11	11	11	11

Name	450F09A	450F11A	450F11I	450F11M	450F13A
Normal Stress (kPa)	450	450	450	450	450
Peak Strength (kPa)	286.1	237.3	294.9	229.8	154.6
Residual Strength (kPa)	N/A	N/A	219.7	127.5	N/A
Moisture content (%)	9	11	11	11	13

A series of test on frozen specimens with 7% water content was done as preliminary testing. Those tests did not use the same normal stresses chosen for the testing program. However, those results were found to be worth indicating since the trend found was comparable to the one obtained during the pull-out program. Table 6 shows those preliminary test results.

Table 7: Preliminary interface test series results

Name	100JF07A	150JF07A	300JF07A	300JF07B	450JF07A
Normal Stress (kPa)	100	150	300	300	450
Peak Strength (kPa)	67.1	103	183	168.8	238.6
Residual Strength (kPa)	N/A	N/A	N/A	N/A	N/A
Moisture content (%)	7	7	7	7	7

Since all samples were compacted under the same normal stress, only 2 curves were made from the data generated. Figure 44 shows the relationship obtained between the adfreeze strength and moisture content of the samples under each normal pressure.

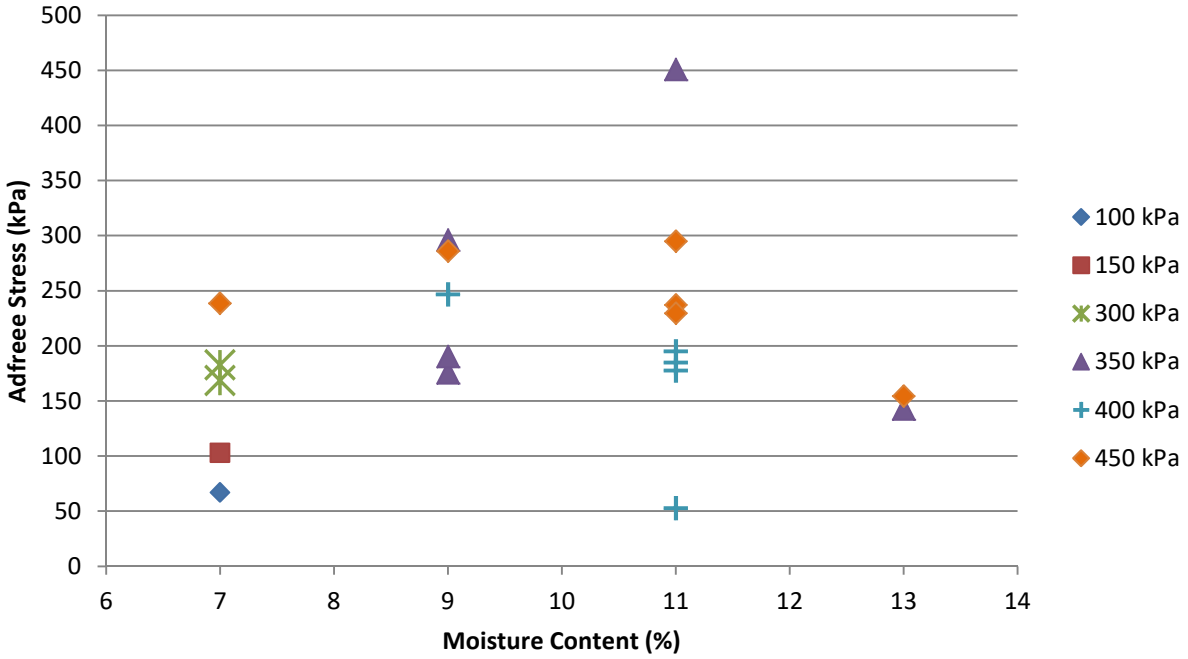

Figure 44: Interface testing relationship between moisture content and adfreeze stress in function of normal stress

No observable trend could be identified in relation to moisture content due to water seeping out of the sample during the freezing process.

The second data arrangement is shown in Figure 45. It graphically represents the relationship between normal stress and maximum adfreeze shear stress in function moisture content of the specimen.

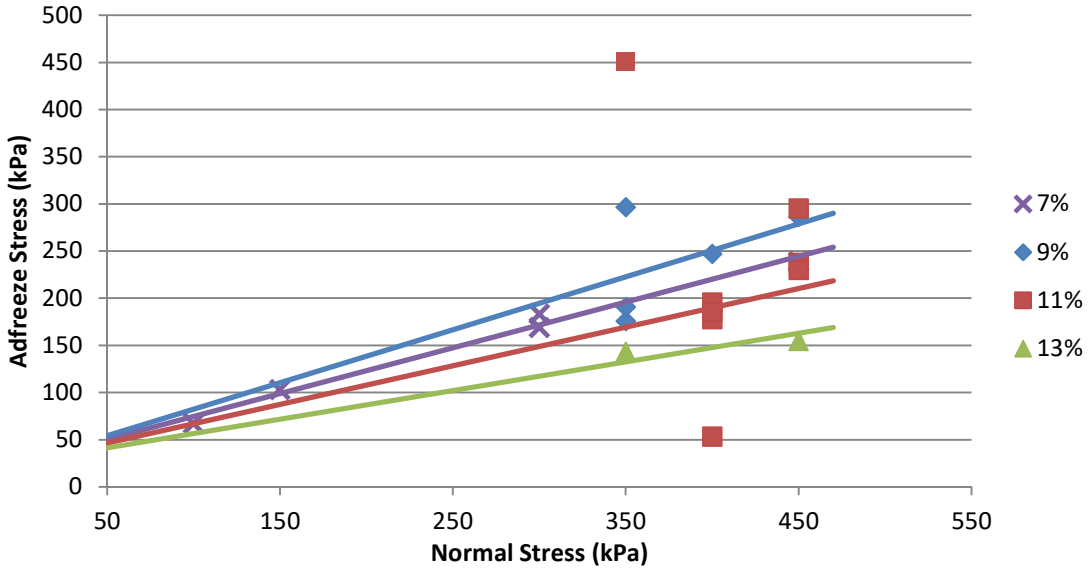

Figure 45: Interface testing relationship between normal stress and adfreeze stress in function of sample moisture content

Ignoring the outliers, it is possible to observe 4 distinctive linear trends. In this case each curve is separated by 5° and tends towards 0.

4.8. Observations

4.8.1. Reproducibility

The limited results from the series of test conducted shows that the machine is consistent and that the results obtained can be reproduced. The cluster of results tested at 400 kPa with 11% water content is a good indication that each test was completed in the same way and reacted in the same way. It is to note that some outliers are also present and could not be explained.

4.8.2. Moisture seepage and sample consolidation

During the 13% water content testing phase, water was observed seeping down and out of the sample. This free water would not seep immediately and be observable before installing the testing plate in the apparatus. This slow process would let water under the shear box which would freeze in place and bind the box to the testing plate.

The tested values for those tests were lower than to previously obtained results of the pull-out test series. On closer inspection, the water did not just seep out of the soil sample but also accumulated at the bottom of the soil boundary and under the shear box. Parameswaran (1978), Weaver and Morgenstern (1981), Crory (1966) and Andersland (2004) indicated that shear strength of frozen soil is inversely proportional to ice content. This indicates that adfreeze strength tends towards the adfreeze strength of pure ice only, which according to Saeki (2011) ranges from 50 kPa to 100 kPa approximately for the shear rate and normal pressure used during these tests. The added bond did not increase the strength of the system but reduced it.

The concentrated high moisture content layer that was observed in some of the 11% tests and all the 13% tests, diminish the actual adfreeze strength expected for those samples. It also shows that the lower level of the sample is over saturated.

For water contents lower than the optimum water content, the suction of the dry soil is able to retain the water between the particles during the small consolidation time before the water freezes.

4.8.3. Boundary effect

It is well known that the direct shear apparatus induces stress concentration in samples. This apparatus is already known to cause stress concentration from the applied normal load if the sample is not perfectly levelled after compaction. (Fakharian & Evgin, 1996)

It was also observed, as shown in Figure 46, that the boundary also deforms the sample. The shear box is held in placed by the vertical loading ram while the sample is frozen to the testing table as well as the shear box side. However, the frozen samples are much stiffer than room

temperature samples. The adfreeze bond itself is approximately 60 to 70% of the shear strength of the sample according to Weaver & Morgenstern (1981). This force can deform the edge of the sample.

As shown in Figure 46 the deformation is maximum at the centre of the edge boundary were the other boundaries are not influencing the sample. The extent of the border effect on the result is unknown and is difficult to control. Some specimens were observed to have larger deformations, and some did not show an effect of the edge.

This effect is an indication of the shear for of the sample but also indicates stress concentration in corners and along the opposite edge. This stress concentration would fail the adfreeze locally and diminish the global observed strength. It is probably the reason the results and curves resemble more the residual data found in the literature and observed previously in the pull-out testing sequence.

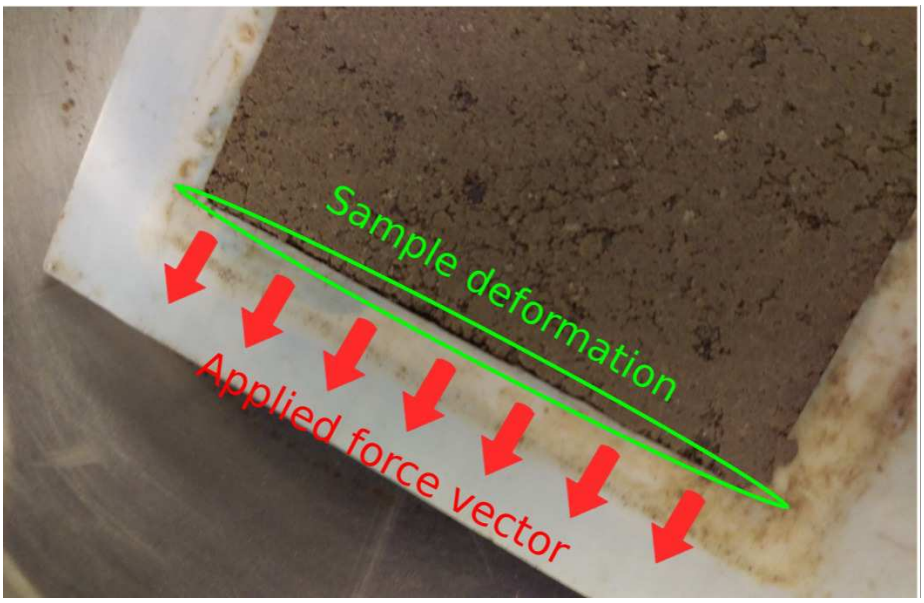

Figure 46: Sample deformation due to border effect

4.8.4. Apparatus limitations

The apparatus used was initially designed to test dry soils. To execute saturated interface tests on frozen samples, the soil would need to freeze in a sealed shear box.

During testing 400F11A the LPT recording the specimen movements jammed. It is unclear why this device's movement was impeded, but the possibility that moisture may have frozen and affected the free movement of the slider should be considered for future modification of the equipment. For the specimen with the missing displacement information, the data had to be plotted in function of time since the record was incomplete. The system also makes it complicated to change or switch over components. There were also occasional issues with the vertical LPT (vertical displacement) and the stepper motor, responsible for the horizontal displacement, is starting to show its age and would on occasion block and overheat. Upgrades to the system components and software in the future should ensure better performance in the development of new test programs.

Chapter 5. Testing method discussion

The two methods used for this study are newly developed techniques, which are low cost alternatives for frost testing. With global warming and the loss of permafrost all around the world, engineers tend to ignore seasonally frozen grounds and design for full saturation. When frozen ground is considered a highly conservative adfreeze value is used. For cases at the boundary of continuous permafrost the effect of creep and frost heave during the freezing season are more likely to be studied. When permafrost is present on site more consideration is given to the properties of the soil. However, most design will have to consider protecting and maintaining the integrity of the frozen layer.

Adopting a testing technique that is easy and affordable is to the best interest of the northern communities around the world and could be used in seasonal frost regions. This section will compare the observations and discuss their relationship with data and observation presented in literature.

5.1. Pull out test discussion

The pull-out laboratory test is commonly used to test interface bond strength of various material and stratum. In soil mechanic it is often used for soil anchors, soil nails and geo-grid reinforcement.

5.1.1. Field representation

Pull out laboratory test are the closest laboratory test representing field testing condition. Just as for field procedures this test can be adapted and scaled, if necessary, to represent parts of the field condition at a much lower cost. Figure 47 shows the set up for a field pull test side by side with a laboratory pull test.

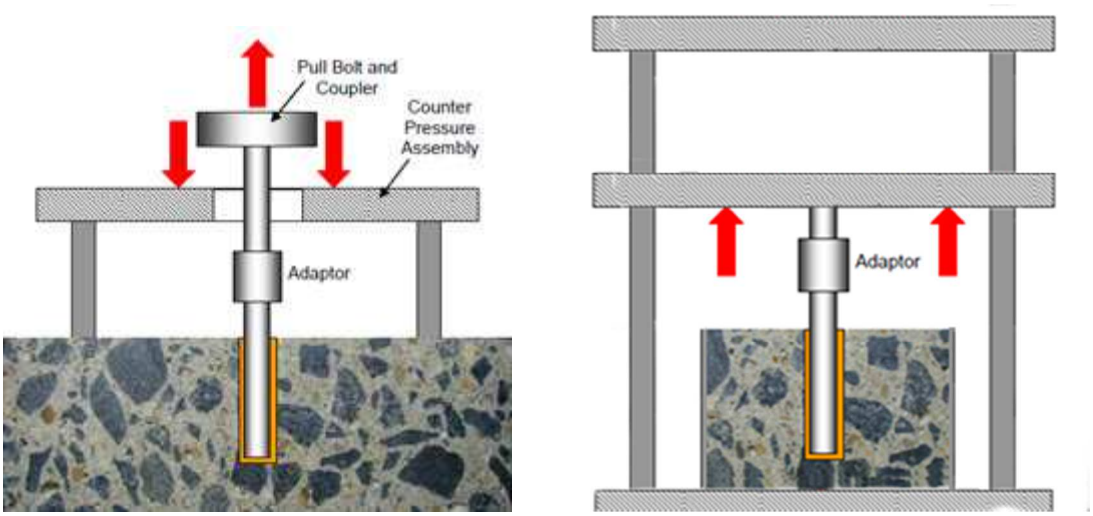

Figure 47: Field pull test set up (left) lab pull out test (right)

Small scale testing is possible with the laboratory setup and multi-layered soils can also be tested if necessary. The method is also versatile in its way to prepare and use different types of piles and soil.

5.1.2. Test versatility

In addition to scaling and field representation, the pull-out test also proves easy to modify when needed. The easiest and simplest parameters to modify for testing were water content and embedded depth. The water content could range from completely dry to over-saturated or submerged conditions, since the test box is fully enclosed and impermeable.

This method also allows for the user to quickly change the setup to test different types of pile shape and materials. The only modification required is the type of attachments. Clamps can be used with H-pile sections, an embedded bar can be installed in a concrete pile or a screw in bolt can be installed on top of a lumber pile. The options are only dependent on the size and type of the universal test machine available.

Since the testing box is a small-scale element of ground the installation process can also be modified. For this study the piles were assumed to be augered and put-in-place. It is also possible to install driven in place or mud back filled fill if necessary. This option is practical for concrete

and H-pile testing. It is known that the installation method has an important influence on the bearing capacity of piles (Randolph et al., 1979; Johnston & Ladanyi, 1972) and most small element laboratory test do not capture the effect of the installation process.

5.1.3. Test results

The behaviour for this type of adfreeze test procedure is comparable to field tests. They are however complicated to compare to other results obtained by direct shearing. The data obtained from this test is limited to displacement, depth and force. It is not an element model in which all forces are known in all direction.

The test is easily scalable by modifying the physical properties like depth, size of pile and soil layer. There are very limited ways to observe and collect data on the effect of lateral stress on the pile (normal loads) or isolate local effects and conditions.

The data obtained is to be computed with depth as a main parameter. Weaver and Morgenstern (1981) described those lateral normal forces on piles (effective stress) to be negligible with little effect on the adfreeze bond. This statement was proven wrong by Ladanyi and Theriault in 1990 when they presented the effect of effective stress for different type of soil under freezing conditions. This is an issue of importance when modelling the problem. While using finite member element to model the pile under axial load could be done using those results, it is a lot more complicated to modify the data to fit a finite element model.

5.1.4. Testing equipment

When it comes to laboratory testing, using large laboratory specimens like the ones needed for this set up, is expensive and requires a lot of resources. The size of the test box alone is considerable and requires planning for transportation, installation and storage. Laboratories don't typically have the storage or resources to equip themselves with large pieces of equipment that are rarely used.

5.2. Soil Interface testing discussion

The interface shear testing is a method easily modified from standard simple shear test apparatus, which are common in laboratories and easy to use.

5.2.1. Field representation

Simple shear tests are extensively used in soil mechanics. This type of test has been largely studied. It has been found to show discrepancies with in-situ stress conditions (Prevost, 1976). It does so due to the lateral stress induced by the walls of the shear box while under normal stress. Prevost showed that the increase in normal stress is proportionate to the increase of those lateral forces. In sand the effect is increased when shear distortion is imposed to the sample. This test procedure is also known to induce additional stress by slippage.

Pure shear elements are rarely found under practical conditions. Simple shear and direct shear test both shows the same issues but are commonly used to find design criteria even if they are not accurate element representations of field conditions. An adaptation for interface testing under triaxial condition is the optimal element representation. This type of test would be highly expensive and complicated to develop.

The way samples are prepared and frozen under a constant normal stress is not highly representative of the conditions found on site. No considerations are given to the stress and other effects occurring during the pile installation process. In addition, there is no way to study the effect of different shapes or cast in place piles.

5.2.2. Test versatility

Simple shear tests offer a very limited range of test conditions. The variable parameters of this test are the application of normal stress and shear rate. It was found that due to the undrained characteristics of this type of test, water content cannot be easily modified. The increase in pore water pressure under high normal stress influences the freezing process and the increase in internal stress due to the expansion of water between the particles.

The nature of frozen soils, where ice impedes free movement of water, does not allow for drained and consolidated tests. In addition, there is no instrument in the apparatus for monitoring pore water pressure buildup.

The stresses created by the installation and freezing process are known to dissipate over time. A small sample would dissipate those stresses faster and represent long term strength. This effect varies in the type of soil.

5.2.3. Test results

The data obtained from simple shear test can be manipulated and plotted in different ways. Generating a Mohr circle and plotting the stress path is easy to do after a series of individual tests. It is important to note the test is completed under undrained conditions. Even frozen, the soil contains a liquid phase that is still able to influence local stress under undrained conditions.

5.2.4. Testing equipment

The testing equipment used for this study has been modified from a well-known testing process. Any laboratory's simple or direct shear apparatus can be used to test adfreeze bond with many type of interfaces. Different steel plates, precast concrete or planks can be inserted in the apparatus to act as pile material.

6.3 Data discussion

The data obtained by both techniques are not comparable. Not only regarding absolute values but also on shape and response. The common published data available presents maximum and residual values with only a description of the behaviour. Parameswaran (1978 & 1981) and Ladanyi & Theriault (1990) have presented values using similar testing methods. Both using saturated sands, the difference in the values publish shows similar variations. The push through values ranged around 725 kPa for the same push rate against steel (Parameswaran 1981) while the interface test yielded maximum adfreeze bonds in ranges of 140 kPa to 550 kPa (Ladanyi 1990) at high normal stresses.

While this study showed a range of adfreeze bond between 400 to 650 kPa in this pull-out series of test, the results are comparable to Parameswaran (1978) with is push through tests, the series of interface tests showed a lower range of values. Due to the limitation of the interface apparatus the full range tested by Ladanyi & Theriault could not be completely compared. The trend between each test was still the same with the exception of the brittle response. Some interface test showed a brittle response right after reaching the maximum peak strength. However most of the tested samples did not respond in that way. They showed a small peak and a small fall in strength for the rest of the testing period. It is important to note that some tests show a plateau after 1 to 2 mm of displacement before reaching peak strength. A ratio of tested adfreeze strength from larger scale test to interface testing for both this study and literature is approximately 2.0 to 2.2.

The water seeping under the specimens at high water content was likely due to the low matric suction capacity of the tested sand. It explains why the lower water content tests (7-9%) behaved in a more comparable way to the pull-out series of test were the volume of sand was large enough to allow freezing on the vertical surface before seeping down. Direct shear interface testing allows for a larger range of water content testing for finer soils. Selecting proper water content and freezing process for testing is crucial to obtain the proper results. The maximum water content needs to be selected in function of the specimen's height and its soil water characteristic curve.

The normal stresses used were also found to be exceeding both expected in-situ effective stress for this soil, as well as the maximum pure ice adfreeze bond. While the earlier studies found that effective stress in frozen soils could be neglected, more recent research shows that lateral stresses are large for short term freezing. Higher normal stresses were chosen for this reason. The results showed that the lateral stresses created during the freezing of unsaturated soil are negligible.

Under this high normal force, the friction from the soil particles is more important and overcomes the adfreeze strength contribution of the ice. After the testing program was completed a thawed sample was tested for comparison, at 400 kPa normal stress the data obtained ranged from 100 kPa to 215 kPa. Since ice has an adfreeze bond value of approximately 100 kPa the

effect of ice on adfreeze soil bond will slowly fade after the soil bond is under enough normal stress to exert a strong friction particle.

During the pull-out test series, it was observed that the tests could easily be disturbed by moving or hitting the box or pile previous to testing. This issue raises the concern of the usefulness of this test in practical applications. The high cost of testing would require the test to be reliable and easily repeatable. If the equipment is available, the issues of moving the sample can be avoided by installing the boxes and the universal testing machine in a cold room.

The pull-out test was a lot more representative of the expected behaviour previously described by Crory (1966). The fragile and brittle failure are easy to observe, and both the effect of water content and depth can be tested with very little secondary effect compared to the effect caused by the increase of water content in the interface test. More study on unsaturated frozen grounds as well as the effect of depth on adfreeze tests should be completed to verify the entire behaviour and find a proper constitutive expression to demonstrate it.

Chapter 6. Conclusion

In conclusion, this study observed the various effects of unsaturated freezing including, water migration, separation and fragile bonding.

1) The modifications made to Fakharian and Evgin (1996) interface apparatus allowed to prepare, freeze and test specimen on place avoiding handling disturbances.
2) It was observed that unsaturated adfreeze strength shows the same behavior as previously studied for saturated freezing.
3) After comparing literature data of similar testing procedures used for this study as well as the data presented, it can be concluded that the results between large scale pull/push out testing are not completely compatible.
4) The results obtained by direct interface shear testing proved both in literature and this series of test to be smaller than the strength obtained from large scale testing. The results of both types of tests are difficult to correlate, due in part to the unknown lateral normal stresses existing on the embedded pile, A ratio of maximum adfreeze strength of 2.0 to 2.2 was observed.
5) The behavior of unsaturated frozen ground, bearing capacity and strength is closely related to the water content. Once the saturation point is passed, the strength characteristics tend towards pure ice properties.
6) Unsaturated frozen soils are submitted to lower effective stress due to their shallow depth and the amount of void available for the water to expand while freezing.

The series of tests conducted under this study also observed a marked difference in the several testing techniques used and the data available. This was to conclude if any techniques available was economically viable. While larger scale test gives comparable results to field testing, they require more resources. Interface shear testing uses more available testing apparatus and smaller installation. Since frozen ground applications are rarely encountered interface testing would provide the required data. Larger scale testing would be more suited for larger and more complicated projects.

7.1 Suggestion for further studies

The interface apparatus developed by Fakharian and Evgin (1996) used for this study is a basic version of the apparatus used by & Theriault (1990) for this application. A modern version of these apparatuses should be developed. This updated version of the machine would not only be useful for frozen soil applications but versatile enough for all interface shear testing.

1) Complete a series of saturated and over-saturated test using the large-scale pull-out method to compare the hypotheses suggested.
2) Complete a series of test freezing the interface under a gradient of temperature to simulate the effect of freeze piles and thermosyphon.
3) Observe the effect of freeze thaw cycles on adfreeze bond and the effect each cycle has on the strength of the bond.
4) Complete a similar series of test using a fine grain soil to observe the effect matric suction has on the freezing process
5) Observe the field requirement and testing procedure do better approach the practical side of the design

References

- Aldaeef A.A., Rayhani M.T. (2018) Adfreeze Strength and Creep Behavior of Pile Foundations in Warming Permafrost. In: Abu-Farsakh M., Alshibli K., Puppala A. (eds) Advances in Analysis and Design of Deep Foundations. GeoMEast 2017. Sustainable Civil Infrastructures. Springer, Cham
- Andersland, O. B., & Ladanyi, B. (2004). Frozen ground engineering. John Wiley & Sons.
- Arenson, L. U., Springman, S. M., & Sego, D. C. (2007). The rheology of frozen soils. Applied Rheology, 17(1), 12147.
- Arenson, L.U. and Springman, S.M.(2005) Mathematical description for the behaviour of ice-rich frozen soils at temperatures close to zero centigrade. Canadian Geotechnical Journal 42 431-442.
- Arteau, J. (1984) Étude de la consolidation des sols gelés. Ph.D. diss., École Polytechnique, Montreal.
- Baker, T.H.W. (1976). Transportation, preparation and storage of frozen soil samples for laboratory testing. In Soil Specimen Preparation for Laboratory Testing. ASTM Spec. Tech. Pub. 559, pp.88-112
- Bishop, A.W. (1973) The influence of an undrained change in stress on pore pressure in porous media of low compressibility. Géotechnique 23(3):435-42
- Black, P. B., & Tice, A. R. (1989). Comparison of soil freezing curve and soil water curve data for Windsor sandy loam. Water Resources Research, 25(10), 2205-2210.
- Catana, M. C. (2006). Compaction and water retention characteristics of Champlain sea clay (Doctoral dissertation, University of Ottawa (Canada)).
- Crory, F. E. (1966). Pile foundations in permafrost. In Permafrost: Proceedings of North American Contribution to First International Conference on Permafrost (pp. 467-476).
- Domaschuk, L. (1982). Frost heave forces on embedded structural units. In Proceedings of 4th Canadian Permafrost Conference (pp. 487-496).

- Faizi, K., Kalatehjari, R., Nazir, R., & Rashid, A. S. A. (2015). Determination of pile failure mechanism under pullout test in loose sand. Journal of Central South University, 22(4), 1490-1501.
- Fakharian, K., and E. Evgin. "A three-dimensional apparatus for cyclic testing of interfaces." Proc. 46th Annual Canadian Geotechnical Conference. 1993.
- Fakharian, K. and Evgin, E., "An Automated Apparatus for Three-Dimensional Monotonic and Cyclic Testing of Interfaces," Geotechnical Testing Journal, Vol. 19, No. 1, 1996, pp. 22-31, https://doi.org/10.1520/GTJ11404J. ISSN 0149-6115
- Gold, L.W., (1970) Process of failure in ice. Canadian Geotechnical Journal 7 405-413.
- Goodman,M.A. (1975). Mechanical properties of simulated deep permafrost. ASME J. Eng. Ind. Ser. B 97(2):417-25
- Hammer, T. A., Ryan, W. L., & Zirjacks, W. L. (1985). Ground temperature observations. In Thermal Analysis,Construction, and Monitoring Methods for Frozen Ground (pp. 9-46). ASCE.
- Harris, S.A. (2015). Permafrost. In the Canadian Encyclopedia. Retrieved from http://www.thecanadianencyclopedia.ca
- Heydinger, A. G. (1987). Piles in permafrost. Journal of cold regions engineering, 1(2), 59-75.
- Hillel, D. (1980) Applications of Soil Physics. New York: Academic Press.
- Johnston, G. H., & Ladanyi, B. (1972). Field tests of grouted rod anchors in permafrost. Canadian Geotechnical Journal, 9(2), 176-194.
- Kelly, R. B., Houlsby, G. T., & Byrne, B. W. (2006). A comparison of field and laboratory tests of caisson foundations in sand and clay.
- Koopmans, R. W. R., & Miller, R. D. (1966). Soil freezing and soil water characteristic curves. Soil Science Society of America Journal, 30(6), 680-685.
- Ladanyi, B. (1985) Stress transfer mechanism in frozen soils. Invited lecture. In 10th Canadian Congress on Applied Mechanics, London, Ontario, Canada, vol. 1, pp. 11-15.
- Ladanyi. B. (2002). Behavior of ice-rock mixture on slopes. 11th Int. Conf on cold regions Engrg., Anchorage, Alaska:632-699.

- Ladanyi, B. (2003). Rheology of ice/rock systems and interfaces. In Proceedings of the 8th International Conference on Permafrost, Zurich (pp. 22-25).
- Ladanyi,B., and G.H. Johnston. (1978) Field investigations of frozen ground. Chap. 9 in Geotechnical Engineering for Cold Regions, ed. O.B Anderlsand and D.M. Anderson. New York: McGraw-Hill
- Ladanyi, B., & Theriault, A. (1990). A study of some factors affecting the adfreeze bond of piles in permafrost. In Proc. of Geotechnical Engineering Congress GSP (Vol. 27, pp. 213-224).
- Marcuson III, W. F., & Franklin, A. G. (1979). State of the art of undisturbed sampling of cohesionless soils (No. WES-MP-GL-79-16). Army Engineer Waterways Experiment Station Vicksburg MS.
- Miller, R. D. (1965). Phase equilibria and soil freezing. In Permafrost: Proceedings of the Second International Conference. Washington DC: National Academy of Science-National Research Council (Vol. 287, pp. 193-197).
- Miller, D. L. (1985). Temperature Monitoring/Ground Thermometry. In Thermal Analysis,Construction, and Monitoring Methods for Frozen Ground(pp. 57-75). ASCE.
- Nixon, J. F., & McRoberts, E. C. (1976). A design approach for pile foundations in permafrost. Canadian Geotechnical Journal, 13(1), 40-57.
- Nottingham, D. & Christopherson, A.B. (1983) Design Criteria for Driven Piles in Permafrost. Department of Transport and Public Facilities
- Palmeria, E. M., & Milligan, G. W. E. (1989). Scale and other factors affecting the results of pull-out tests of grids buried in sand. Geotechnique, 39(3), 511-542.
- Parameswaran, V. R. (1978). Adfreeze strength of frozen sand to model piles. Canadian geotechnical journal, 15(4), 494-500.
- Parameswaran, V. R. (1981). Adfreeze strength of model piles in ice. Canadian Geotechnical Journal, 18(1), 8-16.
- Phuong, N. T. V., Van Tol, A. F., Elkadi, A. S. K., & Rohe, A. (2016). Numerical investigation of pile installation effects in sand using material point method. Computers and Geotechnics, 73, 58-71.

- Phukan, A.(1978) Pile Foundations in Frozen Soils. Journal of Pressure Vessel Technology 100, no. 3 : 302–9. doi:10.1115/1.3454471.
- Prevost, J. H., & Høeg, K. (1976). Reanalysis of simple shear soil testing. Canadian Geotechnical Journal, 13(4), 418-429.
- Randolph, M. F., Carter, J. P., & Wroth, C. P. (1979). Driven piles in clay—the effects of installation and subsequent consolidation. Geotechnique, 29(4), 361-393.
- Rostami, H. (2017). Finite Element Analysis of Coupled Thermo-Hydro-Mechanical Processes in Fully Saturated, Partially Frozen Soils (Master's thesis, NTNU).
- Saeki, H. (2011). Mechanical Properties Between Ice and Various Materials Used in Hydraulic Structures: The Jin S. Chung Award Lecture, 2010. International Journal of Offshore and Polar Engineering, 21(02).
- Sheikhtaheri, M. (2014). Experimental and numerical modeling studies for interpreting and estimating the p–δ behavior of single model piles in unsaturated sands (Doctoral dissertation, Université d'Ottawa/University of Ottawa).
- Spaans, E. J., & Baker, J. M. (1996). The soil freezing characteristic: Its measurement and similarity to the soil moisture characteristic. Soil Science Society of America Journal, 60(1), 13-19.
- Stähli, M. (2005). Freezing and thawing phenomena in soils. Encyclopedia of hydrological sciences.
- Ting, J.M., Martin, R.T. &Ladd, C.C. (1983). Mechanisms of strength for frozen sand. J. Geotech. Engrg., ASCE 109(10):1286-1302.
- Veillette, J. (1975). Helicopter portable drill for high artic programs. Geol. Surv. Can. Pap. 75-1, pt .A.
- Weaver, J. S., & Morgenstern, N. R. (1981). Pile design in permafrost. Canadian Geotechnical Journal, 18(3), 357-370.
- Wissa, A.E.Z. (1969) Pore pressure measurement in saturated stiff soils. J.Soil Mech. Found. Civ. ASCE95(SM4): 1063-73
- Xu, X. T., Liu, H. L., & Lehane, B. M. (2006). Pipe pile installation effects in soft clay. Proceedings of the Institution of Civil Engineers-Geotechnical Engineering, 159(4), 285-296.

- Yong, R. N. (1962). Research on Fundamental Properties of Frozen Soils. Proc. 1st Canadian Conf. Permafrost, pp. 84-108.
- Zhang, T., Barry, R. G., Knowles, K., Ling, F., & Armstrong, R. L. (2003, July). Distribution of seasonally and perennially frozen ground in the Northern Hemisphere. In Proceedings of the 8th International Conference on Permafrost (Vol. 2, pp. 1289-1294). AA Balkema Publishers.

Appendix A. Pull out test results

Pull out 1

Test Date: 02/04/15 Embedded depth : 533 mm

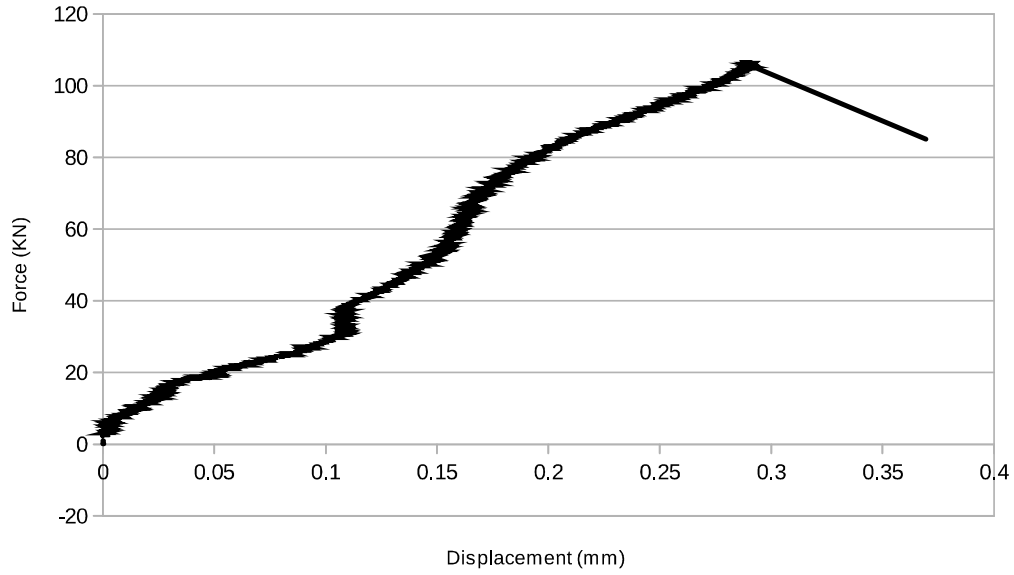

Force Max:	106	KN
Residual:	N/A	KN
Max Stress:	553	Kpa
Res. Stress:	N/A	Kpa

Time (min)	Temperature (°C)

Comments: Pulling arm bolt failed. The test was unconclusive.

Pull out 3

Test Date: 02/13/15 Embedded depth : 533 mm

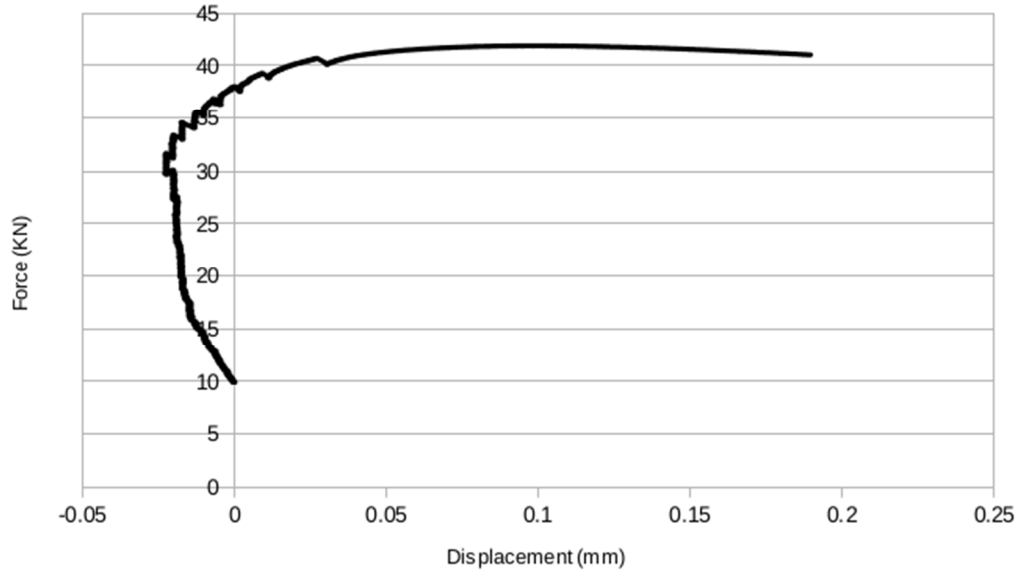

Force Max:	N/A	KN
Residual:	41.8	KN
Max Stress:	N/A	Kpa
Res. Stress:	219	Kpa

Comments: Sample was disturbed when installed on the testing machine. The adfreeze bound was broken. The test yielded the residual friction

Time (min)	Probe 1 (°C)	Probe 2 (°C)	Probe 3 (°C)	Probe 4 (°C)
0	-15.562	-12.812	-13.562	-10.75
20	-11.812	-7.625	-8.375	-5.375
40	-11	-7	-7.7687	-4.562
60	-10.187	-6.187	6.812	-3.875
80	-9.375	-5.5	-6.062	-3.312
100	-8.687	-4.812	-5.312	-2.875

Probe set-up

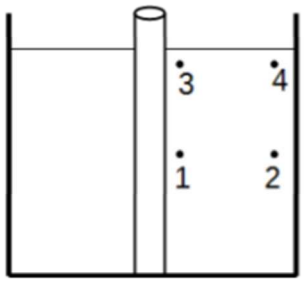

Pull out 4

Test Date: 02/26/15 Embedded depth : 521 mm

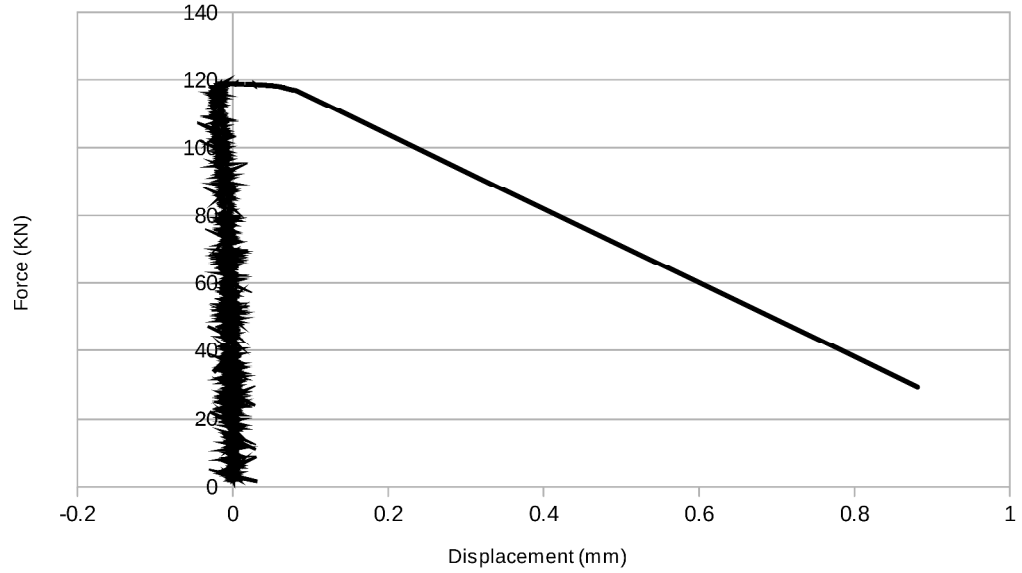

Force Max:	118.796	KN
Residual:	N/A	KN
Max Stress:	536	Kpa
Res. Stress:	N/A	Kpa

Comments: Sudden failure after reaching maximum force. Residual strength not tested

Time (min)	Probe 1 (°C)	Probe 2 (°C)	Probe 3 (°C)	Probe 4 (°C)
0	-11.5	-9.187	-7.562	-7.812
20	-10.825	-8.937	-7.437	-7.25
40	-10.25	-8.625	-7.25	-6.812
60	-9.812	-8.375	-7.062	-6.437
80	-9.25	-8	-6.812	-6
95	-8.812	-7.625	-6.562	-5.5625

Probe set-up

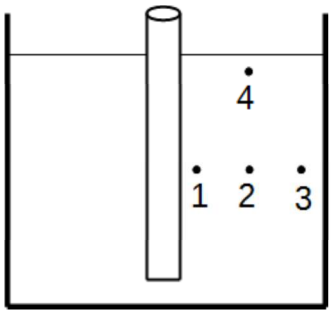

Pull out 5

Test Date: 03/02/15 Embedded depth : 429 mm

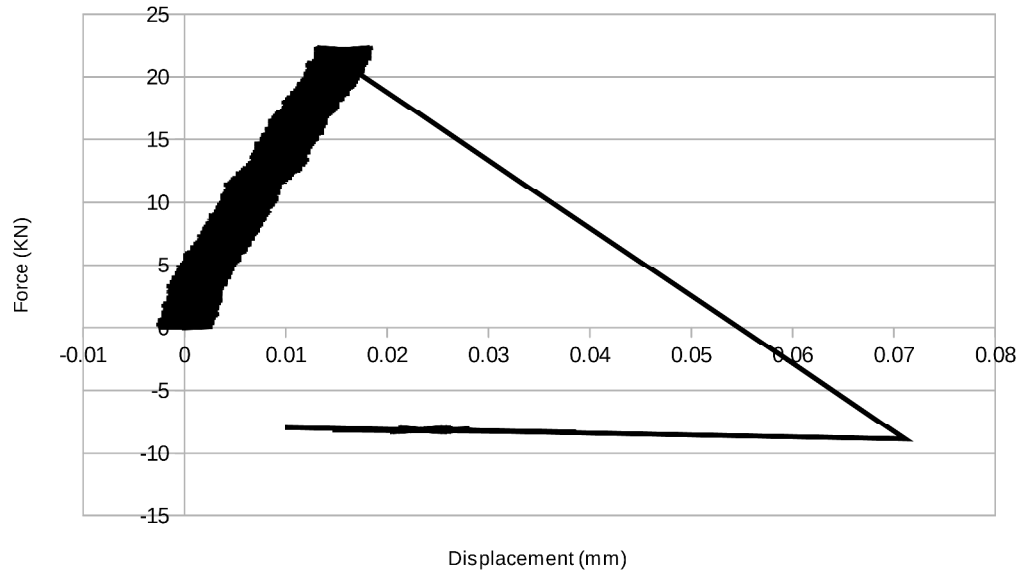

Force Max:	N/A	KN
Residual:	N/A	KN
Max Stress:	N/A	Kpa
Res. Stress:	N/A	Kpa

Comments: Pulling arm failed. Test inconclusive

Time (min)	Probe 1 (°C)	Probe 2 (°C)	Probe 3 (°C)	Probe 4 (°C)
0	-4.5	-4.25	-325	-3.437
5	-4.437	-4.187	-3.25	-3.375
10	-4.375	-4.125	-3.187	-3.25
15	-4.312	-4.062	-3.187	-3.187

Probe set-up

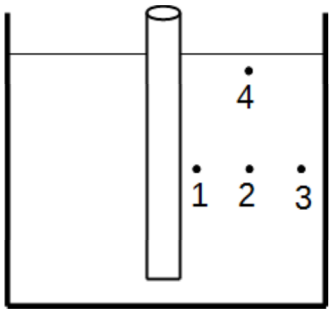

Pull out 6

Test Date: 03/03/15 Embedded depth : 419 mm

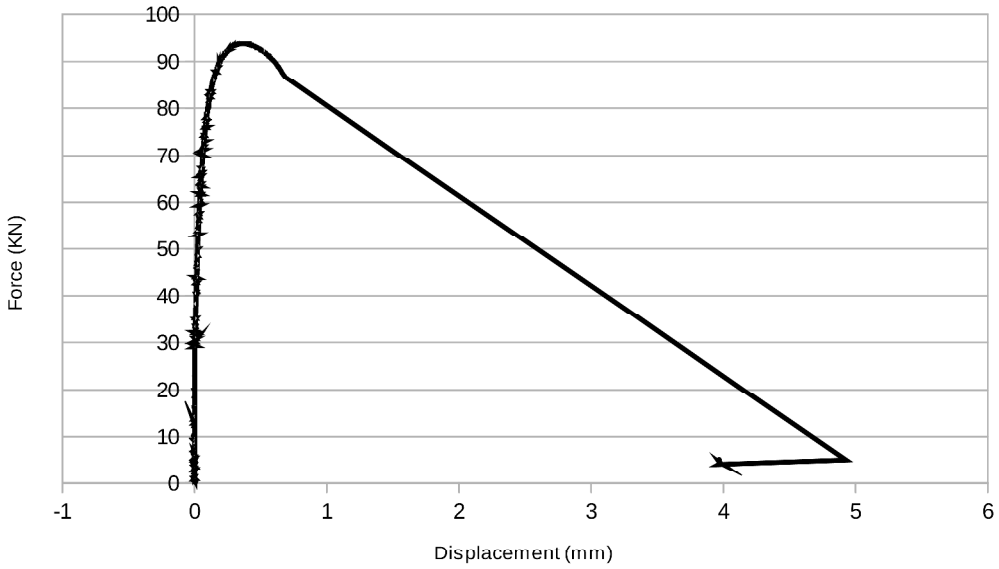

Force Max:	93.843	KN
Residual:	N/A	KN
Max Stress:	624	Kpa
Res. Stress:	N/A	Kpa

Comments: Sudden failure after reaching maximum force

Time (min)	Probe 1 (°C)	Probe 2 (°C)	Probe 3 (°C)	Probe 4 (°C)
0	-6.687	-6.562		
10	-6.562	-6.312		
20	-6.375	-6.187		
30	-6.187	-6		
40	-6	-5.875		
50	-5.812	-5.687		
75	-5.625	-5.562		

Probe set-up

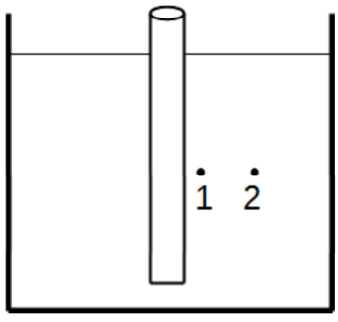

Pull out 6 (residual testing)

Test Date: 03/03/15 Embedded depth : 419 mm

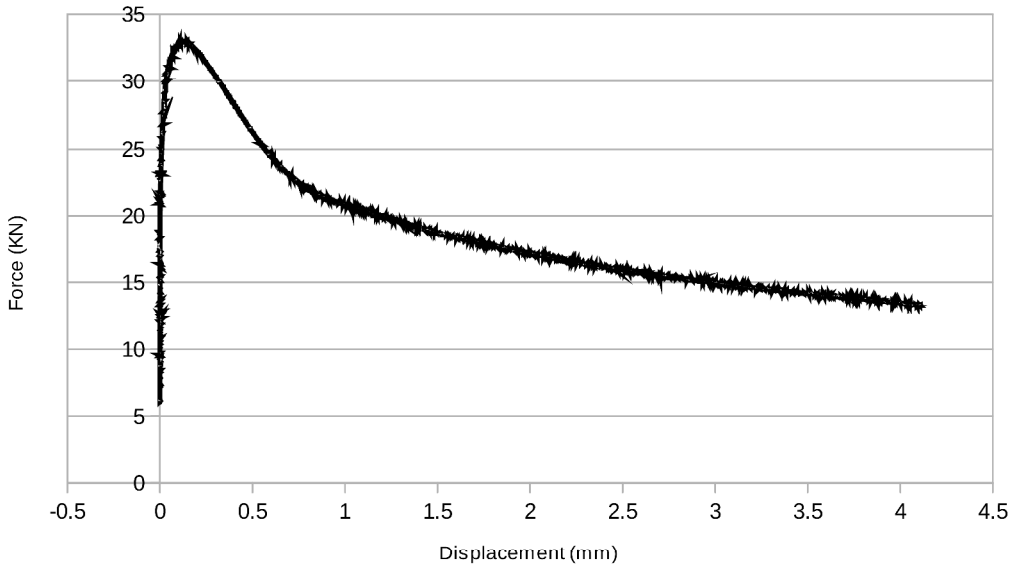

Force Max:	N/A	KN
Residual:	32.9595	KN
Max Stress:	N/A	Kpa
Res. Stress:	222	Kpa

Comments: Pull out test 6 was immediately restarted after failure to test residual strength

Time (min)	Probe 1 (°C)	Probe 2 (°C)	Probe 3 (°C)	Probe 4 (°C)
0	-5.437	-5.375		
10	-5.25	-5.25		
20	-5.062	-5.062		
30	-4.937	-4.937		
40	-4.75	-4.937		

Probe set-up

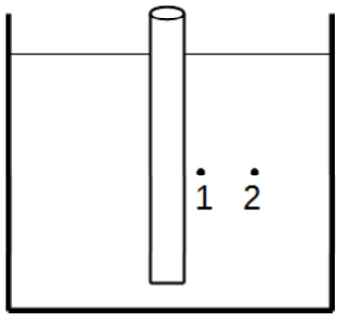

Pull out 7

Test Date: 03/06/15 Embedded depth : 428 mm

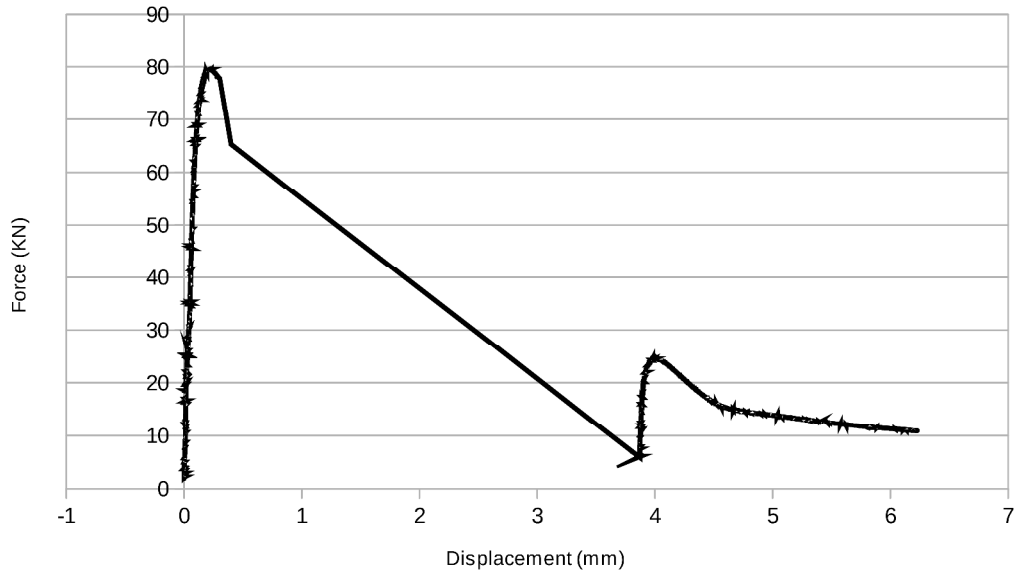

Force Max:	79.449	KN	Comments:
Residual:	24.5198	KN	
Max Stress:	517	Kpa	
Res. Stress:	160	Kpa	

Sudden failure after reaching maximum force. Failure happened at 70min. Test was continued to test for residual strength

Time (min)	Probe 1 (°C)	Probe 2 (°C)	Probe 3 (°C)	Probe 4 (°C)
0	-8.187	-7.375	-6.375	-6.437
5	-8.125	-7.312	-6.375	-63.12
10	-8.0642	-7.25	-6.312	-6.125
20	-7.875	-7.125	-6.312	-5.812
30	-7.812	-7	-6.187	-5.5
40	-7.5	-6.875	-6.125	-5.187
50	-7.312	-6.75	-5.937	-5.187
60	-7.125	-6.562	-5.812	-4.687
70	-6.937	-6.437	-5.687	-4.5
80	-6.87	-6.25	-5.562	-4.187
90	-6.5	-6.062	-5.375	-3.937
100	-6.312	-5.875	-5.25	-3.75

Probe set-up

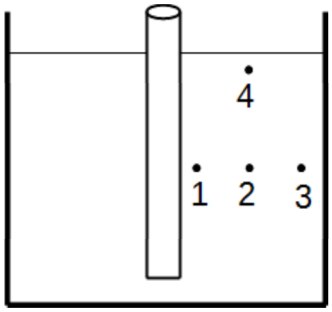

.

Pull out 8

Test Date: 03/17/15 Embedded depth : 406 mm

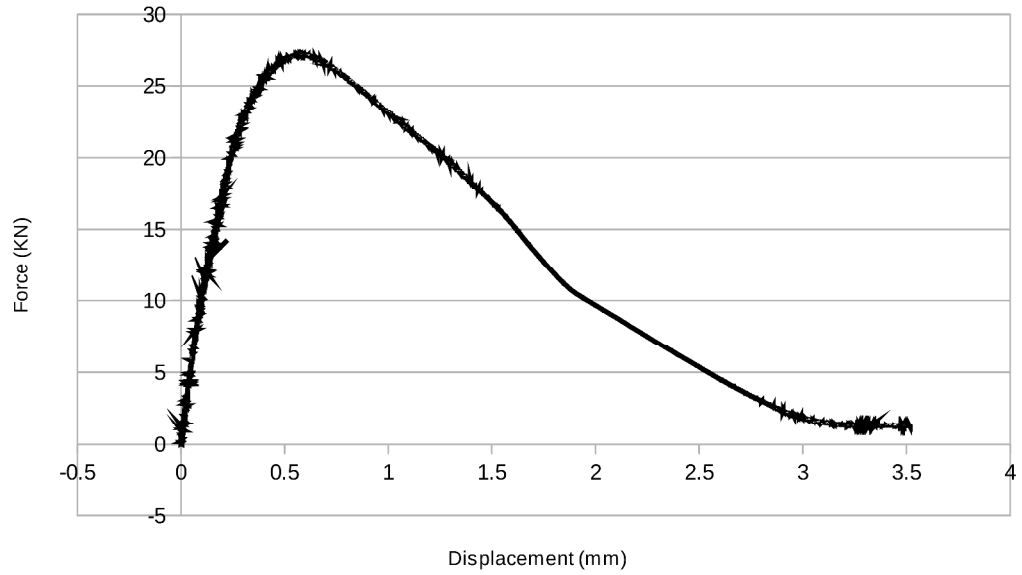

Force Max:	N/A	KN
Residual:	27.1478	KN
Max Stress:	N/A	Kpa
Res. Stress:	186	Kpa

Comments: Pile was hit when installed on the machine. The test only yielded residual strength

Time (min)	Probe 1 (°C)	Probe 2 (°C)	Probe 3 (°C)	Probe 4 (°C)
0	-5.500	-5.437	-3.937	-3.812
5	-5.437	-5.375	-3.937	-3.750
10	-5.375	-5.312	-3.875	-3.562
15	-5.312	-5.250	-3.812	-3.437
20	-5.250	-5.125	-0.381	-3.312
30	-5.062	-5.000	-3.687	-3.000
40	-4.937	-4.875	-3.625	-2.687
44	-4.812	-4.750	-3.625	-2.562
50	-4.750	-4.687	-3.500	-2.500
55	-5.625	-4.625	-3.437	-2.375

Probe set-up

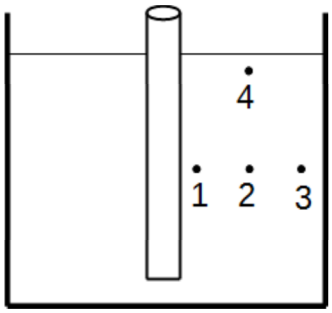

Pull out 9

Test Date: 06/25/15 Embedded depth : 406 mm

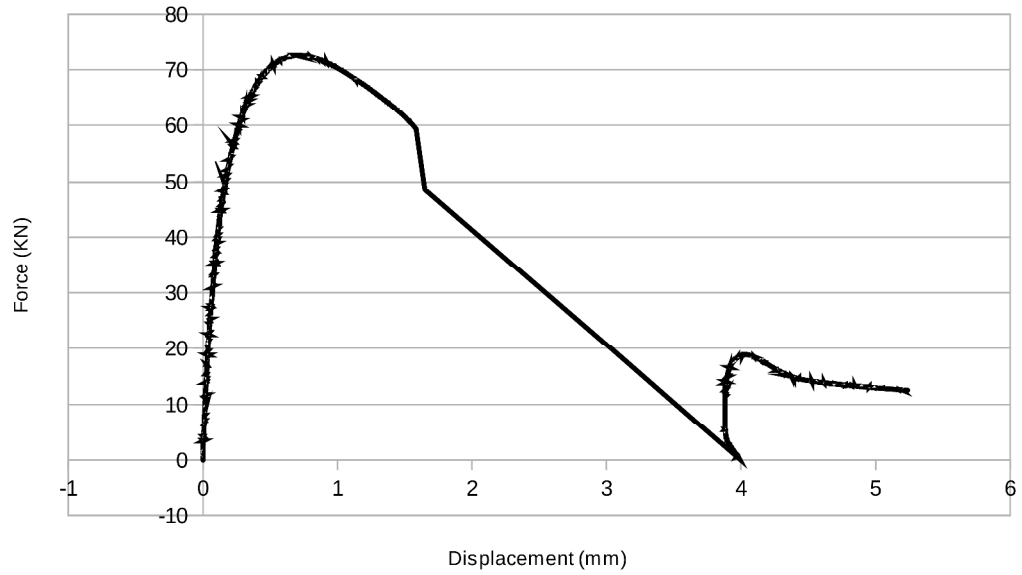

Force Max:	72.552	KN	Comments: Sudden failure after reaching maximum force. Failure occurred at 60min. Test was continued to test residual strength
Residual:	18.8318	KN	
Max Stress:	497	Kpa	
Res. Stress:	129	Kpa	

Time (min)	Probe 1 (°C)	Probe 2 (°C)	Probe 3 (°C)	Probe 4 (°C)
0	-6.000	-6.000	-4.750	-5.125
10	-5.937	-5.875	-4.750	-4.750
20	-5.812	-5.875	-4.687	-4.437
30	-5.625	-5.687	-4.625	-4.125
40	-5.500	-5.500	-4.562	-4.125
50	-5.500	-5.375	-4.437	-3.562
60	-5.125	-5.250	-4.375	-3.312
70	-5.125	-5.062	-4.375	-3.125
78	-4.812	-4.937	-4.125	-2.937

Probe set-up

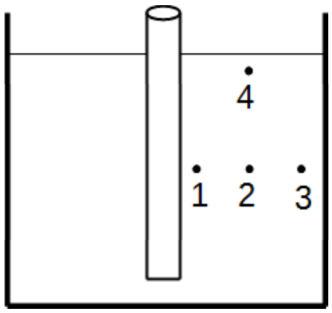

Pull out 10

Test Date: 07/07/15 Embedded depth : 406 mm

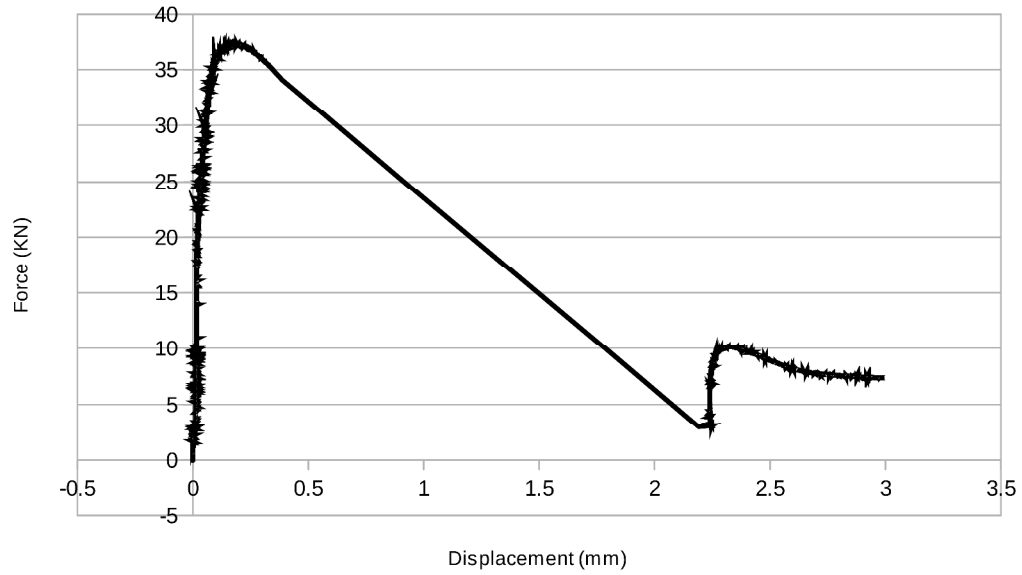

Force Max:	37.2908	KN	Comments:
Residual:	10.1092	KN	
Max Stress:	256	Kpa	
Res. Stress:	69	Kpa	

Sudden failure after reaching maximum force. Pulling clamp on the machine were sliding during the test. Results of test 10 will be ignored

Time (min)	Probe 1 (°C)	Probe 2 (°C)	Probe 3 (°C)	Probe 4 (°C)
0	-5.812	-5.750	-4.062	-4.250
10	-5.750	-5.562	-4.000	-3.937
20	-5.625	-5.375	-3.937	-3.562
30	-5.437	-5.250	-3.877	-3.187
40	-5.312	-5.125	-3.812	-2.875
45	-5.250	-5.000	-3.750	-2.687
50	-5.125	-4.937	-3.687	-2.625
55	-5.062	-4.875	-3.625	-2.500

Probe set-up

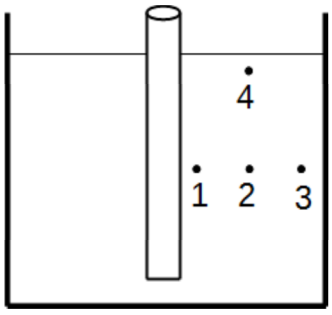

Pull out 11

Test Date: 07/20/15 Embedded depth : 406 mm

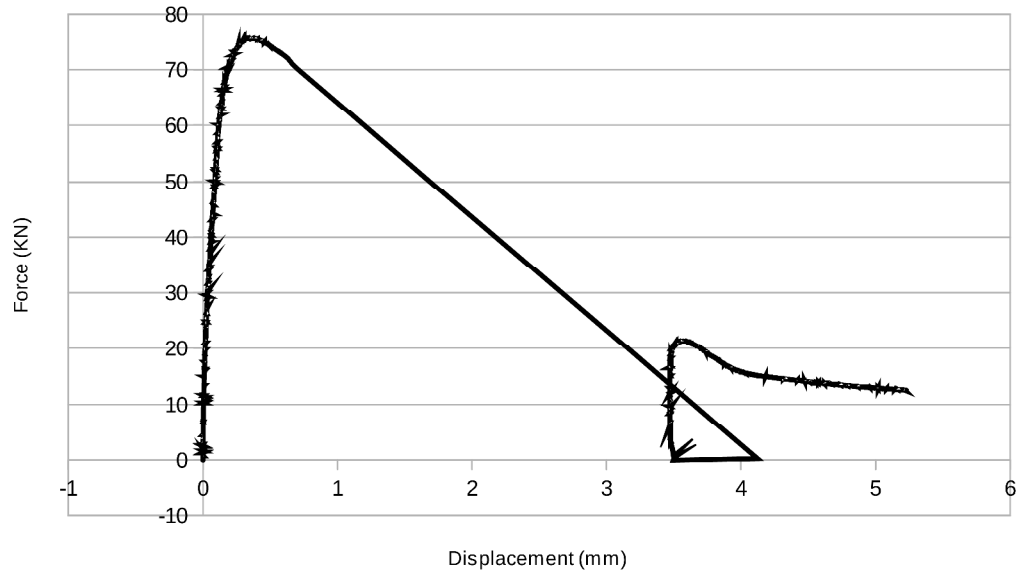

Force Max:	75.6683	KN	Comments: Sudden failure after reaching maximum force. Failure occurred at 72min. The test was continued to test residual strength
Residual:	21.345	KN	
Max Stress:	519	Kpa	
Res. Stress:	146	Kpa	

Time (min)	Probe 1 (°C)	Probe 2 (°C)	Probe 3 (°C)	Probe 4 (°C)
0	-6.187	-6.125	-4.687	-5.062
10	-6.062	-5.937	-4.562	-4.750
20	-6.062	-5.812	-4.500	-4.375
30	-5.812	-5.625	-4.375	-4.062
40	-5.812	-5.500	-4.250	-3.687
50	-5.500	-5.375	-4.125	-3.437
58	-5.312	-5.187	-4.000	-3.187
60	-5.312	-5.181	-3.937	-3.128
70	-5.187	-5.181	-3.875	-2.937
80	-5.000	-4.875	-3.687	-2.687

Probe set-up

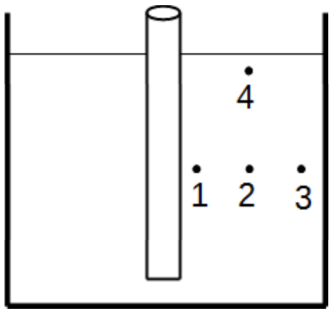

Pull out 12

Test Date: 08/24/15 Embedded depth : 305 mm

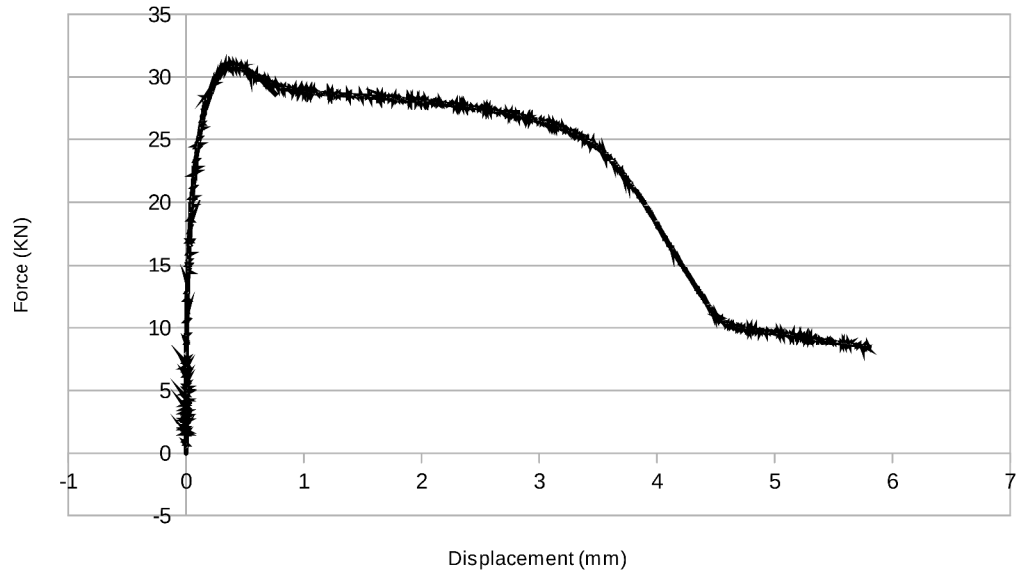

Force Max:	N/A	KN
Residual:	30.828	KN
Max Stress:	N/A	Kpa
Res. Stress:	282	Kpa

Comments: Sample was left to freeze for 1 month. No sudden failure and no second residual curve. Sample was probably damage. The values will be ignored since the cause of the divergence is unknown

Time (min)	Probe 1 (°C)	Probe 2 (°C)	Probe 3 (°C)	Probe 4 (°C)
0				
10	-5.687	-5.625	-4.250	-4.750
20	-5.562	-5.500	-4.000	-4.437
25	-5.375	-5.375	-3.875	-4.312
30	-5.312	-5.250	-3.687	-4.125
35	-5.187	-5.187	-3.562	-4.000
40	-5.062	-5.062	-3.437	-3.875
50	-4.812	-4.812	-3.181	-3.625
60	-4.562	-4.625	-2.937	-3.120
70	-4.375	-4.437	-2.750	-0.062
75	-4.250	-4.312	-2.687	-3.062

Probe set-up

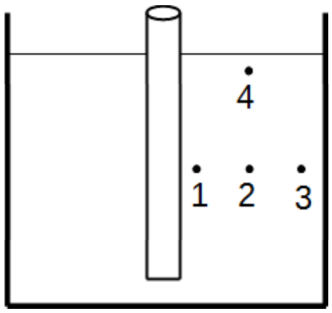

Pull out 13

Test Date: 08/31/15 Embedded depth : 305 mm

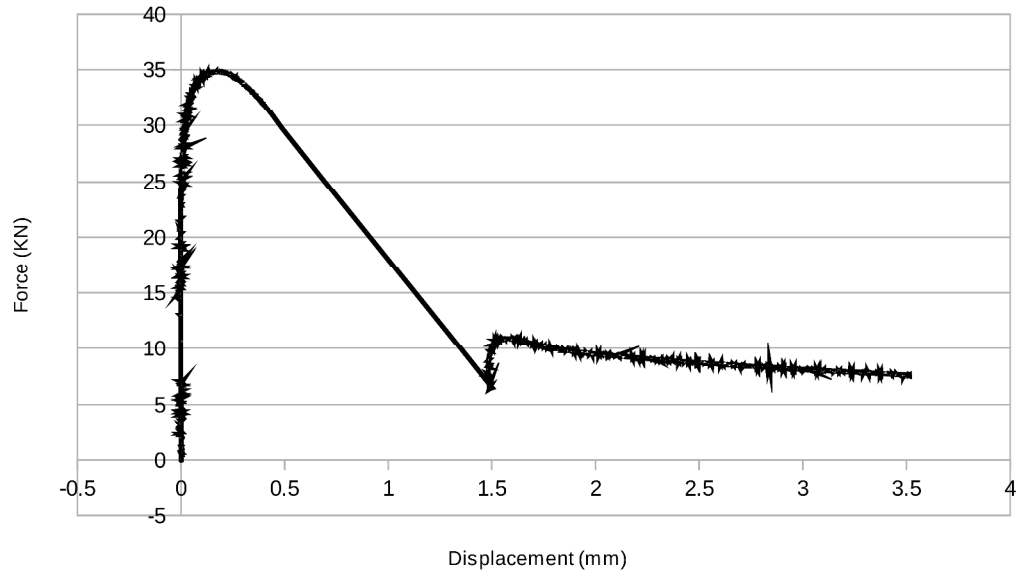

Force Max:	34.8203	KN
Residual:	10.887	KN
Max Stress:	318	Kpa
Res. Stress:	99	Kpa

Comments: Sudden failure after reaching maximum force. Failure occurred at 60min. Test was continued to test residual strength

Time (min)	Probe 1 (°C)	Probe 2 (°C)	Probe 3 (°C)	Probe 4 (°C)
0	-5.875	-5.812	-4.687	-5.250
10	-5.687	-5.562	-4.187	-4.625
20	-5.625	-5.500	-4.125	-4.500
30	-5.437	-5.312	-3.812	-4.187
40	-5.187	-5.125	-3.625	-3.875
50	-5.000	-4.937	-3.625	-3.625
60	-4.750	-4.687	-3.125	-3.312
70	-4.500	-4.500	-3.000	-3.000
80	-4.250	-4.250	-2.812	-2.812
85	-4.250	-4.187	-2.687	-2.750

Probe set-up

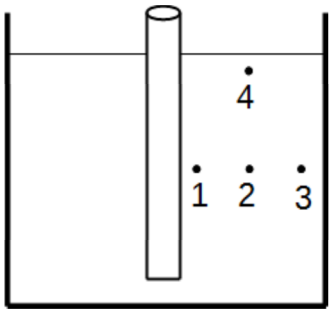

Pull out 14

Test Date: 09/08/15 Embedded depth : 302 mm

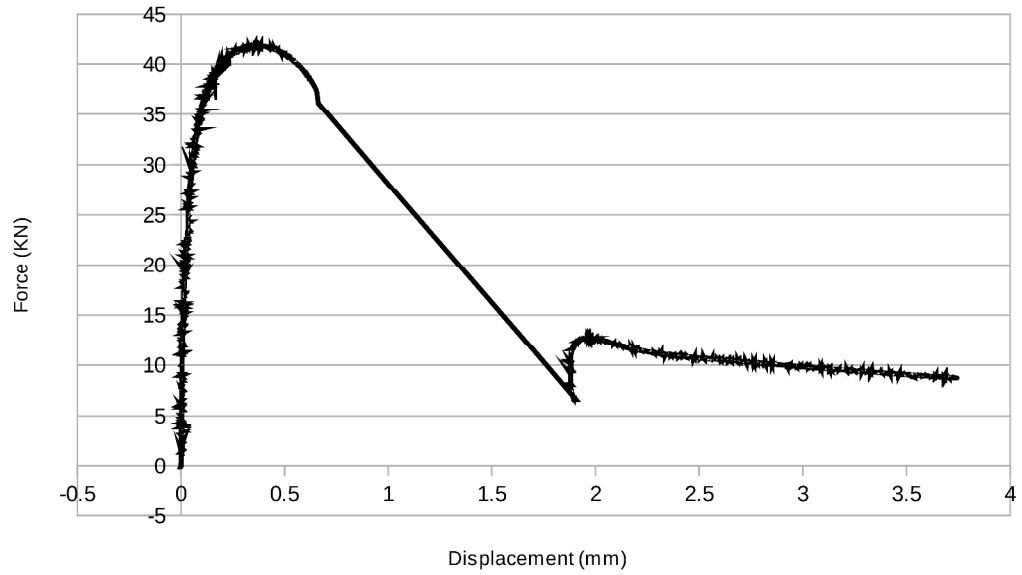

Force Max:	41.817	KN
Residual:	12.696	KN
Max Stress:	386	Kpa
Res. Stress:	117	Kpa

Comments: Sudden failure after reaching maximum force. Failure occurred at 41min. Test was continued to test residual strength

Time (min)	Probe 1 (°C)	Probe 2 (°C)	Probe 3 (°C)	Probe 4 (°C)
0	-5.750	-5.562	-4.250	-4.937
10	-5.625	-5.375	-4.000	-4.437
20	-5.500	-5.125	-3.750	-4.125
30	-5.312	-4.937	-3.500	-4.125
40	-5.062	-4.750	-3.312	-3.437
50	-5.062	-4.500	-3.062	-3.187
60	-4.562	-4.312	-2.875	-2.937

Probe set-up

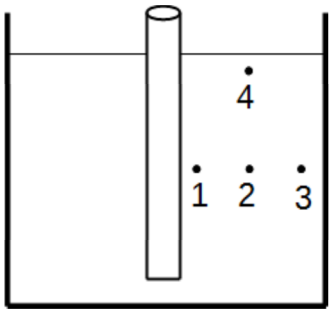

Appendix B. Interface test results

100F07A

Test Date: N/A

Normal Pressure 100 Kpa

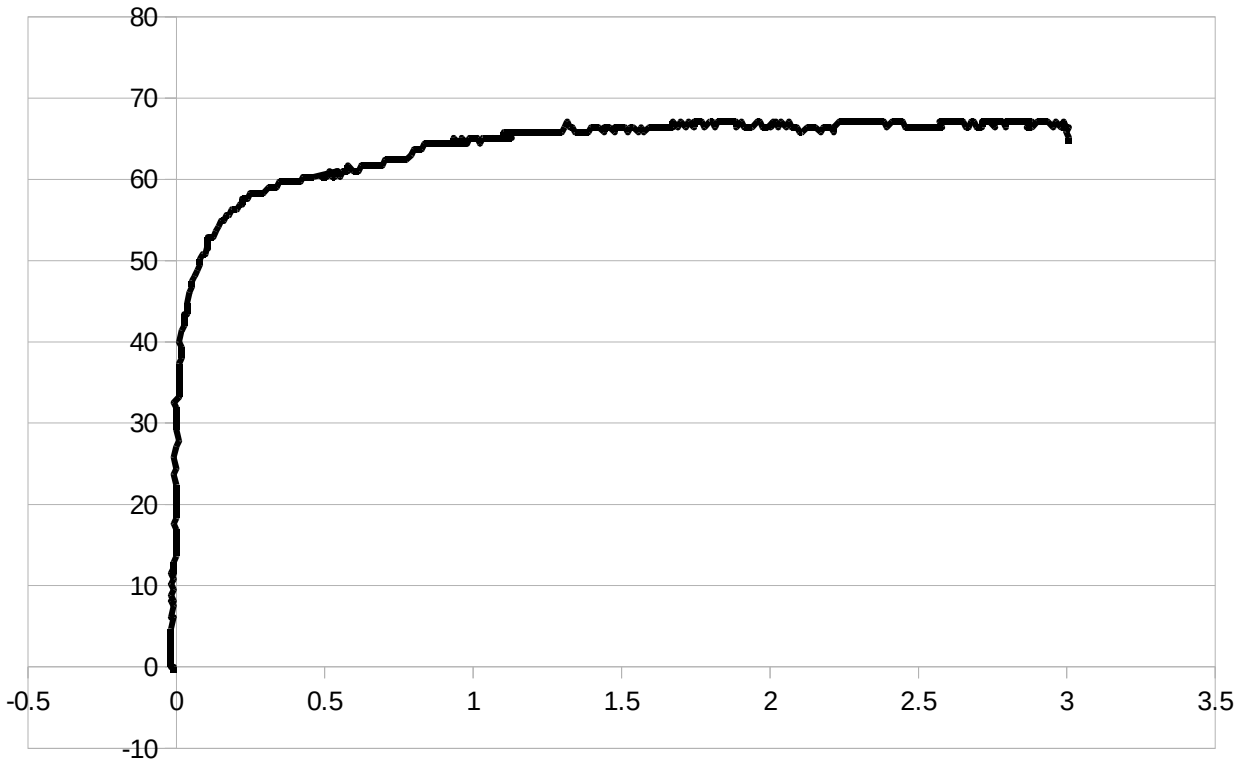

Max Stress: 67.1 Kpa

Res. Stress: N/A Kpa

Moisture : 7 %

Comments:

150F07A

Test Date: N/A

Normal Pressure 150 Kpa

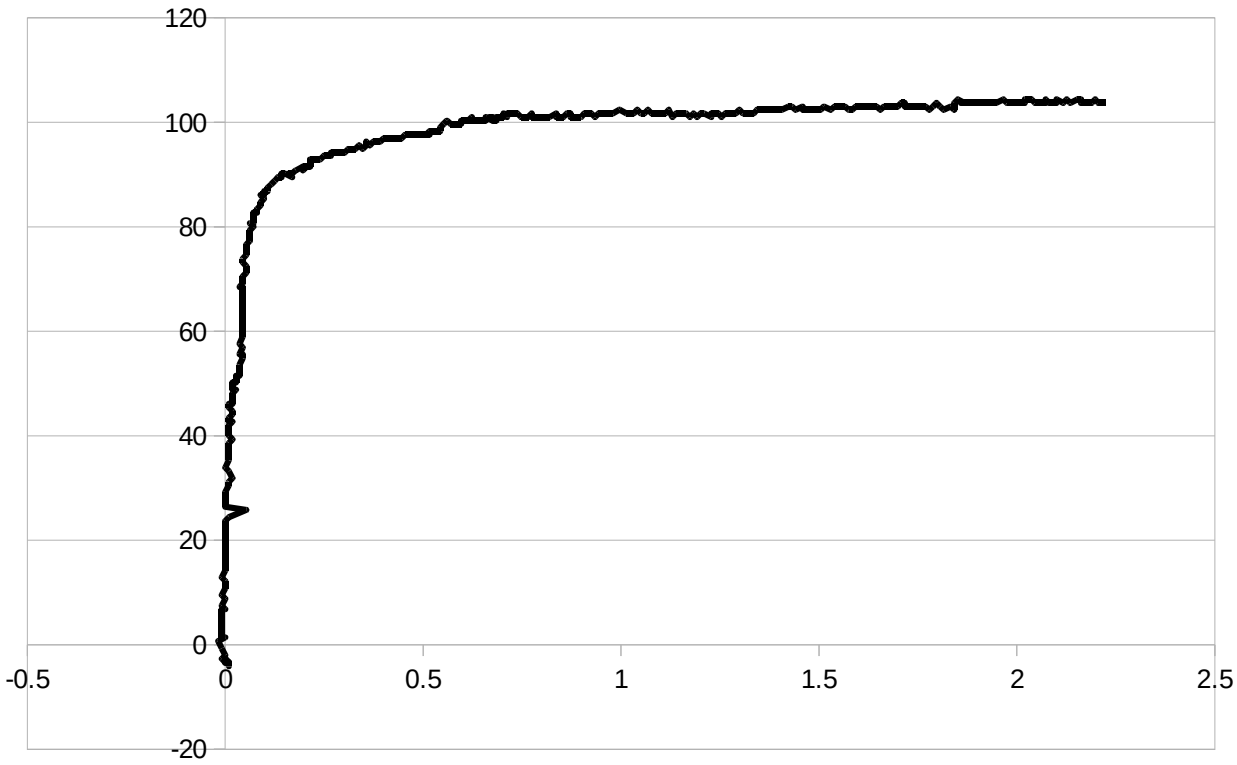

Max Stress: 103.0 Kpa

Res. Stress: N/A Kpa

Moisture : 7 %

Comments:

300F07A

Test Date: N/A

Normal Pressure 300 Kpa

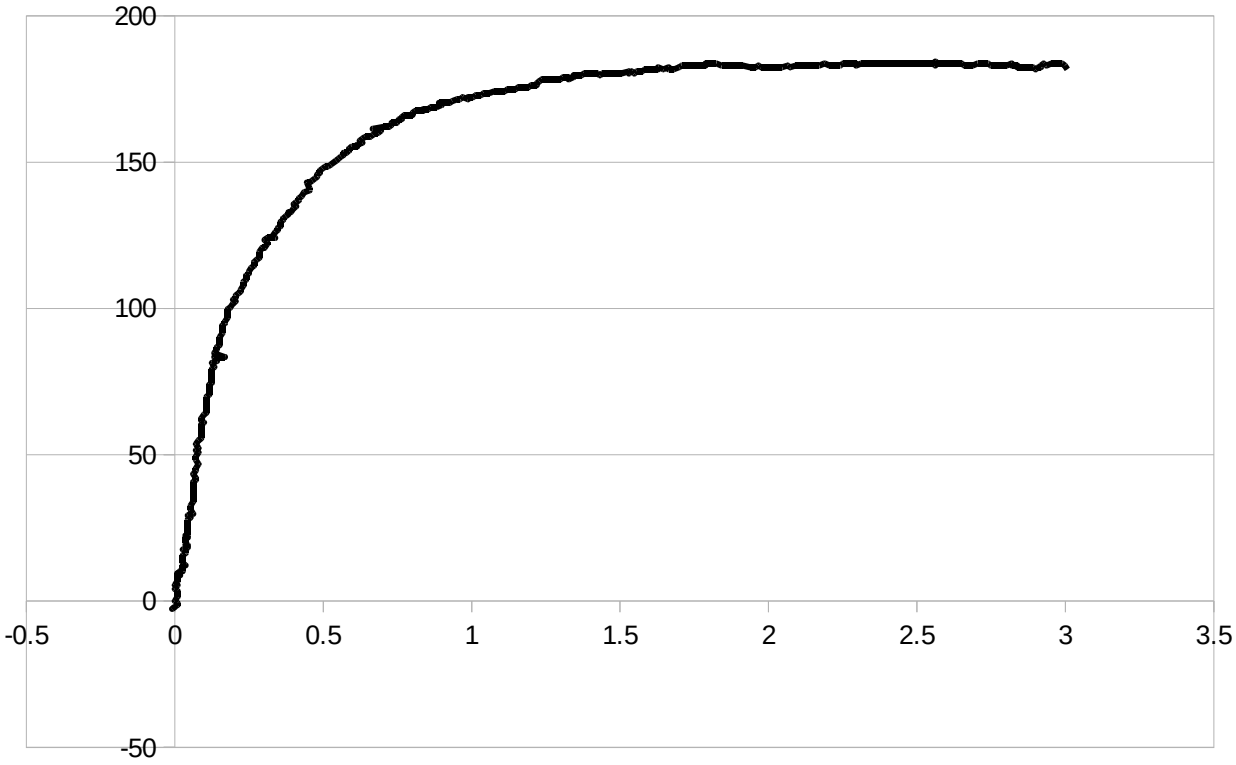

Max Stress: 183.0 Kpa

Res. Stress: N/A Kpa

Moisture : 7 %

Comments:

300F07B

Test Date: N/A

Normal Pressure 300 Kpa

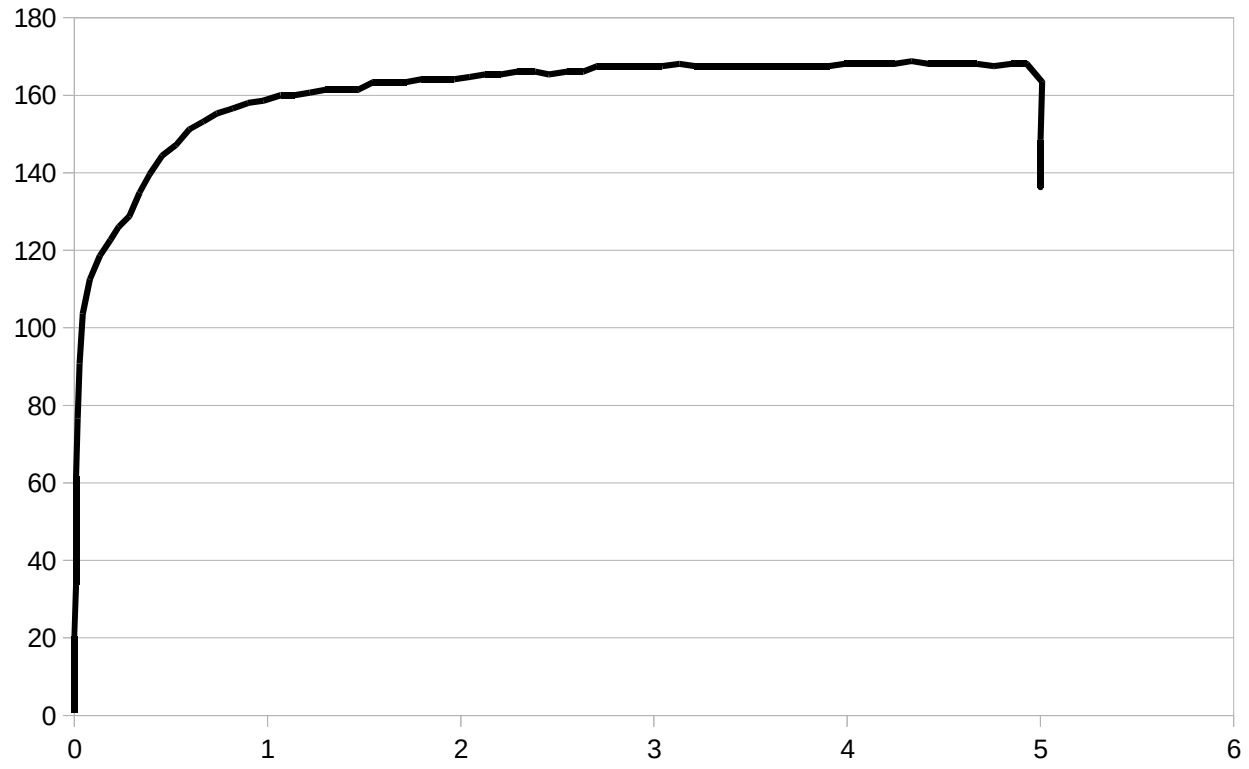

Max Stress: 168.8 Kpa

Res. Stress: N/A Kpa

Moisture : 7 %

Comments:

450F07A

Test Date: N/A

Normal Pressure 450 Kpa

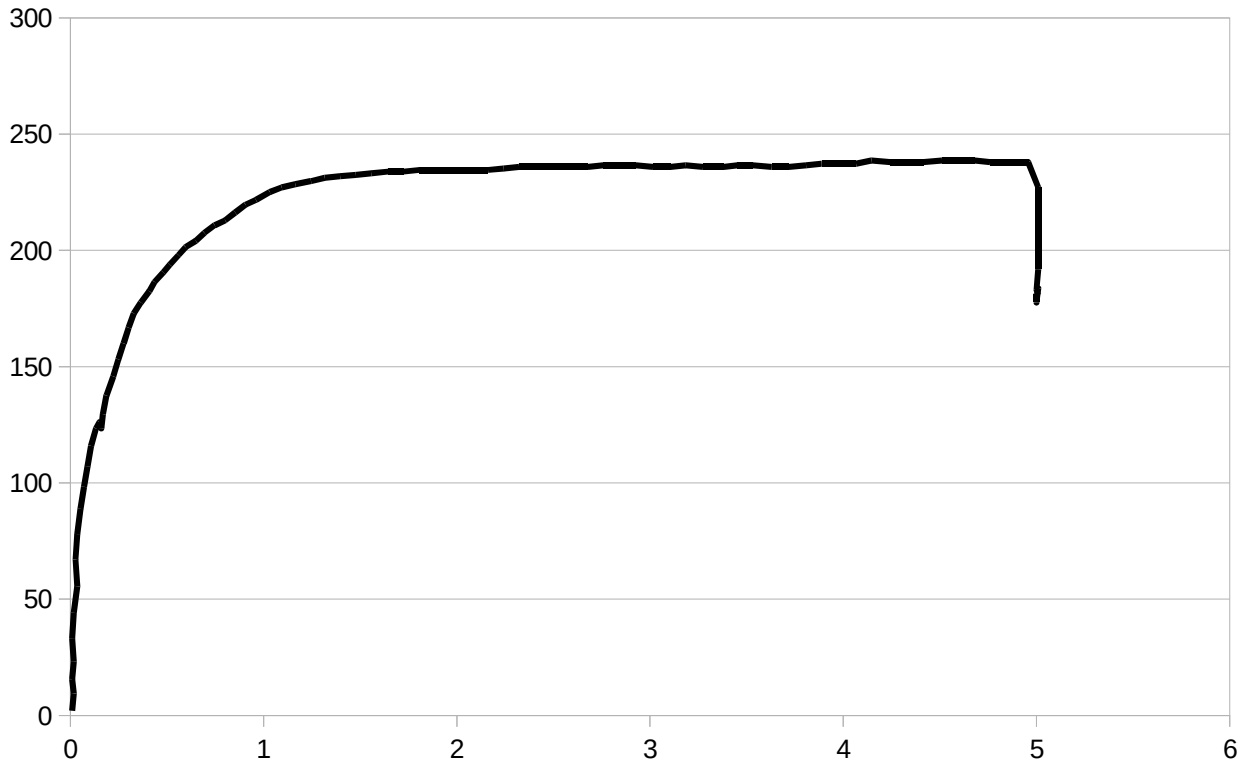

Max Stress: 238.6 Kpa

Res. Stress: N/A Kpa

Moisture : 7 %

Comments:

350F09A

Test Date: 14/04/16 Normal Pressure 350 Kpa

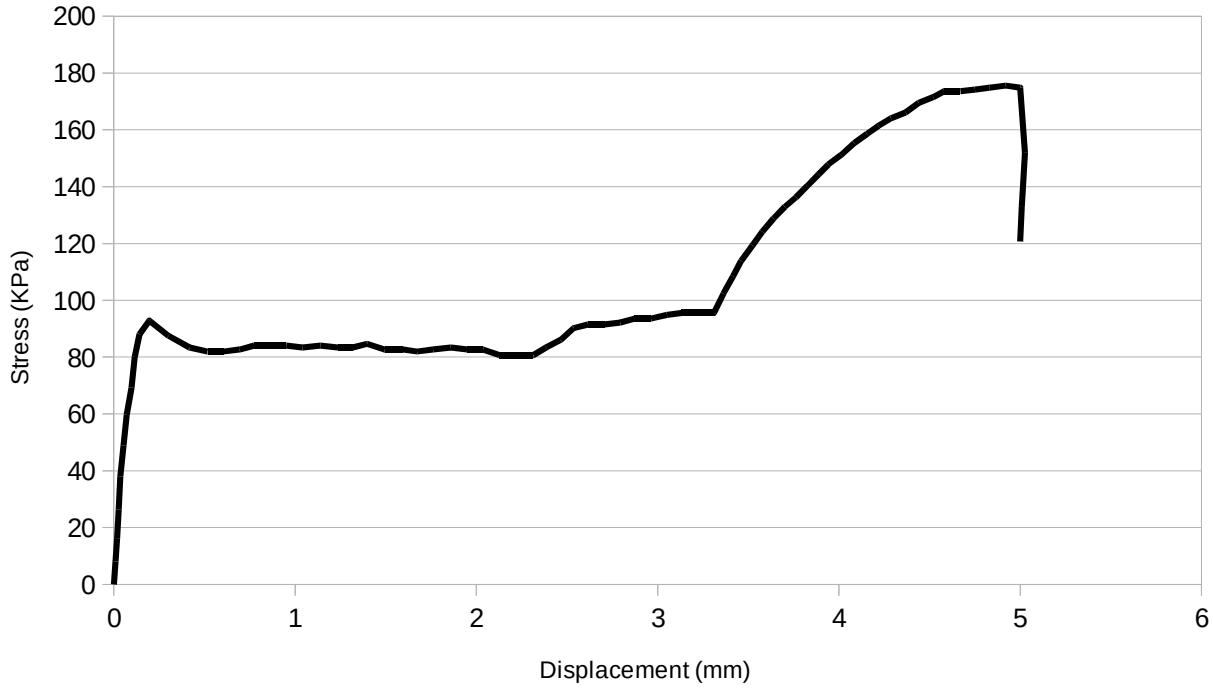

Max Stress: 176 Kpa

Res. Stress: N/A Kpa

Moisture : 9 %

Comments:

350F09B

Test Date: 16-08-05

Normal Pressure 350 Kpa

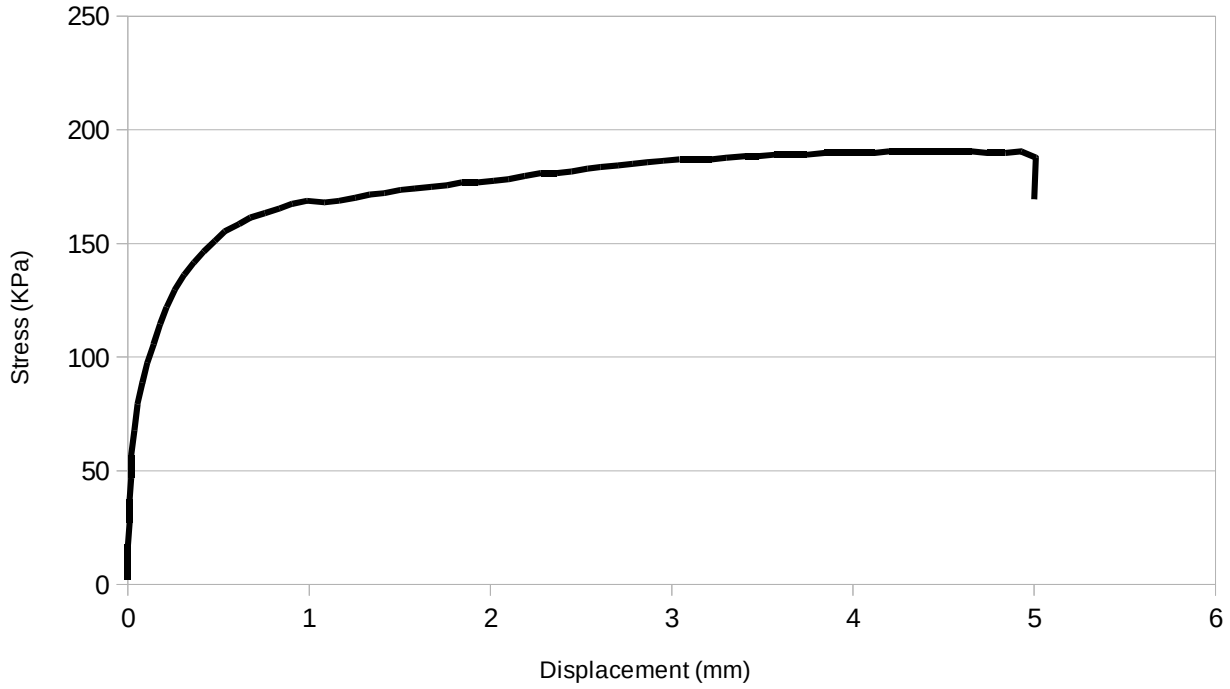

Max Stress: 191 Kpa

Res. Stress: N/A Kpa

Moisture : 9 %

Comments:

350F09I

Test Date: 16-09-07

Normal Pressure 350 Kpa

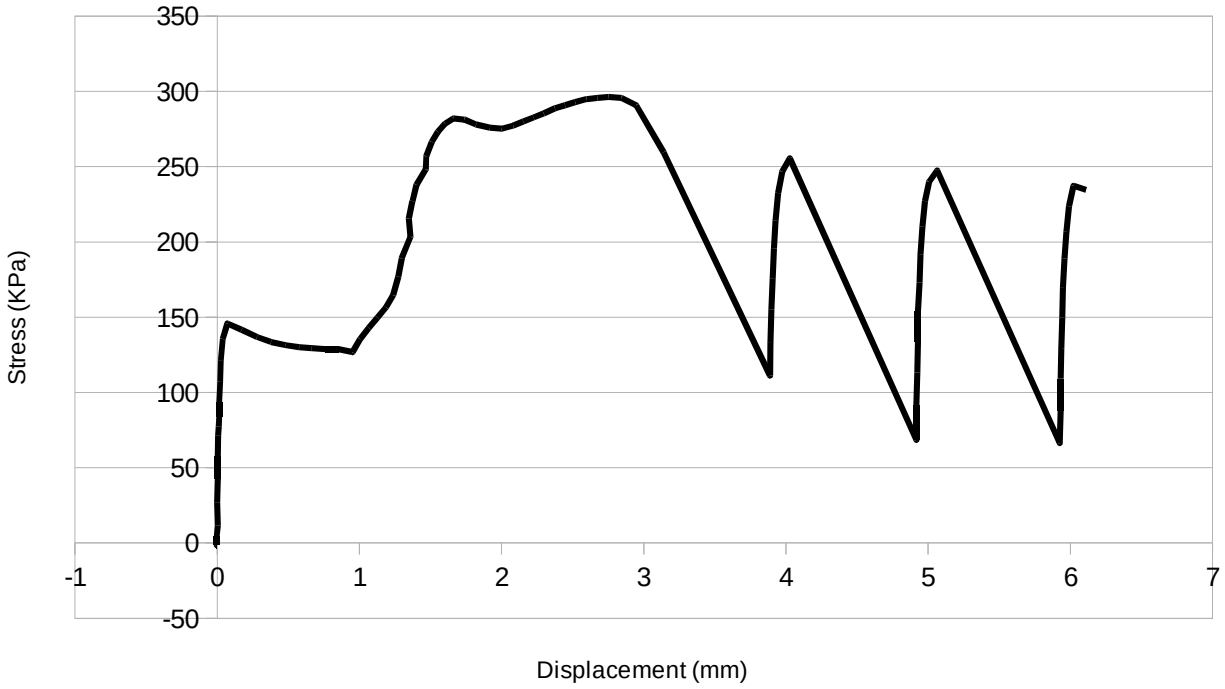

Max Stress: 296 Kpa

Res. Stress: 111.2 Kpa

Moisture : 9 %

Comments:

400F09A

Test Date: 13/04/16 Normal Pressure 400 Kpa

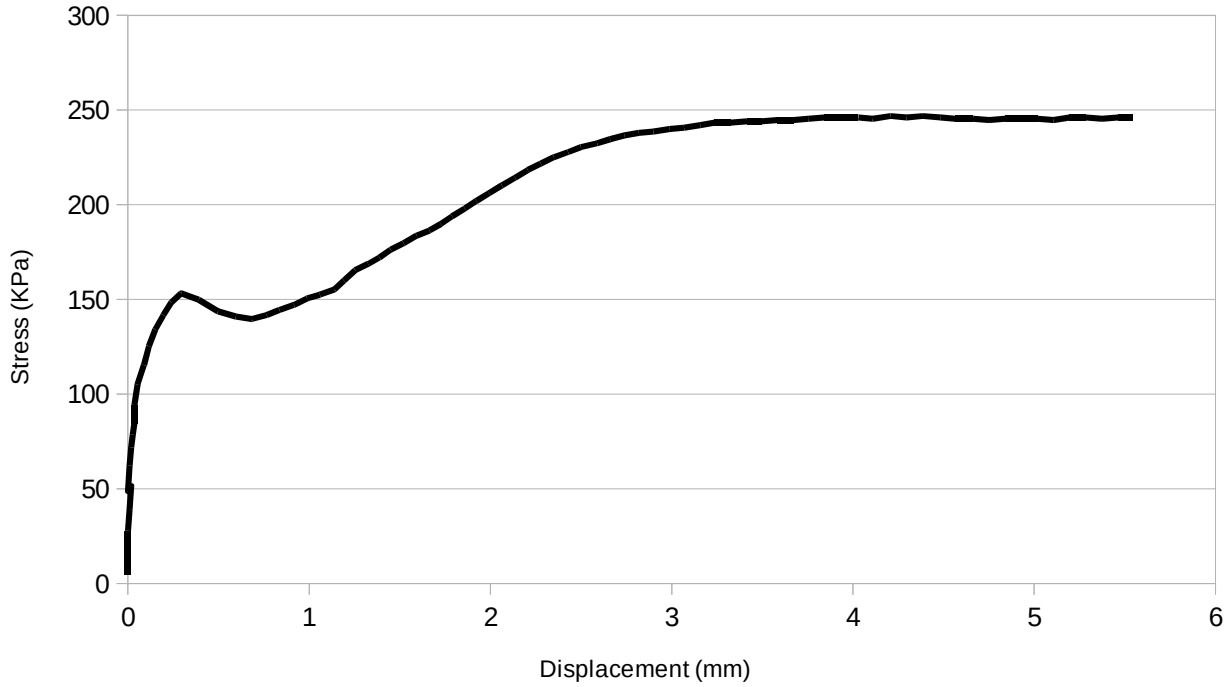

Max Stress: 247 Kpa

Res. Stress: N/A Kpa

Moisture : 9 %

Comments:

450F09A

Test Date: 13/04/16 Normal Pressure 450 Kpa

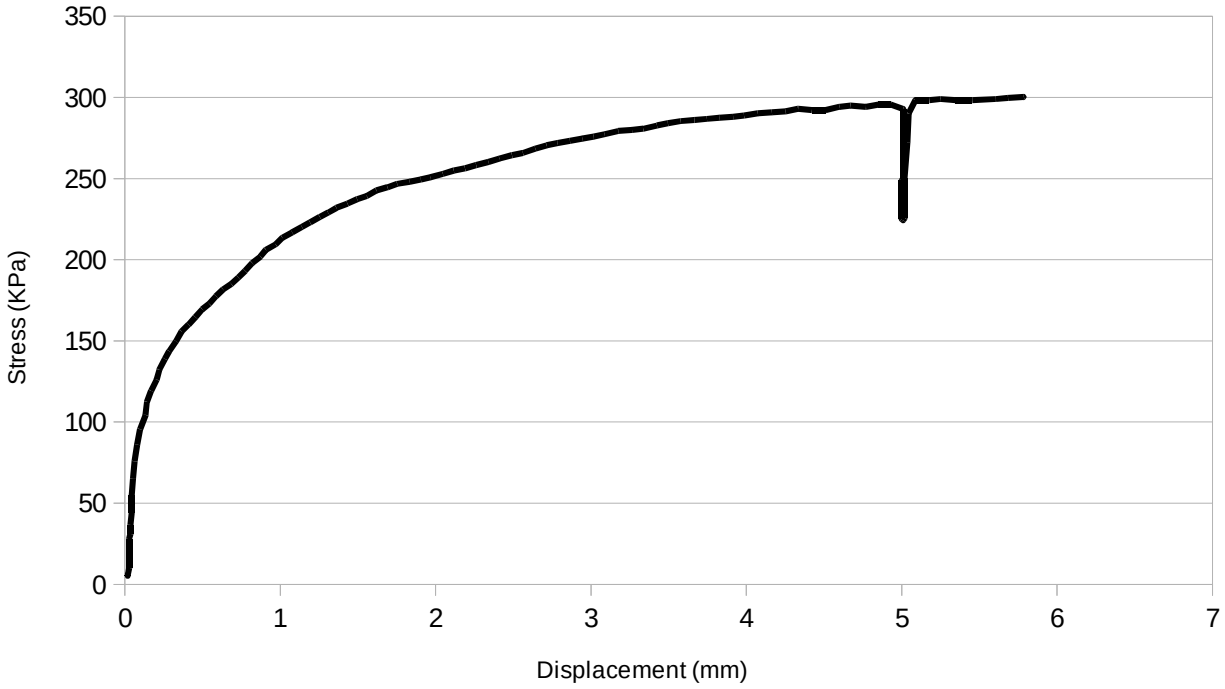

Max Stress: 286.1 Kpa

Res. Stress: N/A Kpa

Moisture : 9 %

Comments:

400F11A

Test Date: 20/06/016 Normal Pressure 400 Kpa

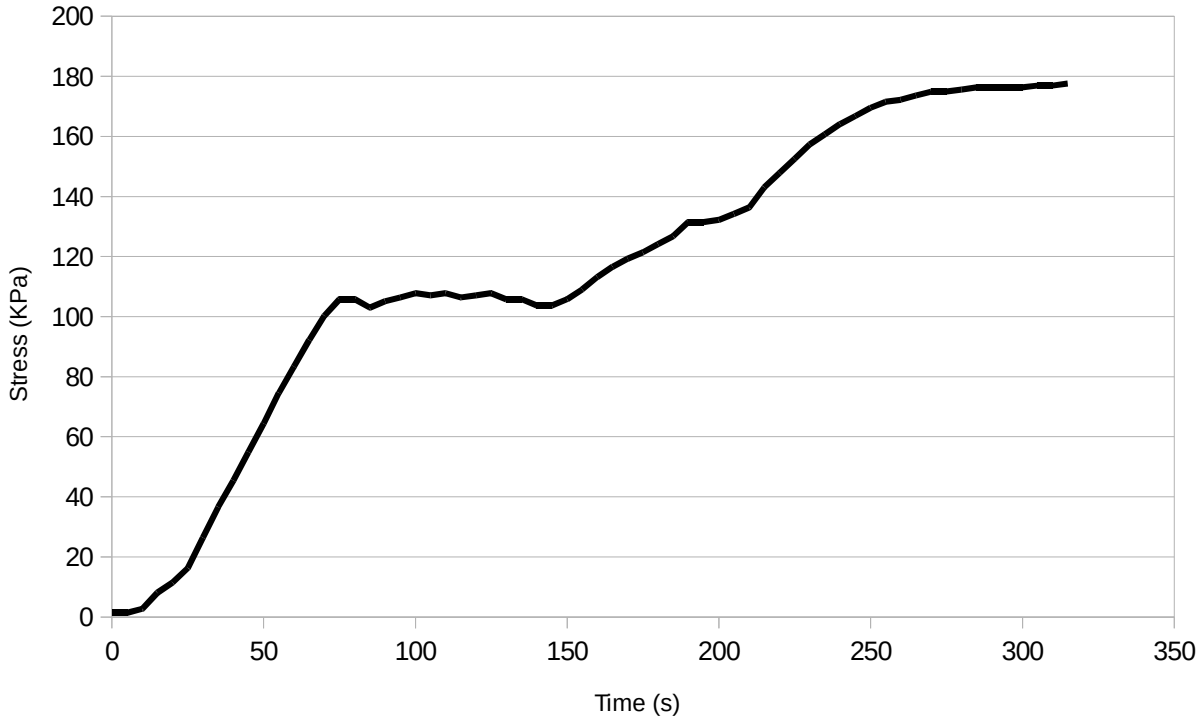

Max Stress: 177.6 Kpa

Res. Stress: N/A Kpa

Moisture : 11 %

Comments: Error with LVDT reading.

400F11I

Test Date: 24/06/16

Normal Pressure 400 Kpa

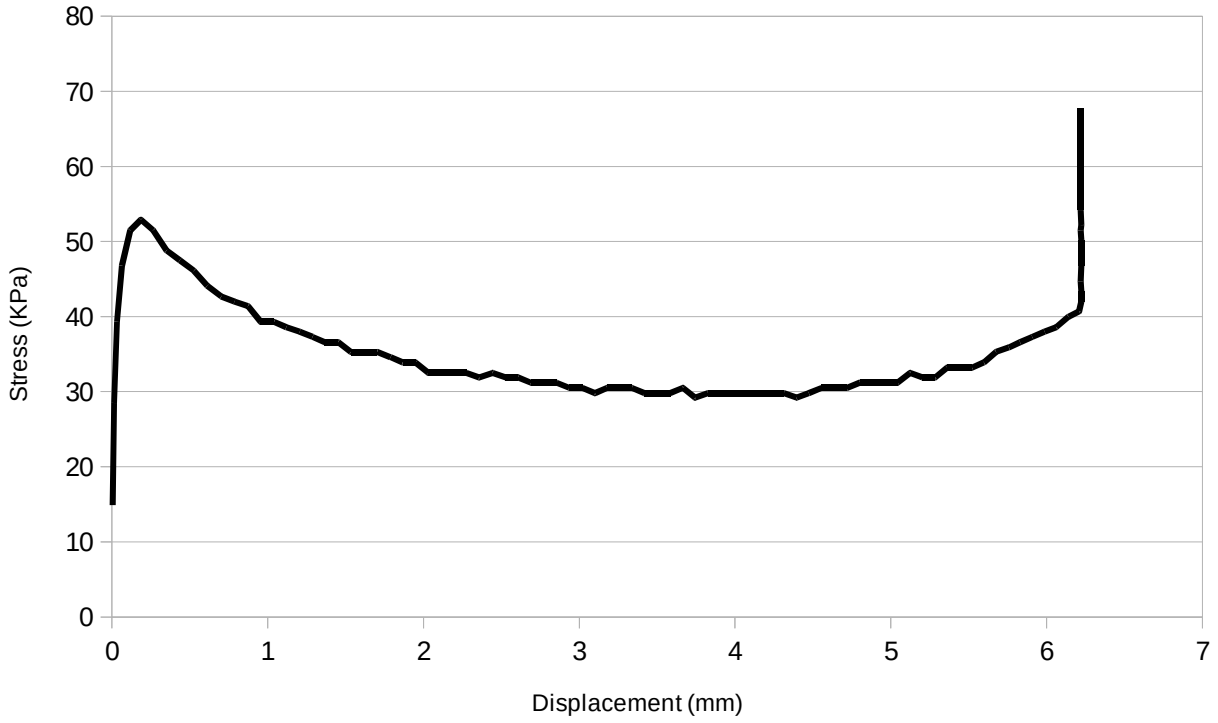

Max Stress: 52.9 Kpa

Res. Stress: 29.8 Kpa

Moisture : 11 %

Comments: Table hit the stopper at the end of the linear bearing. Readjusted position for next test

400F11J

Test Date: 25/06/16 Normal Pressure 400 Kpa

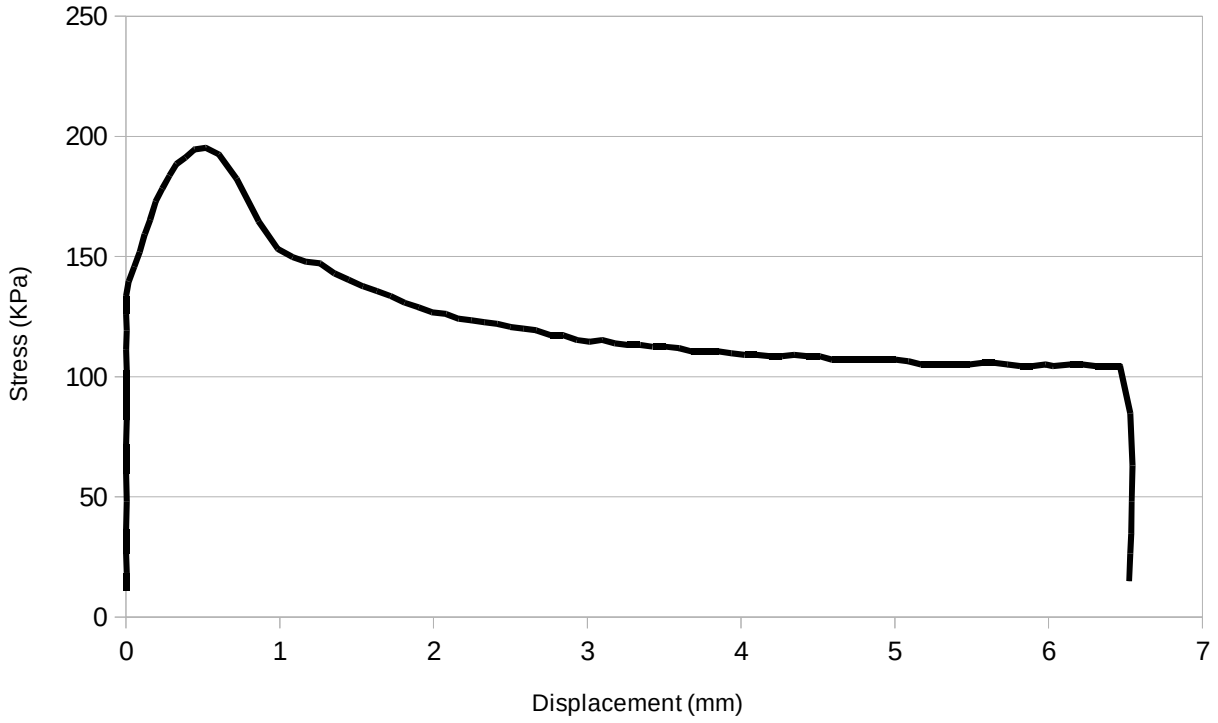

Max Stress: 195.2 Kpa

Res. Stress: 105.1 Kpa

Moisture : 11 %

Comments:

400F11K

Test Date: 26/06/16

Normal Pressure 400 Kpa

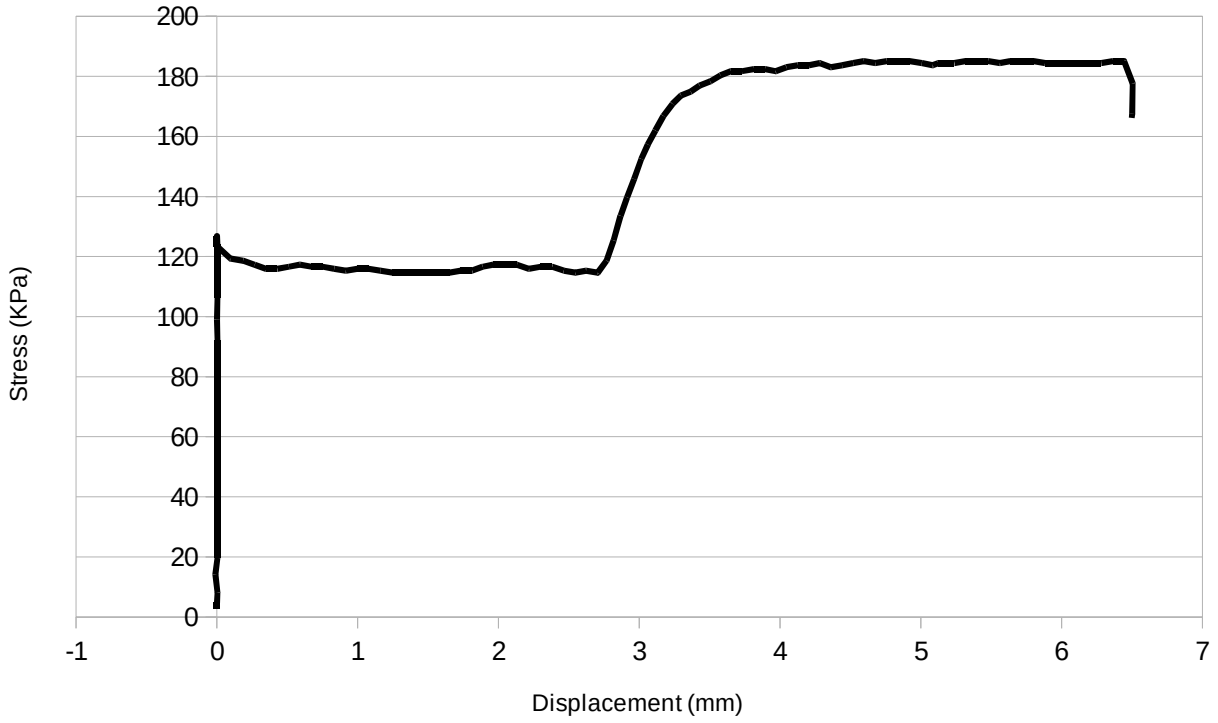

Max Stress: 185.1 Kpa

Res. Stress: N/A Kpa

Moisture : 11 %

Comments:

450F11A

Test Date: 25/05/16

Normal Pressure 450 Kpa

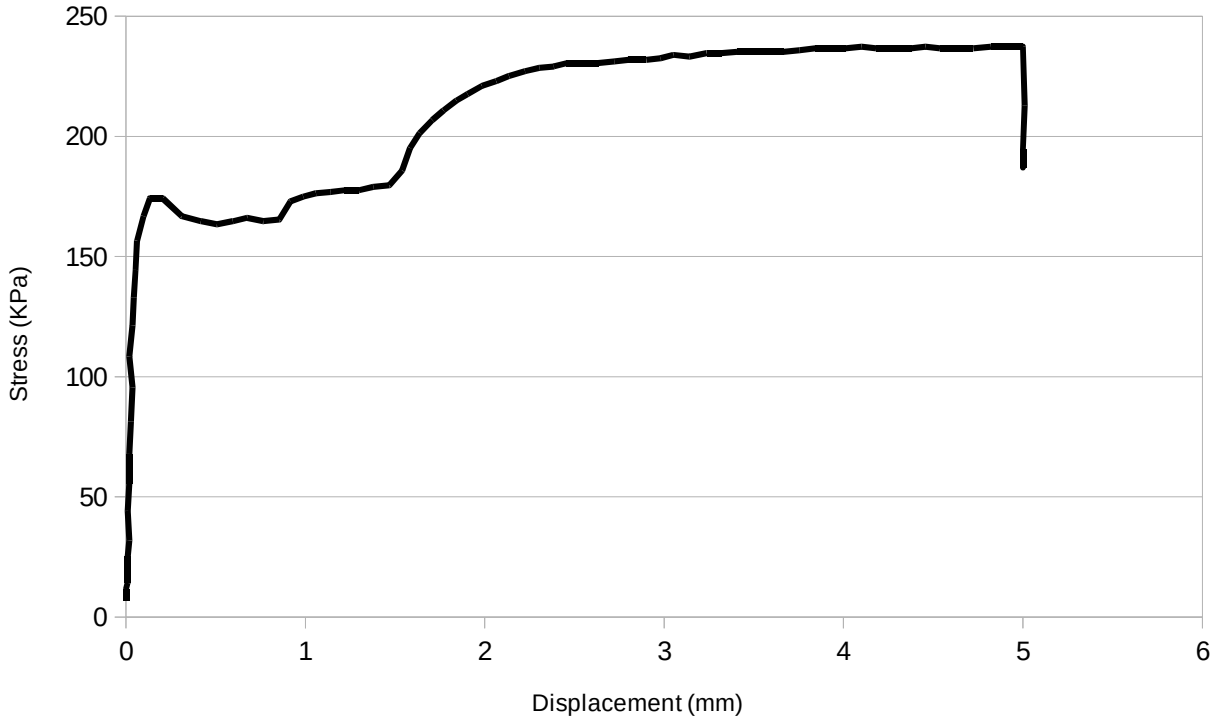

Max Stress: 237.3 Kpa

Res. Stress: N/A Kpa

Moisture : 11 %

Comments:

450F11I

Test Date: 25/08/16 Normal Pressure 450 Kpa

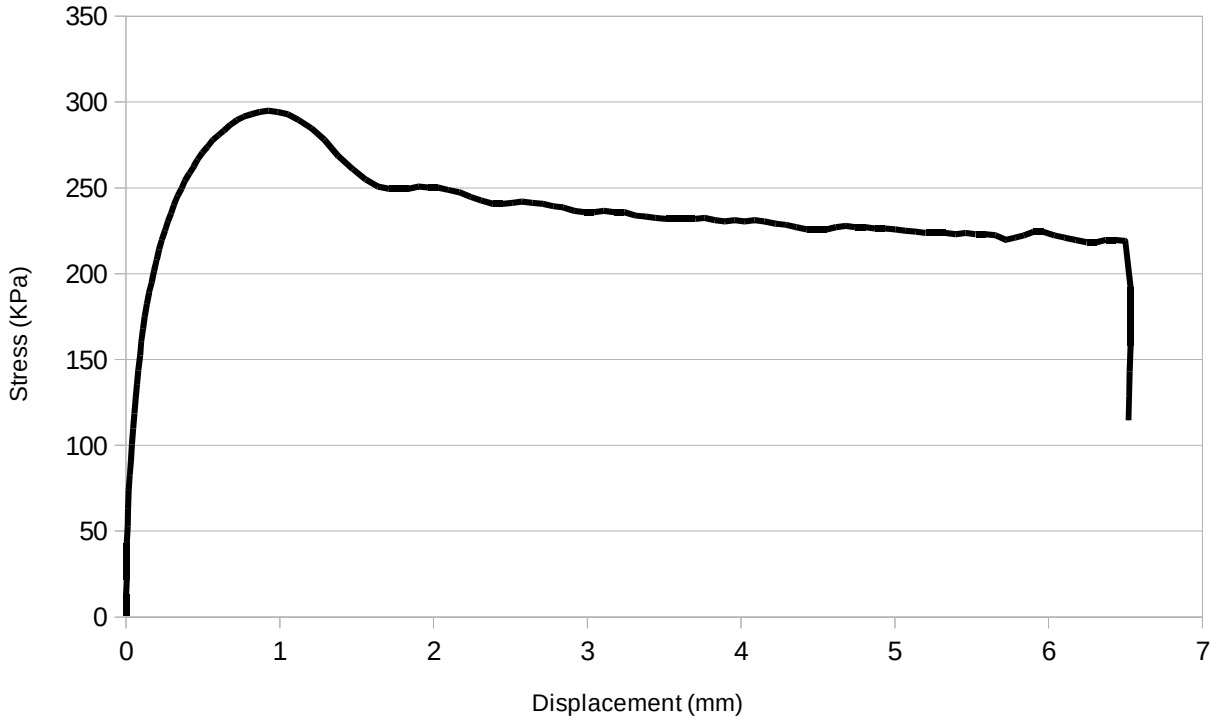

Max Stress: 294.9 Kpa

Res. Stress: 219.7 Kpa

Moisture : 11 %

Comments:

450F11M

Test Date: 28/08/16 Normal Pressure 450 Kpa

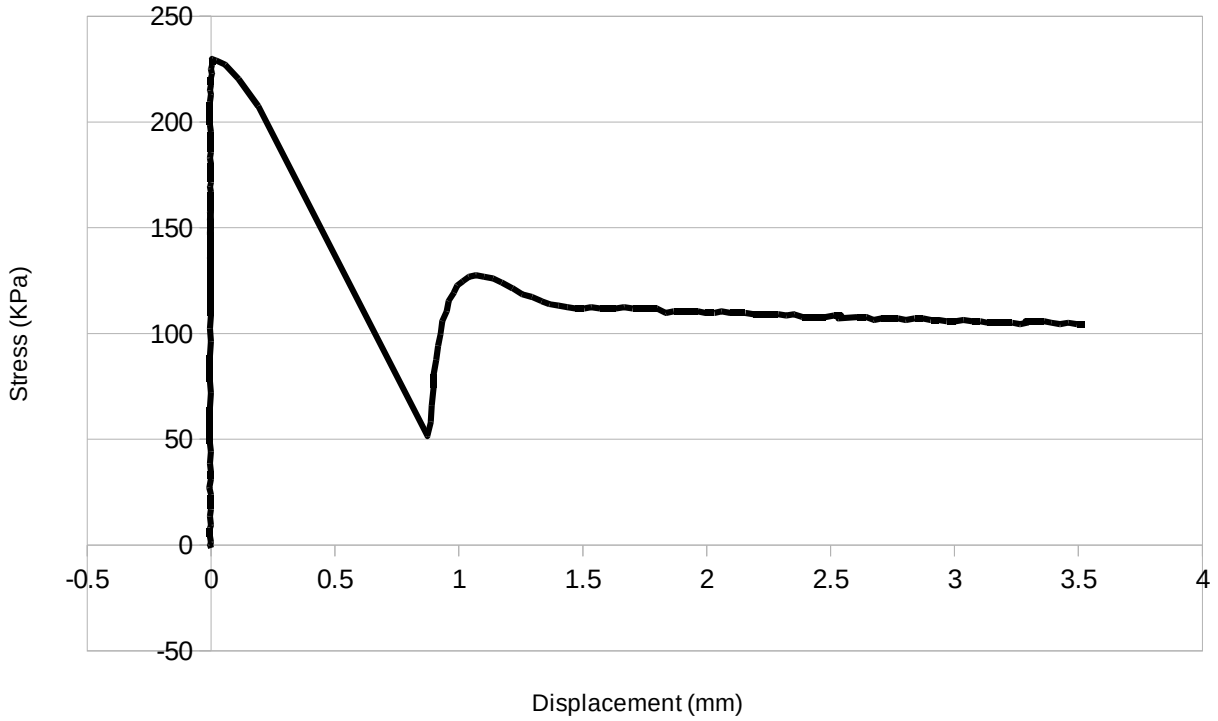

Max Stress: 229.8 Kpa

Res. Stress: 127.5 Kpa

Moisture : 11 %

Comments:

350F11I

Test Date: 16-11-08

Normal Pressure 450 Kpa

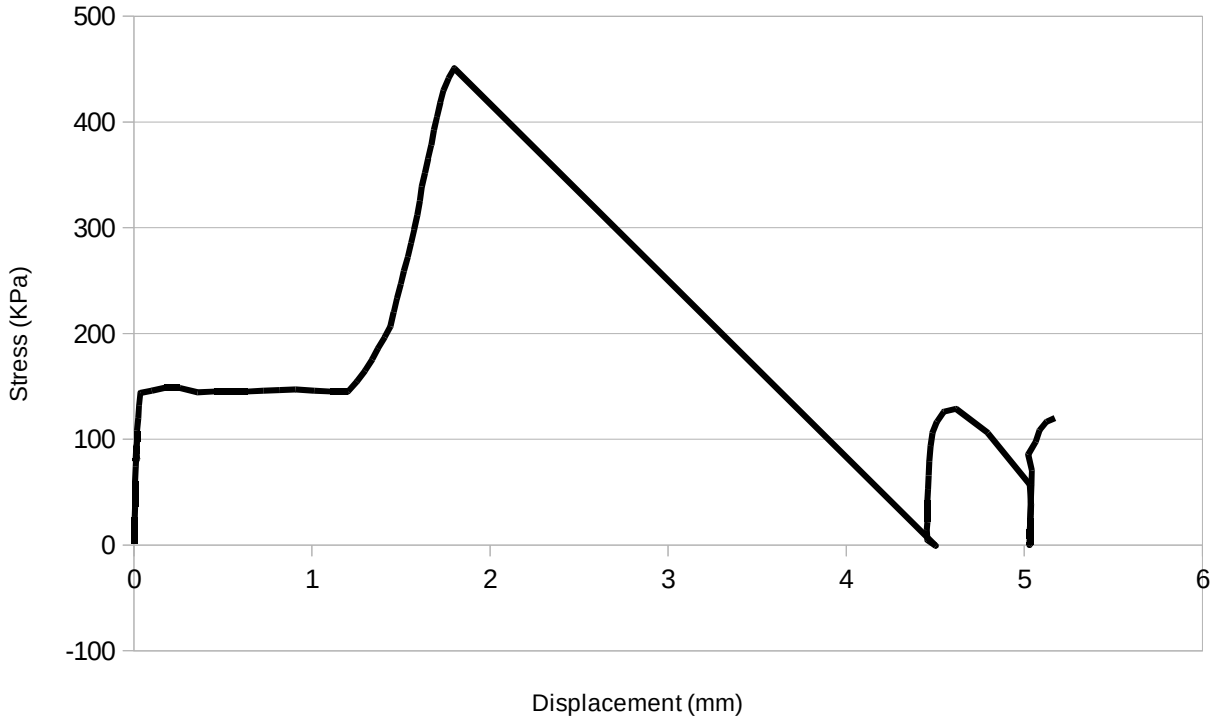

Max Stress: 450.8 Kpa

Res. Stress: 120.0 Kpa

Moisture : 11 %

Comments:

350F13I

Test Date: 16-11-08

Normal Pressure 350 Kpa

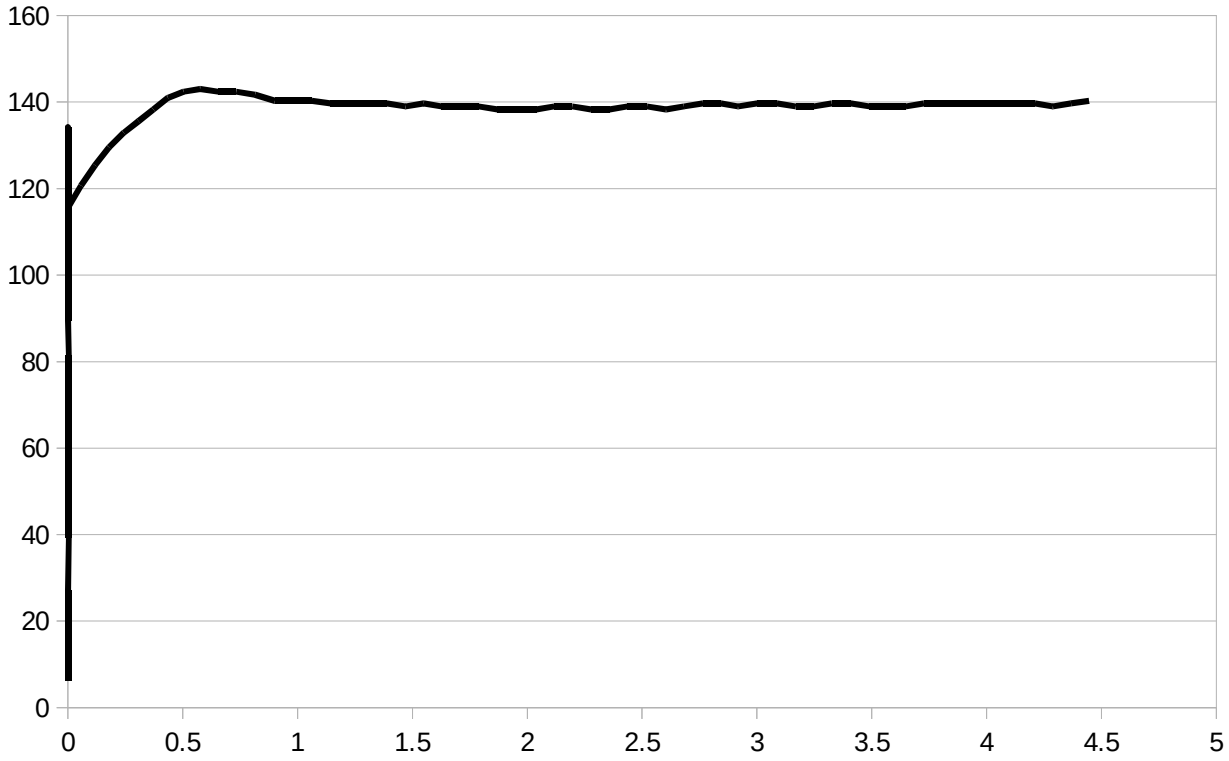

Max Stress: 143 Kpa

Res. Stress: N/A Kpa

Moisture : 13 %

Comments:

450F13A

Test Date: 16-11-08

Normal Pressure 450 Kpa

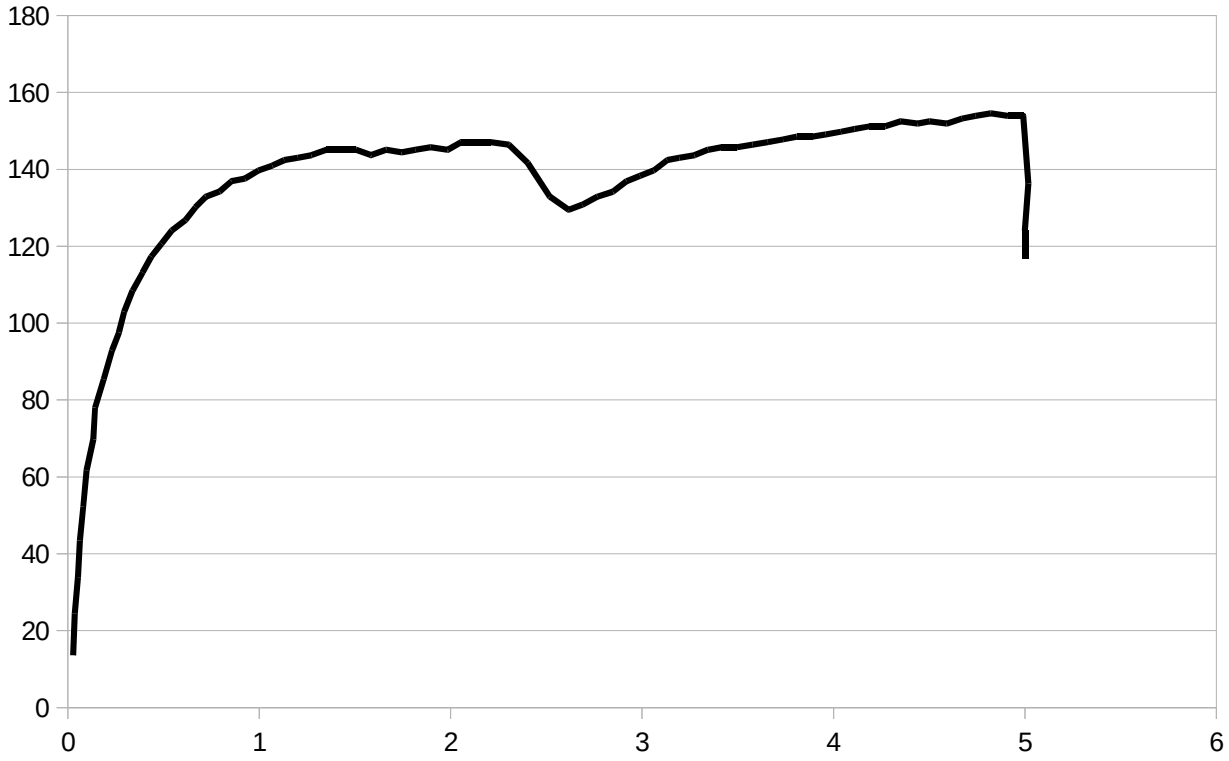

Max Stress: 155 Kpa

Res. Stress: N/A Kpa

Moisture : 13 %

Comments:

Appendix C. Pull out Setup Drawings

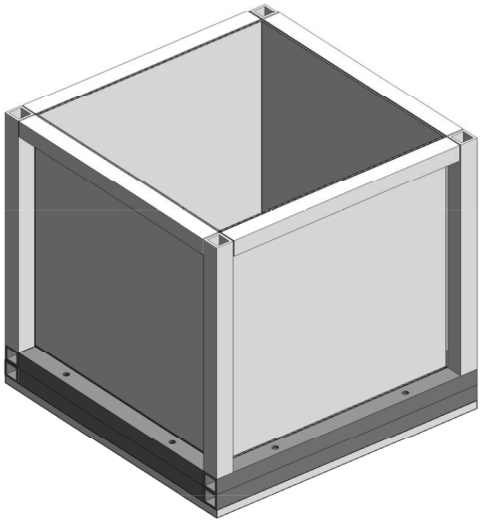

4 ISOMETRIC VIEW
NTS

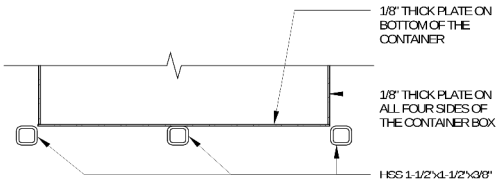

3 SECTION
NTS

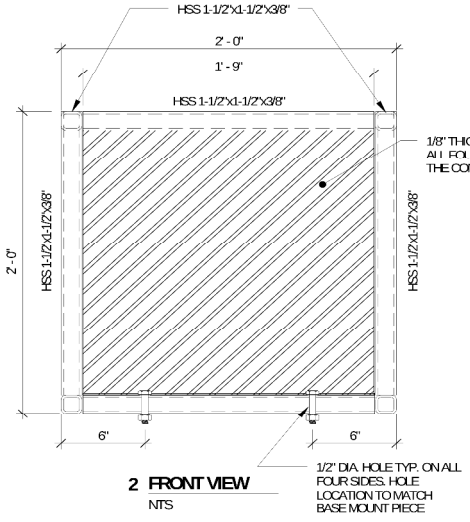

2 FRONT VIEW
NTS

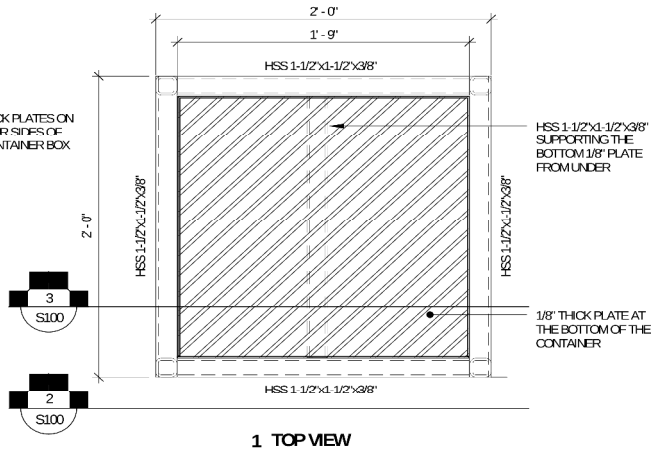

1 TOP VIEW
NTS

MATERIAL LIST:

HSS 1-1/2"X1-1/2"	-	24" LONG x 4 PIECES 21" LONG x 8 PIECES
PLATE 24"X24"	-	1/8" THK x 5 PIECES

No.	Issue Description	Date

ADFREEZE BOND TESTING
UNIVERSITY OF OTTAWA

CONTAINER BOX

Scale	As indicated
Project number	xxxxxxxx
Date	07/23/2014
Drawn by	Author
Checked by	Designer

S100

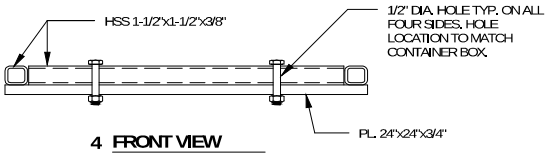

4 FRONT VIEW
NTS

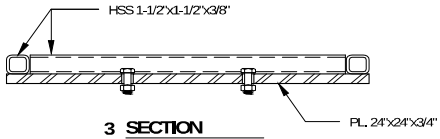

3 SECTION
NTS

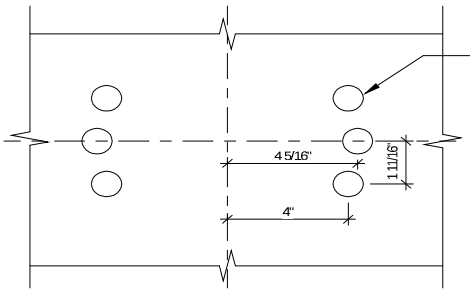

2 ENLARGED PART TOP VIEW
NTS

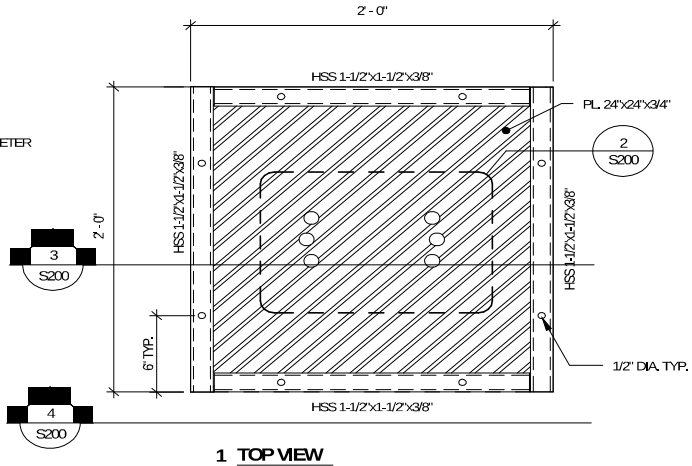

1 TOP VIEW
NTS

MATERIAL LIST:

HSS 1-1/2"x1-1/2"	-	24" LONG x 2 PIECES 21" LONG x 2 PIECES
PLATE 24"x24"	-	3/4" THK x 1 PIECE

No.	Issue Description	Date

ADFREEZE BOND TESTING
UNIVERSITY OF OTTAWA

BASE MOUNT PIECE

Scale	As indicated
Project number	xxxxxxxx
Date	07/23/2014
Drawn by	Author
Checked by	Designer

S200

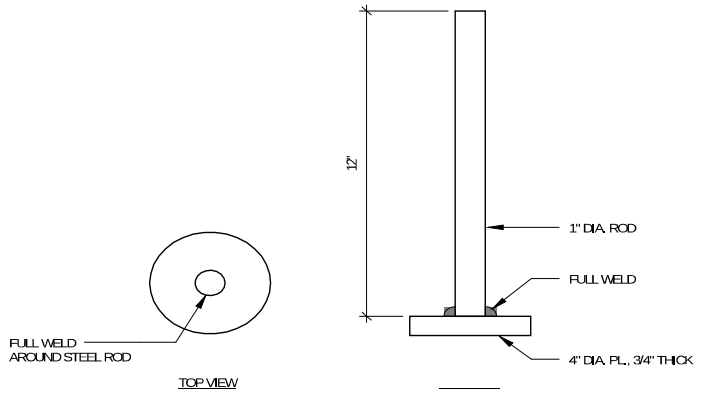

1 TOP MOUNT PIECE

NTS

MATERIAL LIST:

4" DIA. x 1" THK STEEL PLATE	-	1 PIECE
1" DIA. STEEL ROD	-	12" LONG

No.	Issue Description	Date

ADFREEZE BOND TESTING
UNIVERSITY OF OTTAWA

TOP MOUNT PIECE

Scale	As indicated
Project number	xxxxxxxx
Date	07/23/2014
Drawn by	Author
Checked by	Designer

S300